```
=> d his full

     (FILE 'HOME' ENTERED AT 09:48:42 ON 08 MAY 2003)

     FILE 'CAPLUS' ENTERED AT 09:52:25 ON 08 MAY 2003
L1             3 SEA (GEL OR AGAROSE OR ACRYLAMIDE OR POLYACRYLAMIDE) AND
                 IMINOTRIS
                 D 1-3 ALL
L2            50 SEA (GEL OR AGAROSE OR ACRYLAMIDE OR POLYACRYLAMIDE) AND
                 (BIS-TRIS OR BISTRIS)
L3            28 SEA L2 AND PH
                 D 1-28 ALL

     FILE 'STNGUIDE' ENTERED AT 10:00:44 ON 08 MAY 2003
```

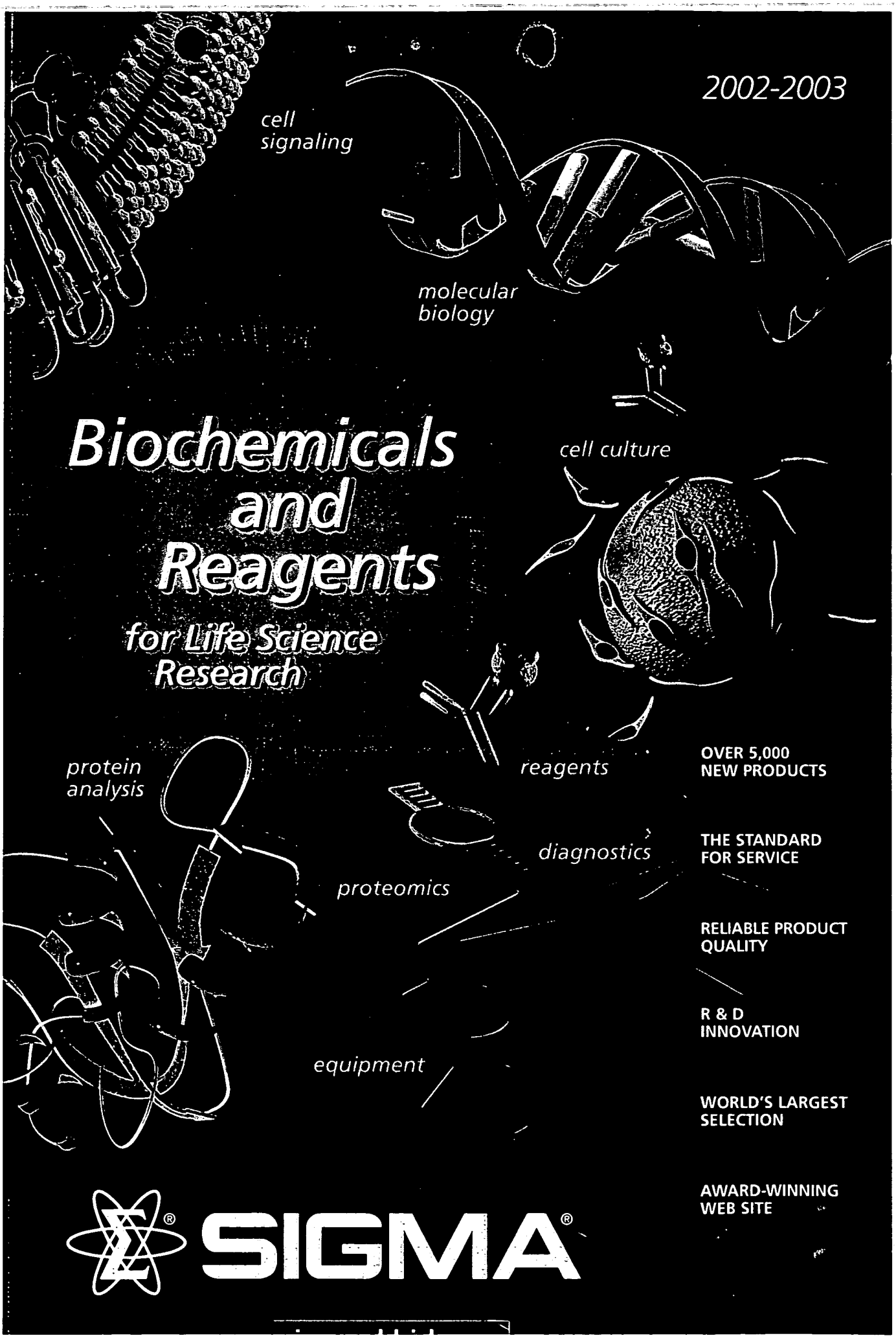
2002-2003
cell signaling
molecular biology
Biochemicals and Reagents
for Life Science Research
cell culture
protein analysis
reagents
diagnostics
proteomics
equipment
OVER 5,000 NEW PRODUCTS
THE STANDARD FOR SERVICE
RELIABLE PRODUCT QUALITY
R & D INNOVATION
WORLD'S LARGEST SELECTION
AWARD-WINNING WEB SITE
SIGMA®

US $

Benzyl 2,2,2-trichloroacetimidate 5 g 19.10
14,033-3 **minimum 99% (titration)** 25 g 63.30
2-8°C Benzyl alcohol ..... ≤1%
R: 36/37/38 S: 26-36

3-Benzyl-6-trifluoromethyl-7-sulfamoyl-3,4-dihydro-2H-1,2,4-benzothiadiazine 1,1-dioxide
See: Bendroflumethiazide *Page 253*

Benzyltrimethylammonium 10 g 225.00
B 5042 **tetrachloroiodate**
RT *[121309-88-4]*
◆ $C_6H_5CH_2N(ICl_4)(CH_3)_3$ FW 419.0
minimum 98% (titration)
Ref.: Kajigaeshi, S., et al., *Bull. Chem. Soc. Japan* **63**, 941 (1990)
R: 34 S: 53-26-45-36/37/39

Benzyl viologen dichloride See: 1,1'-Dibenzyl-4,4'-bipyridinium dichloride *Page 661*

Benzyl Z-α-D-glucosaminide 25 mg 17.75
B 7000 *[2862-10-4]* $C_{21}H_{25}NO_7$ FW 403.4
-0°C

Benzyl Z-β-D-glucosaminide 100 mg 29.25
B 7125 *[14531-02-3]* $C_{21}H_{25}NO_7$
-0°C FW 403.4

Bephenium hydroxynaphthoate 10 g 55.20
B 5650 Benzyldimethyl(2-phenoxyethyl)ammonium 3-hydroxynaphthoate
RT *[3818-50-6]* $C_{28}H_{29}NO_4$ FW 443.5

BePI 1 mg 41.20
B 7417 3-Methoxy-7H-8-methyl-11-([3-aminopropyl]amino)benzo(e)pyrido(4,3-b)indole
-20°C $C_{20}H_{22}N_4O$ FW 334.4
for molecular biology
Selectively intercalates into triple-helical DNA.
DNase, RNase ..... none detected
Ref.: Mergny, J.l., et al., Triple helix-specific ligands. *Science* **256**, 1681-1684 (1992)
R: 36/37/38 S: 26-36

Bepridil hydrochloride 100 mg 77.40
B 5016 1-Isobutoxy-2-pyrrolidino-3-(N-benzylanilino)propane
RT *[74764-40-2]* $C_{24}H_{34}N_2O \cdot HCl$ FW 403.0
Non-selective calcium channel blocker; inhibits Na^+-Ca^{2+} exchange; inhibits growth of brain tumor cells *in vitro*.
Ref.: 1. Kischel, P., et al., *Brit. J. Pharmacol.* **128**, 767 (1999)
2. Li, Y., et al., *J. Pharmacol. Exper. Therap.* **291**, 562 (1999)

Berberine chloride 5 g 17.75
B 3251 Natural Yellow 18 10 g 30.25
RT *[633-65-8]* CI 75160 25 g 66.45
$C_{20}H_{18}NO_4Cl$ FW 371.8
Fluorescent stain for heparin in mast cells
Ref.: 1. Berlin, G. and Enerback, L., *Agents and Actions* **14**, 401 (1984)
2. Dimlich, R.V.W., et al., *Stain Technol.* **55**, 217 (1980)
R: 20/21/22 S: 22-24/25

Berberine hemisulfate 10 g 40.85
B 3412 Natural Yellow 18
RT *[633-66-9]* CI 75160 $C_{20}H_{18}NO_4 \cdot 1/2SO_4$ FW 384.4
minimum 95%
Multi-drug resistance pump (MDR) inhibitor in *S. aureus*.
Fluorescent stain for heparin in mast cells
Ref.: 1. Stermitz, F.R., Synergy in a medicinal plant: Antimicrobial action of berberine potentiated by 5'-methoxyhydnocarpin, a multidrug pump inhibitor *Proc. Natl. Acad. Sci. USA* **97**, 1433 (2000)
2. Berlin, G. and Enerback, L., *Agents and Actions* **14**, 401 (1984)
3. Dimlich, R.V.W., et al., *Stain Technol.* **55**, 217 (1980)
R: 20/21/22 S: 36

Berenil See: Diminazene aceturate *Page 711*

Bergamot il 100 mL 61.60
B 4383 *[8007-75-8]*
RT Density ..... 0.88 g/mL

Bergapten See: 5-Methoxypsoralen *Page 1358*

Bergenin monohydrate 100 mg 17.95
B 6776 *[477-90-7]* $C_{14}H_{16}O_9 \cdot H_2O$ 1 g 92.75
RT FW 346.3
R: 36/37/38 S: 26-36

Beryllium atomic absorption 100 mL 19.35
20,698-9 **standard solution**
RT R: 49-34-43-23/25-48/23 S: 53-26-45-36/37/39

Beryllium oxide 5 g 41.30
20,277-0 R: 49-25-26-43-48/23-51/53-36/37/38 S: 53-45-61 20 g 109.20
2-8°C 100 g 432.15
◆

BES
Useful pH range 6.4-7.8

N,N-bis(2-Hydroxyethyl)taurine; N,N-Bis(2-hydroxyethyl)-2-aminoethanesulfonic acid; BES
[10191-18-1] $C_6H_{15}NO_5S$ FW 213.3
pKa (25 °C) 7.1
R: 36/37/38 S: 26-36

B 9879 **minimum 99% (titration)** 25 g 18.15
RT 100 g 58.70
250 g 129.00
1 kg 418.65

B 4554 **minimum 99% (titration), Biotechnology Performance Certified, cell culture tested** 25 g 19.40
RT 100 g 62.65
500 g 268.30
1 kg 447.10
Endotoxin and bioburden ..... tested
DNase, RNase, protease none detected

B 6420 **minimum 99% (titration), SigmaUltra** 25 g 44.35
RT 100 g 143.60
Aluminum (Al) ..... <0.0005%
Ammonium (NH_4) ..... <0.05%
Calcium (Ca) ..... <0.0005%
Copper (Cu) ..... <0.0005%
Iron (Fe) ..... <0.0005%
Lead (as Pb) ..... <0.001%
Magnesium (Mg) ..... <0.0005%
Potassium (K) ..... <0.005%
Sodium (Na) ..... <0.005%
Zinc (Zn) ..... <0.0005%
Chloride (as Cl) ..... <0.05%
SO_4 ..... <0.05%
Insoluble matter ..... <0.1%
Phosphorus (P) ..... <0.0005%
Residue on ignition ..... <0.2%
A_{260}, 1 M, water ..... <0.095
A_{280}, 1 M, water ..... <0.080
Solubility
water ..... 1 M at 25 °C, clear, colorless

B 2891 **BES s dium salt** 25 g 26.70
RT N,N-Bis(2-hydroxyethyl)-2-aminoethanesulfonic acid sodium salt 100 g 89.95
500 g 354.35
[66992-27-6] $C_6H_{14}NO_5SNa$ FW 235.2
pKa (25 °C) ..... 7.1 (Free acid)
S: 22-24/25

HEPBS 25 g 119.30

H 6903 RT — N-(2-Hydroxyethyl)piperazine-N'-(4-butanesulfonic acid) 100 g 331.30

[161308-36-7] $C_{10}H_{22}N_2O_4S$ FW 266.4

minimum 99% (titration)

Homolog of HEPES and EPPS with higher pKa and similar utility in biological systems.

pH range 7.6-9.0
pKa (25 °C) 8.3

Ref.: Thiel, T., et al., *J. Biochem. Biophys. Meth.* **37**, 117 (1998)

R: 36/37/38 S: 26-36

HePC See: Choline hexadecyl phosphate *Page 512*

15(S)-HEPE See: 15(S)-Hydroxy-(5Z,8Z,11Z,13E,17Z)-eicosapentaenoic acid *Page 1102*

HEPES

N-(2-Hydroxyethyl)piperazine-N'-(2-ethanesulfonic acid); 4-(2-Hydroxyethyl)piperazine-1-ethanesulfonic acid

[7365-45-9] $C_8H_{18}N_2O_4S$ FW 238.3

Useful pH range 6.8-8.2
pKa (25 °C) 7.5

H 3375 RT ◆	**minimum 99.5% (titration)** S: 22-24/25	25 g	21.95
		100 g	49.85
		6 × 100 g	245.15
		250 g	112.40
		500 g	182.75
		6 × 500 g	831.95
		1 kg	301.90
		5 kg	1170.10

H 4034 RT	**minimum 99.5% (titration), Biotechnology Performance Certified**	25 g	24.00
		100 g	53.35
		500 g	192.50
		6 × 500 g	871.50
		1 kg	316.30

Heavy metals (as Pb) ... ≤5 ppm
Iron (Fe) ..... <5 ppm
A_{260}, 0.1 M, water ..... <0.05
A_{280}, 0.1 M, water ..... <0.05
S: 22-24/25

H 7523 RT	**>99.5% (titration), pH 5.0-6.5 (20 °C), SigmaUltra**	50 g	79.35
		250 g	317.30

Aluminum (Al) ..... <0.0005%
Arsenic (As) ..... <0.0001%
Barium (Ba) ..... <0.0005%
Bismuth (Bi) ..... <0.0005%
Cadmium (Cd) ..... <0.0005%
Calcium (Ca) ..... <0.001%
Chromium (Cr) ..... <0.0005%
Cobalt (Co) ..... <0.0005%
Copper (Cu) ..... <0.0005%
Iron (Fe) ..... <0.0005%
Lead (as Pb) ..... <0.0005%
Lithium (Li) ..... <0.0005%
Magnesium (Mg) ..... <0.0005%
Manganese (Mn) ..... <0.0005%
Molybdenum (Mo) ..... <0.0005%
Nickel (Ni) ..... <0.0005%
Potassium (K) ..... <0.005%
Sodium (Na) ..... <0.005%
Strontium (Sr) ..... <0.0005%
Zinc (Zn) ..... <0.0005%
Chloride (as Cl) ..... <0.005%
Insoluble matter ..... passes filter test
Residue on ignition ..... <0.1% (as SO_4)
Loss on drying ..... <1%, 110°C
A_{260}, 1 M, water ..... <0.045
A_{280}, 1 M, water ..... <0.035
Solubility
water ..... 1 M at 20 °C, clear, colorless
S: 22-24/25

H 6147 RT	**≥99.5% (titrati n), Powder, Embryo tested**	25 g	28.35
		100 g	85.05
	Useful pH range: 6.8 - 8.2	500 g	299.15

Heavy metals (as Pb) ..... ≤5 ppm
A_{290}, 1.5 M ..... ≤0.05
pKa (25 °C) 7.5
S: 22-24/25

H 0887 2-8°C	**HEPES solution**	20 mL	12.85
	HEPES	100 mL	38.45

[7365-45-9]

1 M, pH 7.0-7.6, cell culture tested

Prepared from HEPES free acid and cell culture grade water.

sterile-filtered
Endotoxin ..... tested
S: 22-24/25

HEPES hemisodium salt

N-(2-Hydroxyethyl)piperazine-N'-(2-ethanesulfonic acid); 4-(2-Hydroxyethyl)piperazine-1-ethanesulfonic acid hemisodium salt

[103404-87-1] $C_{16}H_{35}N_4NaO_8S_2$ FW 498.6

S: 22-24/25

H 9897 RT	**Dry powder** foil pouches	10 packets	101.25
		5 × 10 packets	404.70

Contents of each pouch dissolved in 1 liter deionized water will yield 0.1 M sodium HEPES buffer, pH 7.5 at 25°C.

H 7637 RT	**minimum 99.5% (titration)**	25 g	23.40
		100 g	57.00

H 0527 RT	**HEPES potassium salt**	25 g	24.95
	N-(2-Hydroxyethyl)piperazine-N'-(2-ethanesulfonic acid); 4-(2-Hydroxyethyl)piperazine-1-ethanesulfonic acid potassium salt	100 g	61.20
		250 g	142.70

[82207-62-3] $C_8H_{17}N_2O_4SK$ FW 276.4

minimum 99.5% (titration)

S: 24/25

HEPES sodium salt

N-(2-Hydroxyethyl)piperazine-N'-(2-ethanesulfonic acid); 4-(2-Hydroxyethyl)piperazine-1-ethanesulfonic acid sodium salt

[75277-39-3] $C_8H_{17}N_2O_4SNa$ FW 260.3

Useful pH range 6.8-8.2
pKa (25 °C) 7.5
S: 22-24/25

H 7006 RT	**minimum 99.5% (titration)**	25 g	22.55
		100 g	58.00
		500 g	206.75
		1 kg	382.80

H 3784 RT	**minimum 99.5% (titration), Biotechnology Performance Certified, cell culture tested**	25 g	25.40
		100 g	66.45
		500 g	243.15
		1 kg	438.15

Heavy metals (as Pb) ..... ≤5 ppm
Iron (Fe) ..... <5 ppm
Endotoxin and bioburden ..... tested
DNase, RNase, protease ..... none detected
A_{260}, 0.1 M, water ..... <0.05
A_{280}, 0.1 M, water ..... <0.05

H 8651 RT	**minimum 99.5% (titration), SigmaUltra**	25 g	44.55
		100 g	104.90
		500 g	365.60

Aluminum (Al) ..... <0.0005%
Ammonium (NH_4) ..... <0.05%
Calcium (Ca) ..... <0.0005%
Copper (Cu) ..... <0.0005%
Iron (Fe) ..... <0.0005%
Lead (as Pb) ..... <0.001%
Magnesium (Mg) ..... <0.0005%
Potassium (K) ..... <0.005%
Zinc (Zn) ..... <0.0005%
Chloride (as Cl) ..... <0.05%
SO_4 ..... <0.05%
Insoluble matter ..... <0.1%
Phosphorus (P) ..... <0.005%
A_{260}, 1 M, water ..... <0.2
A_{280}, 1 M, water ..... <0.2
pH ..... 10.0-12.0 (20 °C, 1 M in water)
Solubility
water ..... 1 M at 20 °C, clear, colorless

US $

(Continuation of)
MOPSO

M 8389 RT — 3-(N-Morpholino)-2-hydroxypropanesulfonic acid; 3-Morpholino-2-hydroxypropanesulfonic acid
[68399-77-9] $C_7H_{15}NO_5S$ FW 225.3
25 g 24.45; 100 g 55.80; 250 g 132.25; 500 g 215.10
minimum 99% (titration)
pH range 6.2-7.6
pKa (25 °C) 6.9
R: 36/37/38 S: 26-36

MOPSO sodium salt
3-(N-Morpholino)-2-hydroxypropanesulfonic acid; 3-Morpholino-2-hydroxypropanesulfonicacid sodium salt
[79803-73-9] $C_7H_{14}NO_5SNa$ FW 247.2
Useful pH range 6.2-7.6
pKa (25 °C) 6.9

M 8767 RT — **minimum 99% (titration)** 25 g 26.20; 100 g 59.85; 250 g 141.55; 500 g 230.30

M 5914 RT — **minimum 99% (titration), pH 10.0-12.0 (20 °C), SigmaUltra** 25 g 48.60; 100 g 107.50; 250 g 258.65
Aluminum (Al) ..... <0.0005%
Ammonium (NH_4) ..... <0.05%
Calcium (Ca) ..... <0.0005%
Copper (Cu) ..... <0.0005%
Iron (Fe) ..... <0.0005%
Lead (as Pb) ..... <0.001%
Magnesium (Mg) ..... <0.0005%
Potassium (K) ..... <0.005
Zinc (Zn) ..... <0.0005%
Chloride (as Cl) ..... <0.05%
Insoluble matter ..... <0.1%
Phosphorus (P) ..... <0.005%
A_{280}, 1 M, water ..... <0.05
Solubility
water ..... 1 M at 20 °C, clear, colorless

Morantel
R: 20/21/22 S: 36

M 5404 RT — **Morantel citrate salt** 5 g 33.95
1,4,5,6-Tetrahydro-1-methyl-2-(2-[3-methyl-2-thienyl]ethenyl)pyrimidine
[69525-81-1] $C_{12}H_{16}N_2S \cdot C_6H_8O_7$ FW 412.5

M 5529 RT — **Morantel tartrate salt** 25 g 115.20
1,4,5,6-Tetrahydro-1-methyl-2-(2-[3-methyl-2-thienyl]ethenyl)pyrimidine Morantel tartrate monohydrate
[26155-31-7] $C_{12}H_{16}N_2S \cdot C_4H_6O_6$ FW 370.4

Mordant Black 11 See: Eriochrome Black T *Page 794*

Mordant blue 1 See: Chromeazurol B *Page 518*

Mordant Blue 14 See: Celestine blue *Page 437*

Mordant Blue 29 See: Chromeazurol S *Page 518*

Mordant Red 5 See: Anthracene Chrome Red A *Page 190*

Mordant Violet 25 See: Gallein *Page 917*

Morin 2 g 12.55; 5 g 24.20; 10 g 39.00
M 4008 RT — 2',3,4',5,7-Pentahydroxyflavone
[480-16-0] $C_{15}H_{10}O_7$ FW 302.2
Powder
A flavonoid with anti-oxidant properties. Shown to protect cells against the oxygen radical damage. It not only scavenges oxyradicals, but also moderately inhibits xanthine oxidase, a free-radical generating enzyme. At concentrations of 75-100 micromolar, it inhibits oxidation of low density lipoprotein (LDL) by free radicals or Cu^{2+}. Reported to inhibit rat brain phosphatidylinositolphosphate kinase activity *in vitro* and *in vivo*.
Color ..... yellow
Solubility
aqueous base ..... soluble
ethanol ..... 50 mg/mL
Ref.: 1. Wu, T.W., et al., Molecular properties and myocardial salvage effects of morin hydrate. *Biochem. Pharmacol.* **49**, 537-543 (1995)
2. Cheng, C.H., In vitro and in vivo inhibitory actions of morin on rat brain phosphatidylinositolphosphate kinase activity *Life Sci.* **61**, 2035-2047 (1997)
3. Wu, T.W., et al., Morin hydrate inhibits azo-initiator induced oxidation of human low density lipoprotein. *Life Sci.* **58**, PL17-PL22 (1996)
4. Wu, T.W., et al., Antioxidation of human low density lipoprotein by morin hydrate. *Life Sci.* **57**, PL51-PL56 (1995)
5. Zeng, L.H., et al., Morin hydrate protects cultured rat glomerular mesangial cells against oxyradical damage. *Life Sci.* **55**, PL351-PL357 (1994)
6. Zeng, L.H., et al., Comparative protection against oxyradicals by three flavonoids on cultured endothelial cells *Biochem. Cell Biol.* **75**, 717-720 (1997)
R: 36/37/38 S: 26-36

Morphiceptin hydrochloride See: Opioid Peptides *Page 1566*

(+)-9α,13α,14α-Morphinan-3ol See: (±)-3-Hydroxymorphinan *Page 1110*

Morphine sulfate salt

M 9524 -0°C ◆ — *[64-31-3]* 1 mL 32.50
1.0 mg/mL (w/v)±5% in methanol

M 8777 RT ◆ — **Morphine pentahydrate** 25 mg 21.10; 50 mg 37.25; 250 mg 145.50
Morphine hemi[sulfate pentahydrate]
[6211-15-0] $C_{34}H_{40}N_2O_{10}S \cdot 5H_2O$ FW 758.8
Narcotic analgesic; prototypic μ-agonist; also agonist at κ-receptors.
Solubility
ethanol ..... 1.8 mg/mL
water ..... 64 mg/mL
DEA Schedule II; see p. 17.
Ref.: 1. Katsumata, S., et al., Pharmacological study of dihydroetorphine in cloned mu-delta- and kappa-opioid receptors *Eur. J. Pharmacol.* **291**, 367-373 (1995)
2. Martin, G., et al., Chronic morphine treatment alters NMDA receptor-mediated synaptic transmission in the nucleus accumbens. *J. Neurosci.* **19**, 9081-9089 (1999)
3. Stanasila, L., et al., Coupling efficacy and selectivity of the human mu-opioid receptor expressed as receptor-Galpha fusion proteins in Escherichia coli *J. Neurochem.* **75**, 1190-1199 (2000)
4. Napier, L.D., et al., Canine cardiac muscarinic receptorsG proteinsand adenylate cyclase after long-term morphine *J. Pharmacol. Exper. Therap.* **291**, 725-732 (1999)
R: 22 S: 22-36

Morphine-d_3 hydrochloride ◆
R: 26/27/28 S: 53-22-45-36/37/39

M 3402 RT — **Morphine-d_3 trihydrate** 5 mg 404.10
7,8-Didehydro-4,5-epoxy-17-(methyl-d_3)morphinan-3,6-diol
$C_{17}H_{16}D_3NO_3 \cdot HCl \cdot 3H_2O$ FW 378.9
98 atom % D
DEA Schedule II; see p. 17.

M 6380 -0°C — **Morphine-d_3 solution** 1 mL 57.25
100 μg/mL

Morphine 3-ethyl ether See: Ethylmorphine *Page 817*

Morphine 3-β-D-glucuronide solution

M 4266 2-8°C ◆ — **1.0 mg/mL (w/v)±5% in methanol** 1 mL 32.50
R: 23/25-36/38 S: 53-7-16-24-33-45

Piperidine 100 mL 13.40
P 5881 Hexahydropyridine 250 mL 30.85
RT *[110-89-4]* $C_5H_{11}N$ 500 mL 36.40
◆ FW 85.15 6 x 500 mL 195.90
minimum 99.0% (GC) 1 L 68.80
Density . . . . . 0.86 g/mL
R: 11-34-23/24 S: 53-16-26-27-45

(S)-Piperidine-2-carboxylic acid See: L-Pipecolic acid *Page 1698*

L-2-Piperidinecarboxylic acid See: L-Pipecolic acid *Page 1698*

(±)-Piperidine-2-carboxylic acid See: DL-Pipecolinic acid *Page 1698*

3-Piperidinecarboxylic acid See: (±)-Nipecotic acid *Page 1514*

***cis*-2,3-Piperidinedicarboxylic acid** 25 mg 39.45
P 8782 *[46026-75-9]* $C_7H_{11}NO_4$ 250 mg 219.05
RT FW 173.2
NMDA receptor agonist at the glutamate recognition site.
Ref.: 1. Collingridge, et al., Excitatory amino acid receptors in the vertebrate central nervous system *Pharmacol. Rev.* **40**, 143 (1989)
2. Priestley, T., and Kemp, J.A., Kinetic study of the interactions between the glutamate and glycine recognition sites on the N-methyl-D-aspartic acid receptor complex *Mol. Pharmacol.* **46**, 1191-1196 (1994)
3. Crewther, et al., Changes in eye growth produced by drugs which affect retinal ON or OFF responses to light. *J. Ocul. Pharmacol. Ther.*, **12**, 193 (1996)
4. Hansen, et al., Structural, conformational, and stereochemical requirements of central excitatory amino acid receptors *Ed. Res. Rev.* **10**, 55 (1990)
5. Neal, et al., Selective release of nitric oxide from retinal amacrine and bipolar cells *Invest. Ophthalmol. Vis. Sci.* **39**, 850 (1998)

Piperidine-4-sulfonic acid 25 mg 43.40
P 9159 P4S 250 mg 306.15
RT *[72450-62-5]* $C_5H_{11}NO_3S$
FW 165.2
$GABA_A$ agonist
Ref.: 1. Galvez-Ruano, et al., Identifying agonistic and antagonistic mechanisms operative at the GABA receptor. *J. Neurosci. Res.* **42**, 666 (1995)
2. Helen, et al., Muscimol-scopolamine interactions in the rat brain: A study with 2-deoxy-D-[1-14 C]glucose. *J. Neurosci.* **4**, 1405 (1984)
3. Krogsgaard, L., et al., *J. Neurochem.* **34**, 756 (1980)
4. *Merck Index* 12th ed.,

Piperidinic acid See: γ-Aminobutyric acid *Page 136*

3-(1-Piperidinyl)-1,2-propanediol bis(phenylcarbamate) See: Diperodon *Page 720*

3-(2-Piperidinyl)pyridine See: (±)-Anabasine *Page 180*

6-(1-Piperidinyl)pyrimidine-2,4-diamine 3-oxide See: Minoxidil *Page 1411*

N-(2-Piperidylmethyl)-2,5-*bis*-(2,2,2-trifluoroethoxy)benzamide See: Flecainide *Page 863*

Piperine 1 g 8.35
P4,900-7 $C_{17}H_{19}NO_3$ FW 285.3 5 g 21.85
RT Assay . . . . . approx. 97% 25 g 92.15
R: 22 S: 22-24/25

Piperlongumine 100 mg 24.45
P 8588 **from long pepper** 500 mg 97.30
RT 5,6-Dihydro-1-(1-oxo-3-[3,4,5-trimethoxyphenyl]-trans-2-propenyl)-2[1H]-pyridinone
[20069-09-4] $C_{17}H_{19}NO_5$ FW 317.3
long pepper

PIPES
Useful pH range 6.1-7.5
pKa (25 °C) 6.8

Piperazine-N,N'-bis(2-ethanesulfonic acid); 1,4-Piperazinediethanesulfonic acid; Piperazine-1,4-bis(2-ethanesulfonic acid)
[5625-37-6] $C_8H_{18}N_2O_6S_2$ FW 302.4
S: 22-24/25

P 6757 **minimum 99% (titration)** 25 g 25.05 US $
RT 100 g 70.30
6 x 100 g 336.25
500 g 253.30
1 kg 476.15

P 1851 **minimum 99.5% (titration), Biotechnology Performance Certified, cell culture tested** 25 g 28.60
RT 100 g 79.25
500 g 284.85
1 kg 509.30
Heavy metals (as Pb) . . . . . ≤5 ppm
Endotoxin and bioburden . . . tested
DNase, RNase, protease none detected

P 8203 **minimum 99% (titration), SigmaUltra** 50 g 81.90
RT 250 g 312.90
Aluminum (Al) . . . . . <0.005%
Barium (Ba) . . . . . <0.0005%
Bismuth (Bi) . . . . . <0.0005%
Cadmium (Cd) . . . . . <0.0005%
Calcium (Ca) . . . . . <0.005%
Chromium (Cr) . . . . . <0.0005%
Cobalt (Co) . . . . . <0.0005%
Copper (Cu) . . . . . <0.0005%
Iron (Fe) . . . . . <0.0005%
Lead (as Pb) . . . . . <0.0005%
Lithium (Li) . . . . . <0.0005%
Magnesium (Mg) . . . . . <0.0005%
Manganese (Mn) . . . . . <0.0005%
Molybdenum (Mo) . . . . . <0.0005%
Nickel (Ni) . . . . . <0.0005%
Potassium (K) . . . . . <0.005%
Sodium (Na) . . . . . <0.1%
Strontium (Sr) . . . . . <0.0005%
Zinc (Zn) . . . . . <0.0005%
Chloride (as Cl) . . . . . ≤0.2%
Insoluble matter . . . . . passes filter test
Residue on ignition . . . . . <0.5% (as SO_4)
Loss on drying . . . . . <0.5%, 110°C
A_{260}, 0.5 M, 1 N NaOH . . . . . <0.1
A_{280}, 0.5 M, 1 N NaOH . . . . . <0.1
Solubility
1 N NaOH . . . . . 0.5 M at 20 °C, clear, colorless

P 7643 **PIPES dipotassium salt** 25 g 26.25
RT Piperazine-N,N'-bis(2-ethanesulfonic acid); 100 g 72.80
500 g 271.75
1,4-Piperazinediethanesulfonic acid; Piperazine-1,4-bis(2-ethanesulfonic acid) dipotassium salt 1 kg 499.15
[108321-27-3] $C_8H_{16}N_2O_6S_2K_2$ FW 378.6
minimum 99% (titration)

P 3768 **PIPES disodium salt** 25 g 26.25
RT Piperazine-N,N'-bis(2-ethanesulfonic acid); 100 g 72.80
250 g 163.90
1,4-Piperazinediethanesulfonic acid; Piperazine-1,4-bis(2-ethanesulfonic acid) disodium salt 500 g 271.75
1 kg 499.15
[76836-02-7] $C_8H_{16}N_2O_6S_2Na_2$ FW 346.3
minimum 99% (titration)
S: 22-24/25

P 8655 **PIPES sesquisodium salt** 25 g 24.15
RT Piperazine-N,N'-bis(2-ethanesulfonic acid); 100 g 66.90
500 g 264.95
1,4-Piperazinediethanesulfonic acid; Piperazine-1,4-bis(2-ethanesulfonic acid) sesquisodium salt 1 kg 459.25
[100037-69-2] $C_8H_{18}N_2O_6S_2$ FW 670.7
minimum 99% (titration)
S: 22-24/25

P 2949 **PIPES sodium salt** 25 g 23.10
RT Piperazine-N,N'-bis(2-ethanesulfonic acid); 1,4-Piperazinediethanesulfonic acid 100 g 64.05
500 g 239.30
[10010-67-0] $C_8H_{17}N_2O_6S_2Na$ FW 324.4
minimum 99% (titration)

US $

Terrific Broth, Modified EZMix™ Powder See: Media for E.coli *Page 1405*

α-Terthienyl See: 2,2':5',2''-Terthiophene *Page 2008*

2,2':5',2''-Terthiophene 100 mg 18.15
T 5406 RT α-Terthienyl; 2,5-Di(2-thienyl)thiophene 250 mg 36.30
[1081-34-1] $C_{12}H_8S_3$ FW 248.4
Natural product occurring in marigold which shows UV-enhanced antibiotic activity.
Ref.: Arora, S.K., *Tetrahedron Lett.* **24**, 4043 (1983)
S: 22-24/25

NEW **Tertiapin** 500 µg 322.30
T 8316 -0°C H-Ala-Leu-Cys-Asn-Cys-Asn-Arg-Ile-Ile-Ile-Pro-His-Met-Cys-Trp-Lys-Lys-Cys-Gly-Lys-Lys-NH_2
$C_{106}H_{176}N_{34}O_{23}S_5$ FW 2455
>95%
A potent inhibitor of the inward-rectifier K+ channels, blcoked a G-protein-gated channel (GIRK1/4) and the ROMK1 channel with nonomolar affinities, however a closely related channel, IRK1, was insensitive to tertiapin. Thus, tertiapin will be a powerful ligand for purifying functional channels as well as for screening pharmaceutical agents against these channels.
Ref.: Jin, W. and Lu, Z., *Biochemistry* **37**, 13291 (1998)

[Gln^{13}]-Tertiapin See: Tertiapin-Q *Page 2008*

NEW **Tertiapin-Q trifluoroacetate salt** 500 µg 333.70
T 1567 -20°C Ala-Leu-Cys-Asn-Cys-Asn-Arg-Ile-Ile-Ile-Pro-His-Gln-Cys-Trp-Lys-Lys-Cys-Gly-Lys-Lys-NH_2 [Disulfide bridges 3–14, 5–18]; [Gln^{13}]-Tertiapin; TPN_Q
$C_{106}H_{175}N_{35}O_{24}S_4$ FW 2452
minimum 97% (HPLC)
Blocks the GIRK1/4 and ROMK1 members of the inward-rectifier K^+ channel family.
Non-air oxidizable tertiapin derivative.
Ref.: 1. Jin, W., et al., Synthesis of a Stable Form of Tertiapin: A High-Affinity Inhibitor for Inward-Rectifier K^+ Channels *Biochemistry* **38**, 14286-14293 (1999)
2. Jin, W., et al., A Novel High-Affinity Inhibitor for Inward-Rectifier K^+ Channels *Biochemistry* **37**, 13291-13299 (1998)
3. Jin, W., et al., Mechanisms of Inward-Rectifier K^+ channel Inhibition by Tertiapin-Q *Biochemistry* **38**, 14294-14301 (1999)

TES
Useful pH range 6.8-8.2
pKa (25 °C) 7.5

2-[(2-Hydroxy-1,1-bis[hydroxymethyl]ethyl)amino]ethanesulfonic acid; N-[Tris(hydroxymethyl)methyl]-2-aminoethanesulfonic acid; TES
[7365-44-8] $C_6H_{15}NO_6S$ FW 229.3
S: 22-24/25

T 1375 RT **minimum 99% (titration)** 25 g 23.30; 100 g 64.40; 500 g 269.65; 1 kg 412.85; 5 kg 1709.80

T 5691 RT **minimum 99% (titration), Biotechnology Performance Certified, cell culture tested** 25 g 29.55; 100 g 80.45; 500 g 318.50
Heavy metals (as Pb) ..... ≤5 ppm
Endotoxin and bioburden ..... tested
DNase, RNase, protease ..... none detected

T 6541 RT **>99.5% (titration), SigmaUltra** 5 g 22.45; 25 g 74.05; 100 g 239.55

Aluminum (Al)	<0.0005%
Arsenic (As)	<0.0001%
Barium (Ba)	<0.0005%
Bismuth (Bi)	<0.0005%
Cadmium (Cd)	<0.0005%
Calcium (Ca)	<0.001%
Chromium (Cr)	<0.0005%
Cobalt (Co)	<0.0005%
Copper (Cu)	<0.0005%
Iron (Fe)	<0.0005%
Lead (as Pb)	<0.0005%
Lithium (Li)	<0.0005%
Magnesium (Mg)	<0.0005%
Manganese (Mn)	<0.0005%
Molybdenum (Mo)	<0.0005%
Nickel (Ni)	<0.0005%
Potassium (K)	<0.02%
Sodium (Na)	<0.01%
Strontium (Sr)	<0.0005%
Zinc (Zn)	<0.0005%
Chloride (as Cl)	<0.005%
Sulfate (SO_4)	<0.005%
Insoluble matter	passes filter test
Residue on ignition	<0.1% (as SO_4)
Loss on drying	<1%, 110°C
A_{260}, 1 M, water	<0.055
A_{280}, 1 M, water	<0.045
pH	3.5-5.0 (20 °C, 1 M in water)
Solubility	
water	1 M at 20 °C, clear, colorless

T 1030 RT **TES hemisodium salt** 100 g 183.50
N-tris-(Hydroxymethyl)methyl-2-aminoethanesulfonic acid; 2-[(2-Hydroxy-1,1-bis[hydroxymethyl]ethyl)amino]ethanesulfonic acid

T 0772 RT **TES sodium salt** 25 g 27.85; 100 g 74.95; 500 g 327.20
2-[(2-Hydroxy-1,1-bis[hydroxymethyl]ethyl)amino]ethanesulfonic acid; N-[Tris(hydroxymethyl)methyl]-2-aminoethanesulfonic acid sodium salt
[70331-82-7] $C_6H_{14}NO_6SNa$ FW 251.2

Testes acetone powder from rat 1 g 109.10
T 4892 -0°C

Testosterone
trans-Testosterone; 17β-Hydroxy-3-oxo-4-androstene; 17β-Hydroxy-4-androsten-3-one; 4-Androsten-17β-ol-3-one
[58-22-0] $C_{19}H_{28}O_2$ FW 288.4

T 1500 RT Testosterone secreted by the testis is converted to dihydrotestosterone in the target tissues where it appears to mediate many of the biological actions of testosterone. Androgens direct the development of the male phenotype during embryogenesis and at puberty. 1 g 9.20; 5 g 31.70; 25 g 106.00
DEA Schedule III; see p. 17.
Ref.: 1. Mainwaring W.I.P., The mechanism of action of androgens *Monogr. Endocrinol.* **10**, 1-178 (1977)
2. Rosenfield, R. L., *Adv. Pediatrics* **19**, 172 (1972)
R: 45-61 S: 53-22-45-36/37/39

T 5411 2-8°C ◆ **1.0 mg/mL (w/v)±2% in 1,2-dimethoxyethane** 1 mL 44.65
R: 10-19-20 S: 24/25

Testosterone-*d*$_3$ solution 1 mL 57.25
T 5536 2-8°C ◆ *[77546-39-5]* **nominal 100 µg/mL in 1,2-dimethoxyethane**
R: 45-61-20/21/22 S: 53-22-45-36/37/39

Mellerson, Kendra

Fr m: Noguerola, Alex
Sent: Thursday, May 08, 2003 10:11 AM
To: STIC-EIC1700
Subject: articles request

Please order the following articles

09/728,378

L3 ANSWER 19 OF 28 CAPLUS COPYRIGHT 2003 ACS
AN 1991:467835 CAPLUS
DN 115:67835
TI A new multiphasic buffer system for sodium dodecyl sulfate-polyacrylamide gel electrophoresis of proteins and peptides with molecular masses 100,000-1000, and their detection with picomolar sensitivity
AU Wiltfang, Jens; Arold, Norbert; Neuhoff, Volker
CS Forschungsstelle Neurochem., Max-Planck-Inst. Exp. Med., Goettingen, 3400, Germany
SO Electrophoresis (1991), 12(5), 352-66
CODEN: ELCTDN; ISSN: 0173-0835

Bistech
QD79.E44E44

Electrophoresis 1991, *12*, 352–366

Jens Wiltfang
Norbert Arold
Volker Neuhoff

Max-Planck-Institut für experimentelle Medizin, Forschungsstelle Neurochemie, Göttingen

A new multiphasic buffer system for sodium dodecyl sulfate-polyacrylamide gel electrophoresis of proteins and peptides with molecular masses 100 000–1000, and their detection with picomolar sensitivity

A novel multiphasic buffer system for high resolution sodium dodecyl sulfate-polyacrylamide gel electrophoresis of dansylated and nondansylated proteins/peptides in the relative molecular mass (M_r) range of 100 000–1000 is described. The system, based on Jovin's theory of multiphasic zone electrophoresis [1–3], allows complete stacking and destacking of proteins/peptides within the above M_r range. The buffer system uses Bicine and sulfate as trailing and leading ion, respectively, and Bistris and Tris as counter ions in the stacking and separating phase, respectively. Through selection of two different counter ions – the characteristic feature of the present ionic system – the stacking limits of a multiphasic buffer system can be further widened, thus making it applicable to gel electrophoresis of a larger spectrum of rapidly migrating species, such as sodium dodecyl sulfate-proteins/peptides and nucleic acids, than has been possible previously. Highly sensitive detection methods for proteins as well as for polypeptides down to approximately M_r 1000 are described. Dansylated proteins/peptides were detected by their fluorescence either directly within the gel or following electroblotting into anion-exchange or polyvinylidene difluoride membranes. The latter procedure resulted in detection sensitivities of approximately 1 ng. Nondansylated proteins/peptides were either detected within the gel by colloidal Coomassie staining or by electroblotting into polyvinylidene difluoride membranes, followed by colloidal gold staining. Prior to both staining procedures the proteins/peptides were pretreated with glutardialdehyde in the presence of borate at near neutral pH values to generate protein/peptide polymers of poor solubility. For a given pH the efficiency of the latter procedure was significantly influenced by the nature of the buffer ion used in the fixation buffer. In contrast to conventional fixation procedures even small polypeptides (M_r 1000) were immobilized and approximately 15 ng and 0.75 ng could be detected after colloidal Coomassie and colloidal gold staining, respectively.

1 Introduction

The purpose of the present study was to set up a discontinuous sodium dodecyl sulfate-polyacrylamide gel electrophoresis (SDS-PAGE) system yielding high resolution in the separation of proteins/peptides in the M_r 100 000–1000 range. High-resolution SDS-PAGE separation of proteins/peptides may be obtained by electrophoretic concentration of the sample components within an ultrathin starting zone (stacking) prior to separation. This can be achieved by placing the electrophoretic net mobilities of the sample components intermediately between those of the leading- and trailing ions of a discontinuous buffer system. Thus the complexes of anionic detergent (SDS) and proteins/peptides are trapped in an ultrathin moving boundary, which is governed by the regulating function for weak electrolytes [1, 4, 5]. Complete liberation of sample components (destacking) within the separation gel demands a trailing ion net mobility faster than that of the smallest peptide to be studied. This can be achieved by introducing discontinuity with regard to pH and/or polyacrylamide pore size between stacking and separating gel. Discontinuous buffer systems for PAGE were introduced by Ornstein [6] and Davies [7], and Ornstein gave a theoretical treatment of "disc" electrophoresis [6]. Note that in this context the terms "discontinuous electrophoresis" and "moving boundary electrophoresis" are synonyms, as well as the terms "discontinuous buffer systems" and "multiphasic buffer systems" [8, 9].

However, ionic systems commonly applied in the separation of small polypeptides by SDS-PAGE often do not provide stacking, such as the method of Swank and Munkres [10], or the stacking is of non-steady state and the trailing ion net mobility is too fast to provide effective stacking over the complete M_r range of interest, such as the ionic system proposed by Anderson *et al.* [11]. In this respect superior results are obtained by the multiphasic buffer system of Kyte and Rodriguez [12], who applied 2-morpholinoethanesulfonic acid as trailing ion, or the Tricine/Tris SDS-PAGE system of Schägger and von Jagow [13]. In this paper we describe a new multiphasic buffer system which allows complete stacking and destacking of proteins as well as peptides in the M_r 100 000–1000 range. The system is based on Jovin's theory of multiphasic zone electrophoresis [1–3].

Correspondence: Dr. J. Wiltfang, Max-Planck-Institut für experimentelle Medizin, Hermann-Rein-Str. 3, DW-3400 Göttingen

Abbreviations: **AMPS**, ammonium peroxydisulfate; **Bicine**, *N,N*-bis(2-hydroxyethyl)-glycine; **Bis**, *N,N'*-methylenebisacrylamide; **Bistris**, bis(2-hydroxyethyl)iminotris-(hydroxymethyl)-methane; **BPB**, Bromophenol Blue; **CBB**, Coomassie Brilliant Blue; **dansyl chloride**, 1-dimethylamino-5-naphthalenesulfonyl chloride; M_r, relative molecular mass; **PBS**, phosphate buffered saline; **%C**, proportion of cross-linking reagent (Bis) per gel total monomer content in g per 100 g; **%T**, total monomer concentration (acrylamide + Bis) in g per 100 mL; **PVDF**, polyvinylidene difluoride; **SDS-PAGE**, sodium dodecyl sulfate-polyacrylamide gel electrophoresis; **TCA**, trichloroacetic acid; **TEMED**, *N,N,N',N'*-tetramethylethylenediamine; **Tris**, 2-amino-2(hydroxymethyl)-1,3-propanediol

0173-0835/91/0505-0352 $3.50+.25/0

Another problem concerns the detecting of small polypeptides in polyacrylamide gels. These peptides are not precipitated by strong acids and/or alcohols and are often lost prior to staining. To overcome this problem, separated proteins/peptides may be insolubilized in the gel with formaldehyde [14, 15] or glutardialdehyde [16]. In the present study, pretreatment of polyacrylamide gels with glutardialdehyde at near-neutral pH in the presence of borate was preferred. Using a recently described colloidal Coomassie stain [17], small polypeptides pretreated in this way may be detected in the lower picomolar range after only 90 min of staining. Due to the colloidal staining principle applied [18], a clear background is obtained without any destaining. Alternatively, small polypeptides may be labeled prior to electrophoresis by fluorescent markers such as fluorescamine [19], *o*-phthaldialdehyde [20], fluorescein isothiocyanate [21], or dansyl chloride [22–24]. In this study dansyl chloride was selected because it yields covalent binding – not only to primary but also to secondary amino groups – as well as stable reaction products, and high detection sensitivity. An increase in detection sensitivity for dansylated proteins/peptides may be obtained by electroblotting the compounds into polyvinylidene difluoride (PVDF) or anion-exchange membranes after electrophoretic separation [25]. Nondansylated proteins/peptides may also be detected by electroblotting the compounds into PVDF membranes, followed by *in situ* dansylation or glutardialdehyde fixation and Auro dye forte staining [26].

2 Materials and methods

2.1 Chemicals

Acrylamide, *N,N'*-methylenebisacrylamide (Bis), and SDS were obtained from Biomol (Ilvesheim, Germany), *N,N,N',N'*-tetramethylethylenediamine (TEMED), bis(2-hydroxyethyl)imino-tris-(hydroxymethyl)-methane (Bistris), and Coomassie Brilliant Blue G-250 (Serva Blue G, CI 42655, research grade) were purchased from Serva (Heidelberg, Germany), glycerol, urea, ammonium peroxydisulfate (AMPS), *N,N*-bis(2-hydroxyethyl)-glycine (Bicine) H_2SO_4 (Titrisol), diethylamine, trichloroacetic acid (TCA), ammonium sulfate and glutardialdehyde for electron microscopy (No. 4239) from Merck (Darmstadt, Germany), 2-mercaptoethanol and Bromophenol Blue (BPB) from Fluka (Buchs, Switzerland), Tris from J. T. Baker Chemicals (Deventer, Netherlands), and dansyl chloride from Sigma (St. Louis, MO, USA). Sucrose (ultrapure) was obtained from Bethesda Research Laboratories (Gaithersburg, MD, USA). For electroblotting, filter paper 3MM was obtained from Whatman (Springfield Mill, Maidstone, UK), Immobilon PVDF membranes (pore size 0.45 µm) from Millipore (Bedford, MA, USA), NA 45 anion-exchange membranes from Schleicher and Schuell (Dassel, Germany) and Auro dye forte from Janssen Biotech N.V. (Olen, Belgium).

2.2 Preparation of samples

2.2.1 Sample components

The low molecular weight (LMW) marker kit composed of (1) phosphorylase b (M_r 94000), (2) bovine serum albumin (M_r 67000), (3) ovalbumin (M_r 43000), (4) carbonic anhydrase (M_r 30000), (5) soybean trypsin inhibitor (M_r 20100), and (6) alpha-lactalbumin (M_r 14400) was obtained from Pharmacia-LKB (Uppsala, Sweden); (7) bovine trypsin inhibitor (M_r 6500), (8) mellittin (M_r 2847), and (9) Met-Lys-bradykinin (M_r 1320) from Serva were added to the LMW marker kit, and this mixture (1)–(9) was used as M_r marker in subsequent experiments. Further M_r markers were the myoglobin polypeptide kit MW-SDS-17 from Sigma, and porcine ACTH (M_r 4567) and cholecystokinin fragment 28–33 (M_r 785) from Serva. The MW-SDS-17 kit consists of cyanogen bromide cleavage products of horse heart myoglobin, supplemented with intact myoglobin. In a previous paper by Kratzin *et al.* [26], gas phase sequencing, amino acid analysis, and UV laser desorption/ionization mass spectrometry demonstrated that the M_r assigned to the generated myoglobin cleavage fragments by the company are not correct. In this paper we apply the new nomenclature, corrected M_r values and amino acid sequence positions, as given by Kratzin *et al.* [26]: horse heart myoglobin, A, M_r 16900, 1–153; fragment B, M_r 14400, 1–131; fragment C, M_r 10700, 56–153; fragment D, M_r 8200, 56–131; fragment E, M_r 6200, 1–55; fragment F, M_r 2500, 132–153. Generation of fragment C was not considered by the company. Crude protein/peptide preparations were obtained from rat hypothalamus, rat suprarenal gland, and total chick brain as follows: Tissues were homogenized in 2 mL of homogenization buffer (0.268 M Bistris, 0.119 M Bicine, pH 7.6) per g fresh weight. Homogenates were boiled for 15 min, centrifuged for 10 min at 16000 *g*, and the upper third of the supernatant was freeze-dried.

2.2.2 Preparation of nondansylated protein/peptide samples

For electrophoresis, samples were made up in the following sample buffer: 0.359 M Bistris, 0.159 M Bicine, 1.0% w/v SDS, 2.5% v/v 2-mercaptoethanol, 15% w/v sucrose, 0.004% w/v Bromophenol Blue, pH 7.7. For dissolution of lyophilized crude protein/peptide preparations from various tissues, Bicine and Bistris were omitted from the sample buffer and 0.5 mL were added per mL freeze-dried supernatant. All samples were incubated for 10 min at 100°C.

2.2.3 Preparation of dansylated protein/peptide samples

Protein/peptide solutions subjected to dansylation should preferably contain no buffers with primary or secondary amino groups or hydroxyl and SH-groups. 2-Mercaptoethanol only needs to be added after dansylation is completed (because dansylation of proteins/peptides is strongly reduced in the presence of 2-mercaptoethanol). For dansylation 20 µL of aqueous protein/peptide solution were added to 10 µL of dansylation buffer (0.3 M sodium borate, 4% w/v SDS, pH 9.5) and incubated for 5 min at 60°C. Five µL of ice-cold 0.4% w/v dansyl chloride dissolved in acetone were added and incubation was continued for 30 min at 60°C. The reaction was stopped by addition of 5 µL of a 98% diethylamine stock solution [27] and incubation continued for 10 min at 60°C. Finally 40 µL of a twofold concentrated sample buffer (see 2.2.2) were added, followed by another 10-min incubation period at 60°C. Tissues were treated as summarized in Section 2.2.1, except for the homogeniza-

tion in an aqueous 0.9% w/v NaCl solution instead of the Bicine/Bistris buffer. Freeze-dried supernatants were incubated for 5 min at 60°C in a dansylation buffer made up of 0.1 M sodium borate, 1% w/v SDS, pH 9.5. Dansyl chloride (0.4% w/v), diethylamine and twofold concentrated sample buffer (see Section 2.2.2) were added in the same ratios as detailed above.

2.3 SDS-PAGE system

2.3.1 Gel dimensions

SDS-PAGE was performed using the vertical microslab gel system described by Poehling and Neuhoff [28] or a miniaturized version of this system. The gel compartments were arranged according to Neuhoff *et al.* [29]. Gel dimensions were: (i) micro gel system: length 35 mm (separation gel 27 mm, stacking gel 3 mm, comb gel 5 mm), width 26 mm, thickness 0.5 mm. (ii) miniaturized gel system: length 70 mm (separation gel 60 mm, stacking gel 5 mm, comb gel 5 mm), width 45 mm, thickness 0.5 mm.

2.3.2 SDS-PAGE of nondansylated proteins/peptides

Comb gel: 7.5%T, 5%C; 0.359 M Bistris, 0.159 M Bicine, 0.1% w/v SDS, 8.6 mM TEMED, 1.75 mM AMPS, pH 7.7 (for buffer composition *cf.* Appendix 6.2). Stacking gel: 6.0%T, 5%C; 0.4 M Bistris, 0.1 M H_2SO_4, 0.1% w/v SDS, 8.6 mM TEMED, 1.75 mM AMPS, pH 6.7 (for buffer composition *cf.* Appendix 6.2). Separation gel: 12%T, 5%C, or 18%T, 5%C; 0.4 M Tris, 0.1 M H_2SO_4, 0.1% w/v SDS, 0.2 mL 87% glycerol per mL gel solution (21.4% w/v), 4.3 mM TEMED, 1.75 mM AMPS, pH 8.1 (for buffer composition *cf.* Appendix 6.5 a). Instead of glycerol, the separation gel may be made up with 8 M urea. Cathode buffer: 0.2 M Bicine, 0.1 M NaOH, 0.1% w/v SDS, pH 8.2. The cathode buffer has to contain 0.25% w/v SDS if 8 M urea is used as additive in the separation gel instead of glycerol. Anode buffer: 0.2 M Tris, 0.05 M H_2SO_4, pH 8.1.

2.3.3 SDS-PAGE of dansylated proteins/peptides

Anodic buffer, stacking and comb gel are the same as described in Section 2.3.2. The cathodic buffer has to contain 0.25% w/v SDS, and the separation gel buffer is composed of 0.4 M Tris, 0.0456 M H_2SO_4, pH 8.6, instead of 0.4 M Tris, 0.1 M H_2SO_4, pH 8.1 (for buffer composition *cf.* Appendix 6.5 b).

2.3.4 Setting up the gel system

For details concerning the preparation of gel chambers, see [28]. To obtain a homogeneous upper separation and stacking gel surface, water was carefully overlayered after filling the respective gel solutions into the chambers. The separating gel was allowed to polymerize for at least 30 min at room temperature before the stacking gel was added. Stacking and comb gel solutions take about 20 min to polymerize. Sample wells were formed with an appropiate comb inserted into the stacking gel. After comb gel polymerization, the slots were rinsed with comb gel buffer (0.359 M Bistris, 0.159 M Bicine, 0.1% w/v SDS), filled with this buffer, and finally the sample was underlayered. Routinely, 1–2 µL of sample were applied; however, due to the effective stacking, up to 7.5 µL could be applied without loss in resolution (miniaturized gel system, slot width 3 mm). For larger volumes the stacking and comb gel height or the slot width have to be increased.

2.3.5 Running conditions

Mini gel system: 5 mA/gel for 10 min, followed by 7.5 mA/gel for approximately 90 min (12%T separation gel) or approximately 2.5 h (18%T separation gel). Micro gel system: 2.5 mA for 10 min followed by 4 mA for approximately 45 min (12%T separation gel) or approximately 75 min (18%T separation gel). Gels were run at room temperature.

2.4 Gel staining methods

2.4.1 Direct colloidal Coomassie staining

Directly following electrophoresis the gel is transferred into a staining solution prepared as follows [17]: 2 g of 85% H_3PO_4 solution are diluted in approximately 80 mL of double distilled H_2O, and 10 g of ammonium sulfate are added. After the salt is completely dissolved, the solution is adjusted to 98 mL with H_2O, and 2 mL of an aqueous 5% w/v Coomassie Brilliant Blue (CBB) G-250 dye stock solution are added. This stock staining solution can be stored for months. Before use, it has to be shaken vigorously to achieve an even distribution of the colloidal dye particles formed in the presence of ammonium sulfate. The colloidal dye particles are crucial for obtaining a low background [18]; therefore, the staining solution should never be passed through a filter. To obtain the final staining solution, 20 mL of methanol are added to 80 mL of the stock staining solution. The final staining solution is prepared just prior to gel staining and discarded after use. If well-visible colloidal dye particles cannot be observed the staining solution should be discarded. During staining the vessels should be carefully sealed to avoid evaporation of methanol, with only a single gel per staining vessel. No destaining step is required to obtain a clear background. After staining, the gel is only briefly rinsed (max. 1 min) in 25% v/v methanol in water to wash off colloidal dye particles attached to the gel surface and then immersed in 25% w/v ammonium sulfate for fixation of the polypeptide dye complexes [17]. In this solution the gel can be stored without destaining of the polypeptides. For further staining, gels may be transferred back into the staining solution. Thus, stepwise staining [18] with periodic inspection and densitometry is possible with this protocol. Dansylated proteins/peptides may also be stained according to this staining procedure.

2.4.2 Glutardialdehyde fixation and colloidal Coomassie staining

For glutardialdehyde fixation the gels were incubated for 1 h at room temperature in a 0.4 M sodium borate/phosphate fixation buffer, pH 6.2, containing 5% glutardialdehyde. (A borate/phosphate stock buffer was prepared by dissolving 30.91 g boric acid in 800 mL H_2O, adjusting the pH to 6.2 with aqueous 1 M Na_2HPO_4 and filling with H_2O to a final volume of 1 L. Prior to use, the fixation buffer is pre-

pared by mixing 20 mL of an aqueous 25% w/w glutardialdehyde solution, as used in electron microscopy, with 80 mL of the borate/phosphate stock buffer). After fixation, the gels were washed 2 × 10 min in H_2O and stained as detailed in Section 2.4.1. Following incubation for 30 min in 25% w/v ammonium sulfate, gels pretreated with glutardialdehyde should be wrapped in aluminum foil and stored at −70°C because slow but significant destaining was observed on prolonged storage in the ammonium sulfate solution. Gels may be thawed and refrozen several times without noticeable damage to the matrix.

2.5 Detection of dansylated proteins/peptides

By monitoring the fluorescent samples at an excitation wavelength of 365 nm (maximal emission: 520 nm) the separation process can be visualized. Following separation, gels may be either photographed directly under UV-illumination or kept frozen at −70°C in the dark for several days prior to photographic documentation because band spreading due to diffusion was not significant.

2.6 Electroblotting

Following SDS-PAGE, proteins/peptides were electroblotted using the semidry electroblotter SM 17556 from Sartorius (Göttingen, Germany). The blotting buffers were prepared according to Hirano [30]; however, methanol was omitted in all buffers and 0.025% w/v SDS included in the cathodic buffer. The following buffers were used: (A) 0.3 M Tris, pH 10.4 (not adjusted); (B) 25 mM Tris, pH 10.4 (not adjusted); (C) 25 mM Tris, 0.025% w/v SDS, pH 9.0 (adjusted with boric acid). The blotting sandwich was erected from the anode to the cathode with one sheet of filter paper immersed in buffer (A), one sheet of filter paper immersed in buffer (B), a PVDF membrane incubated in buffer (B), the gel washed in buffer (C) for only 1 min, a second PVDF membrane [31] incubated in buffer (C), and then two sheets of filter paper immersed in buffer (C). Prior to incubation in buffer (B) or (C) the PVDF membranes were washed for 1 min in methanol and for 5 min in H_2O. For electroblotting of dansylated proteins/peptides, the PVDF membrane at the cathodic side of the gel may be omitted; at the anodic side an anion exchange membrane (NA 45) preincubated in buffer (B) for 10 min may be used alternatively. The transfer was performed at 1 mA/cm² for 30 min at room temperature.

2.7 Detection of proteins/peptides blotted on PVDF or anion exchange membranes

Proteins/peptides dansylated prior to SDS-PAGE can easily be detected by their fluorescence in anion exchange or PVDF membranes after electroblotting with an increase in detection sensitivity as compared to visualizing the compounds within the gel (see Section 2.5). Nondansylated proteins/peptides electroblotted on PVDF membranes may be stained with Coomassie Brilliant Blue G-250 before subsequent gas phase sequencing [26], detected by *in situ* dansylation [26], or stained with Auro dye forte after glutardialdehyde fixation according to the following procedure: After blotting, the PVDF membranes are washed in a 25 mM borate/phosphate buffer, pH 6.2, for 2 × 5 min; incubated in an 80 mM borate/phosphate fixation buffer, containing 1% glutardialdehyde, pH 6.2, for 30 min; washed in phosphate buffered saline (PBS) for 2 × 5 min; stained with Auro dye forte at 37°C for 1–4 h; washed with distilled water for 5 min and finally air dried. To prepare the borate/phosphate washing and fixation buffers, the borate/phosphate stock and fixation buffers described in Section 2.4.2 were diluted 20- and 5-fold, respectively. The PBS solution was prepared as follows [31]: 8 g NaCl, 0.2 g KCl, 1.44 g $Na_2HPO_4 \times 2H_2O$, and 0.2 g KH_2PO_4 were dissolved in 1000 mL H_2O. To guarantee the high detection sensitivity of this procedure, only high quality filter paper should be used and a second PVDF membrane placed at the cathodic side of the polyacrylamide gel (see Section 2.6) to absorb impurities released from the cathodic layers of filter paper. Gels, sheets of filter paper, and blotting membranes should only be handled by their edges with forceps because material released from gloves gives rise to heavy background staining. For the same reason electrode plates of the semidry electroblotter should be only rinsed extensively with distilled water prior to blotting and not be rubbed with gloves. For further details on clean working conditions see [31].

3 Results

3.1 Electrophoresis of dansylated proteins/peptides

Figures 1a–c demonstrate the stacking process for different loading volumes of a dansylated protein/peptide tissue sample from total chick brain. After 30 s (Fig. 1a), 5 min

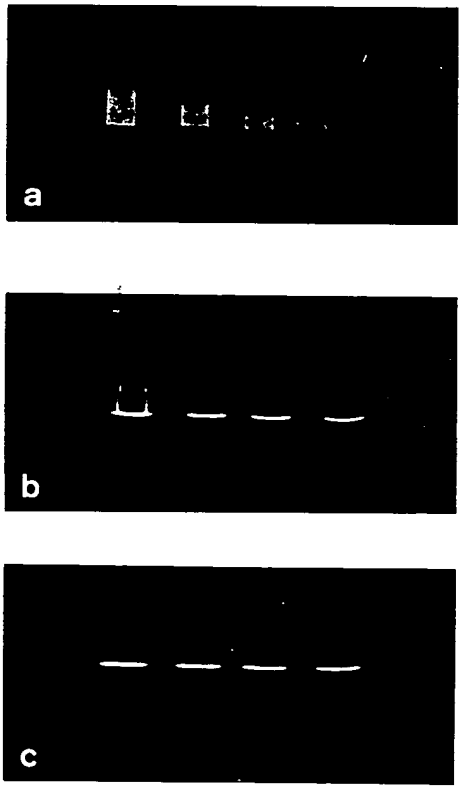

Figure 1. Stacking of protein/peptide samples by the new discontinuous buffer system. From left to right 5, 2.5, 1, and 0.5 µL of a dansylated crude protein/peptide preparation from total chick brain were applied to the sample wells of a vertical minislab gel. Photographs taken after (a) 30 s, (b) 5 min, and (c) 10 min of electrophoresis.

(Fig. 1b), and 10 min (Fig. 1c) of electrophoresis the gel was photographed. In Fig. 1b the sample zone had just reached the second third of the stacking gel (height: 5 mm). Note the pronounced lateral trailing effect in sample wells with a higher sample volume, *i.e.* filling height, as a result of diffusion of part of the sample into the adjoining comb gel. At the same starting level, sample molecules migrating in adjacent gel areas were more retarded than in the middle of the slot under conditions of free electrophoretic mobility. After 10 min this initial effect was compensated (Fig. 1c) and the components were completely stacked in a sharp starting zone before entering the separation gel.

The overall M_r distribution of the tissue sample relative to the myoglobin polypeptide marker kit MW-SDS-17 is shown in Fig. 2. The largest proteins present had an M_r of at least 90 000 as estimated relative to the LMW marker kit (data not shown). Figure 2 demonstrates the complete destacking of dansylated sample components with an M_r < 1000, run in a separation gel composed of 15%T, 5%C and 21.4% w/v glycerol. In lane (a) several peptides, present in the total chick brain preparation, with an apparent M_r < 785, were set free from the moving boundary, and in lanes (a)–(d) at the lower gel end even dansyldiethylamine became destacked. At the present pore size, small polypeptides such as Met-Lys-bradykinin, myoglobin fragment F, and the cholecystokinin fragment 28–33 had only slightly different R_f values. The atypical electrophoretic mobilities of porcine ACTH and myoglobin fragment E in the present system were also observed when we applied the gel systems described by Swank and Munkres [10], with 8 M urea added to the separation gel, or the SDS-PAGE system of Anderson *et al.* [11]. In each case, dansylated porcine ACTH was much more retarded than predicted by its M_r, with the opposite applying to dansylated myoglobin fragment E.

To estimate the detection limit for dansylated proteins/peptides, a dilution series of the MW-SDS-17 marker kit was run in the vertical microslab gel system with the new multiphasic buffer system. The separation gel was composed of 15%T, 5%C and 8 M urea. Approximately 3 ng of a single dansylated protein/peptide could be detected, which corresponds to the detection sensitivity obtained for dansylated Met-Lys-bradykinin or melittin (Fig. 3). The microslab gel dimensions were found to be sufficient for effective employment of the present multiphasic buffer system because destacking is completed after a separation gel length of only 10 mm. Separation of dansylated proteins/peptides from various biological materials did not critically depend on the concentration of glycerol or urea in the gels but was greatly influenced by the ionic strength of the trailing phase and by the presence or absence of SDS during dansylation. In contrast to SDS loading prior to dansylation (Section 2.2.3), the reverse procedure, *i.e.* omitting SDS in the dansylation buffer, led to pronounced trailing of small dansylated polypeptides in the separation gel or their complete insolubility.

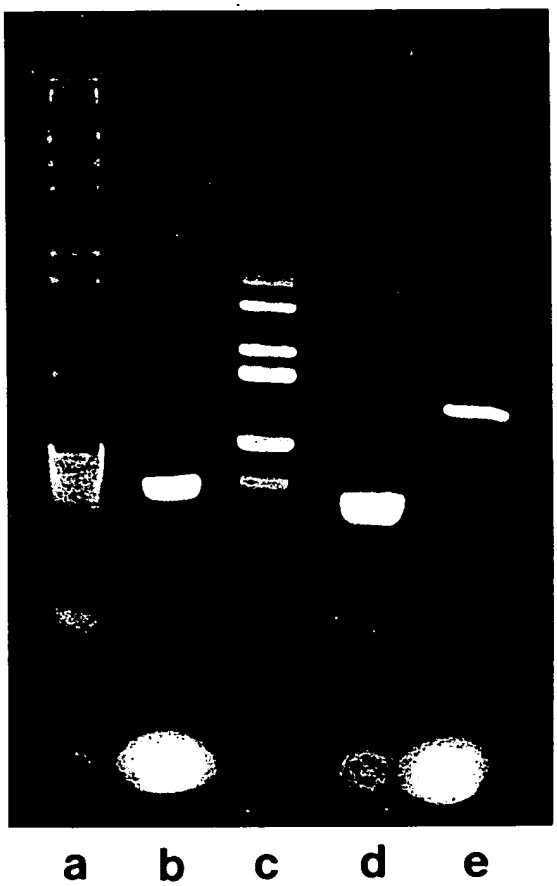

Figure 2. SDS-PAGE of dansylated proteins/peptides with the new multiphasic buffer system. The separation gel was composed of 15%T, 5%C, 21.4% w/v glycerol (minigel version). From left to right: (a) crude protein/peptide preparation from total chick brain, (b) 150 ng Met-Lys-bradykinin (M_r 1320), (c) 600 ng of myoglobin polypeptides A–F (MW-SDS-17), (d) 150 ng cholecystokinin fragment 28–33 (M_r 785), and (e) 100 ng porcine ACTH (M_r 4567).

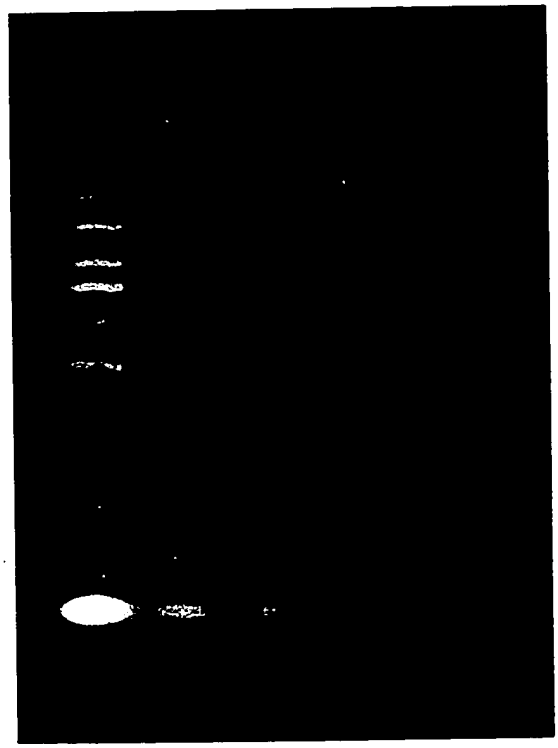

Figure 3. Dilution series of dansylated myoglobin polypeptides A–F (MW-SDS-17) run in the vertical microslab gel system with the new multiphasic buffer system. The separation gel was composed of 15%T, 5%C, 8 M urea. From left to right a total amount of 250 ng, 125 ng, 62.5 ng, 31.2 ng, and 15.6 ng per lane was applied.

A twofold reduction of the separation gel molarity of both Tris and H_2SO_4, *i.e.* approximately halving the ionic strengths of Bicine and Tris in the trailing phase during separation (*cf.* Appendix 6.5b), resulted in increased trailing and irregular banding patterns of proteins/peptides dansylated according to the standard procedure. For a given separation gel composition, the resolving power of the gel system is superior for nondansylated as compared to dansylated proteins/peptides (compare Figs. 2 and 11) due to more pronounced band broadening during separation in the latter case.

3.2 Electroblotting of dansylated proteins/peptides

A mixture of myoglobin polypeptides A–F (MW-SDS-17 kit) plus cholecystokinin 28–33 was dansylated, separated by SDS-PAGE and electroblotted for 90 min at 1.6 mA/cm² into anion-exchange or PVDF membranes as described in [25]. The polypeptides may also be dansylated, separated, and electroblotted according to the present paper; however, in contrast to the standard protocol (Section 2.6) electroblotting should be performed for 90 min at 1 mA/cm² to remove the dansylated compounds completely from the gels, as judged by their fluorescence. Dansylated myoglobin polypeptides A–F were effectively immobilized in NA 45 anion-exchange membranes, whereas for cholecystokinin 28–33 a severe loss was observed, which could be detected in a PVDF control membrane underlayered the detection membrane at the anodic side. In PVDF detection membranes, myoglobin polypeptides A–F and cholecystokinin 28–33 were immobilized with approximately the same efficiency, with a significant loss of all compounds, demonstrated by a PVDF control membrane. Due to a concentration of electroblotted bands within the ultrathin PVDF or anion-exchange membranes, the detection limit for dansylated myoglobin polypeptides A–F could be lowered to about 1 ng/band (results not shown). Binding to PVDF membranes mainly depends on hydrophobic interaction and the increased hydrophobicity of dansylated proteins/peptides improves their immobilization. In the case of anion-exchange membranes the negatively charged SDS protein/peptide complexes will be mainly bound by ionic interaction.

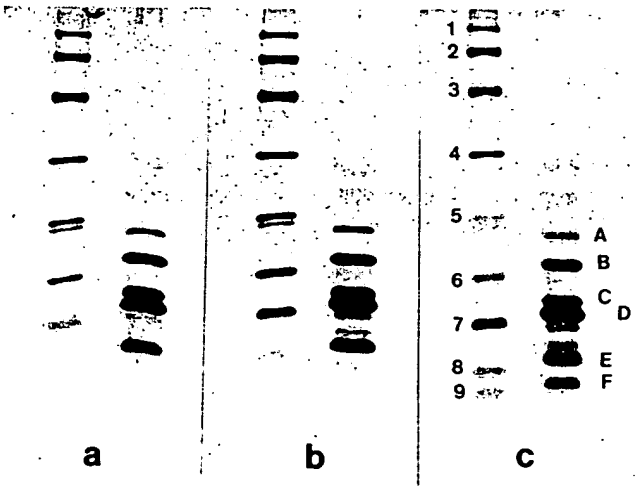

Figure 4. SDS-PAGE of M_r standards (1)–(9) and myoglobin polypeptides A–F (MW-SDS-17) with the new multiphasic buffer system. The separation gel was composed of 12%T, 5%C, 21.4% w/v glycerol. Visualization by (a) 1 h fixation in 10% w/v TCA and colloidal Coomassie staining, (b) direct colloidal Coomassie staining, and (c) glutardialdehyde fixation followed by colloidal Coomassie staining.

3.3 Fixation and Coomassie staining of nondansylated proteins/peptides

In contrast to peptides prelabeled with a fluorochrome prior to separation, detection of nondansylated peptides following electrophoresis was problematic because the compounds could not be fixed in the gel matrix prior to standard staining procedures with such commonly used acid precipitants as acetic acid, sulfosalicylic acid, or TCA. Figure 4 shows a separation of M_r markers (1)–(9) and myoglobin polypeptides A–F (MW-SDS-17) in a 12%T gel followed by: (i) 1 h fixation in 10% w/v TCA and colloidal Coomassie staining, (ii) direct colloidal Coomassie staining, and (iii) glutardialdehyde pretreatment followed by colloidal Coomassie staining. During TCA "fixation", loss of small polypeptides (Met-Lys-bradykinin > myoglobin fragment F > melittin > bovine trypsin inhibitor) was inversely correlated to their M_r. This also applied to direct colloidal staining, but with a shift in immobilization efficiency to lower M_rs: bovine trypsin inhibitor was effectively immobilized, myoglobin fragment F was detectable, and only Met-Lys-bradykinin was completely lost. By contrast, all M_r markers were detected after glutardialdehyde pretreatment of the gels followed by colloidal Coomassie staining, and the intensity by which small polypeptides were stained no longer seemed to be closely correlated to M_r.

To further investigate the effect of glutardialdehyde pretreatment on small polypeptides, Met-Lys-bradykinin was incubated in glutardialdehyde-containing buffers prior to electrophoresis (Fig. 5). Preincubation with glutardialde-

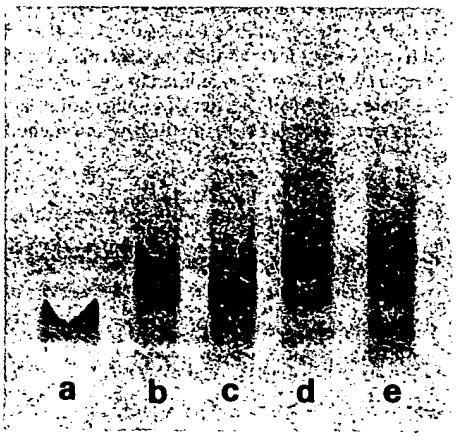

Figure 5. SDS-PAGE of Met-Lys-bradykinin incubated prior to electrophoresis in the presence of 0.08% glutardialdehyde in (b) 0.1 M sodium citrate, pH 4.0, (c) 0.1 M sodium citrate, pH 6.0, (d) 0.1 M sodium borate, pH 8.0, and (e) 0.1 M sodium borate, pH 10.0. The new multiphasic buffer system was applied. The separation gels were 20%T, 5%C, containing 21.4% w/v glycerol. For preincubation, 5 µL of an aqueous 5% w/v solution of Met-Lys-bradykinin were added to 20 µL of buffers (b)–(e), vigorously shaken for 1 min immediately afterwards, left at room temperature for 1 h, and made up to 50 µL by the addition of 25 µL sample buffer. After 10 min incubation at room temperature, 500 ng of Met-Lys-bradykinin were applied per slot. Lane (a) was loaded with 100 ng of unmodified Met-Lys-bradykinin dissolved in sample buffer.

hyde induced a polymer formation of Met-Lys-bradykinin, most effective in the presence of borate at pH values of 8.0 and 10.0. To study the pH dependency of glutardialdehyde fixation within the gel matrix, Met-Lys-bradykinin was electrophoresed and incubated for 1 h at room temperature in different buffers containing glutardialdehyde (Fig. 6). Below pH 3.0, Met-Lys-bradykinin was not immobilized in the gel. On incubation in a borate buffer (Fig. 6j) or 10% w/v TCA (Fig. 6i), without glutardialdehyde, the polypeptide almost completely leached from the gel. We observed a broad plateau between pH 4–7 (Fig. 6c–f) with a steep increase in staining intensity at pH 8.0 (Fig. 6g). As borate buffers were used in (g) and (h), in contrast to citrate and phosphate buffers in (a)–(f), this effect may be more related to the change in buffer composition than pH variation. Irrespective of the pH value tested, fixation by glutardialdehyde was more effective for borate than for phosphate buffers (Fig. 7), with a pH optimum for borate around pH 6.0. To improve the buffering capacity of the borate buffer (pK 9.2), in subsequent experiments the pH was titrated with 1 M Na_2HPO_4 instead of the NaOH used so far (Fig. 4–7). The comparatively low amount of phosphate had no adverse effect on fixation, with the best signal/noise ratio at pH 6.2.

By varying the glutardialdehyde concentration, a concentration of 5% was shown to be adequate. Higher concentrations did not improve fixation significantly and above 15% the polyacrylamide matrix was damaged. The conditions of glutardialdehyde fixation were not optimized with regard to reaction temperature and reaction time. For gels of 0.5 mm thickness, incubation for 1 h at room temperature was

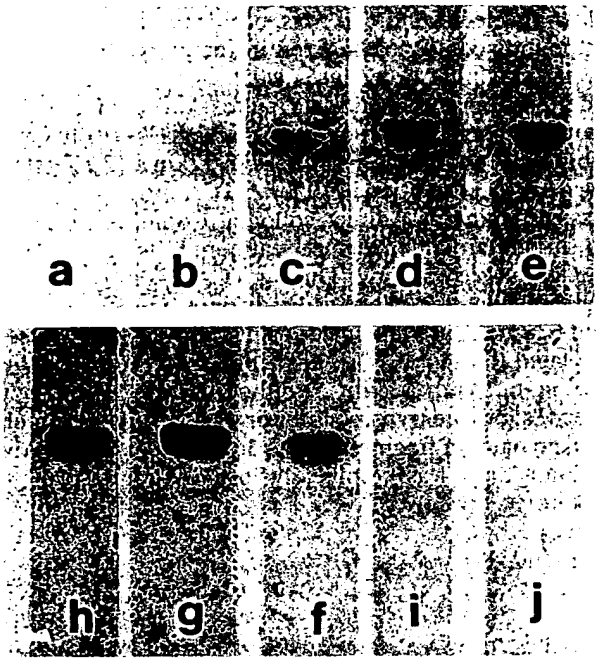

Figure 6. Effect of buffer pH and buffer composition on glutardialdehyde fixation of Met-Lys-bradykinin. Met-Lys-bradykinin (300 ng/lane) was run in a minigel using the new multiphasic buffer system. The separation gel was made up of 12%T, 5%C, containing 21.4% w/v glycerol. Following SDS-PAGE the lanes were cut out and incubated for 1 h at room temperature in the presence of 0.5% glutardialdehyde in 0.25 M NaH_2PO_4, (a) pH 2.0 and (b) pH 3.0, 0.25 M sodium citrate, (c) pH 4.0 and (d) pH 5.0, 0.25 M Na_2HPO_4, (e) pH 6.0 and (f) pH 7.0, 0.25 M sodium borate, (g) pH 8.0 and (h) pH 9.0, respectively. Lanes (i) and (j) were incubated in 10% w/v TCA and 0.25 M sodium borate buffer, pH 8.0, respectively, with no glutardialdehyde added. The gel slices were washed 2 × 10 min in H_2O and stained with colloidal Coomassie.

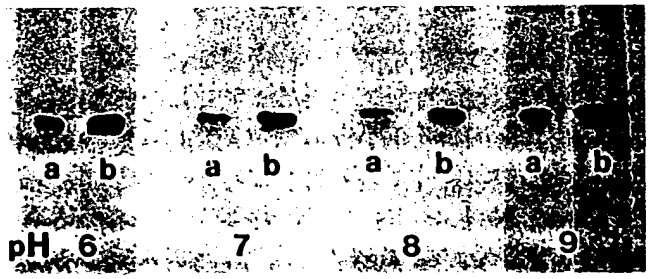

Figure 7. Glutardialdehyde fixation of polypeptides in dependence on the buffer ion applied. Met-Lys-bradykinin (150 ng/lane) was run in a minigel using the new discontinuous buffer system. The separation gel was 12%T, 5%C, containing 21.4% w/v glycerol. Following SDS-PAGE the lanes were excised and incubated for 1 h at room temperature in (a) 0.4 M Na_2HPO_4 buffers at pH 6.0, 7.0, 8.0, and 9.0, or in (b) 0.4 M sodium borate buffers at pH 6.0, 7.0, 8.0, and 9.0, respectively. All buffers contained 0.5% glutardialdehyde. The lanes were washed 2 × 10 min with H_2O and stained with colloidal Coomassie.

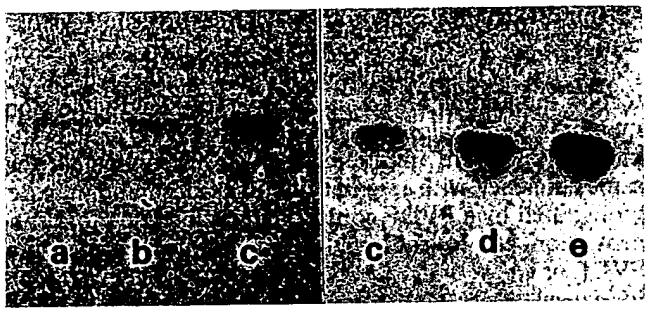

Figure 8. Dilution series of Met-Lys-bradykinin run in a 12%T, 5%C, 21.4% w/v glycerol separation gel (minigel version, new multiphasic buffer system), fixed with glutardialdehyde and stained with colloidal Coomassie for 8 h. Amounts of sample were: (a) 7.5 ng, (b) 15 ng, (c) 30 ng, (d) 60 ng, (e) 120 ng.

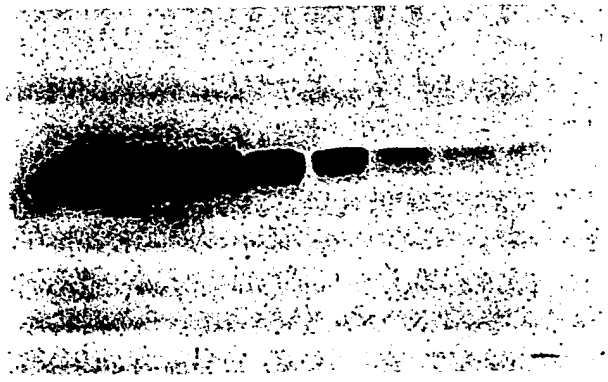

Figure 9. Dilution series of Met-Lys-bradykinin run in a 12%T, 5%C, 21.4% w/v glycerol separation gel (minigel version, new multiphasic buffer system) and electroblotted onto a PVDF membrane (see Section 2.6) subsequent to SDS-PAGE. Following electroblotting the membrane was glutardialdehyde-fixed and stained with Auro dye forte for 2 h at 37°C (see Section 2.7). Samples from left to right: 100 ng, 50 ng, 25 ng, 12.5 ng, 6 ng, 3 ng, 1.5 ng, 0.75 ng. As checked by glutardialdehyde fixation and colloidal Coomassie staining of the gel, the Met-Lys-bradykinin was completely transferred into the PVDF membrane.

adequate. Background staining after glutardialdehyde fixation and colloidal Coomassie staining was slightly more pronounced as compared to direct colloidal Coomassie staining; however, due to the colloidal staining principle applied [13, 18], a destaining step could be omitted in both cases. The detection limit of colloidal Coomassie staining after glutardialdehyde fixation for small polypeptides was determined for a dilution series of Met-Lys-bradykinin (Fig. 8). Approximately 15 ng could be detected in the gel and about 7.5 ng on the photograph after 8 h staining time. Similar detection limits were found for other small polypeptides, such as melittin or porcine ACTH. Staining for only 90 min instead of 8 h yields a detection limit of 30 ng.

3.4 Detection of nondansylated proteins/peptides after electroblotting

Alternatively to fixation and staining of the gel, the SDS protein/peptide complexes may be detected after electroblotting into PVDF membranes by Auro dye forte staining. As opposed to the original method [31] Tween 20 had to be omitted in the initial washing step (see Section 2.7), because small polypeptides were completely washed out of the membrane by the nonionic detergent. With this modification, small polypeptides could be retained but were progressively washed out during staining, because the commercial stain contains Tween 20, added by the company to stabilize the colloidal gold particles. To immobilize small polypeptides in PVDF membranes during staining with Auro dye forte the electroblotted compounds were pretreated with 1% glutardialdehyde in a borate/phosphate fixation buffer (see Section 2.7). As a result of these modifications, staining intensities of polypeptides with M_rs down to approximately 1000 progressively increased with staining time, and in spite of slightly increased background staining, as compared to the original protocol [31], 0.75 ng of Met-Lys-bradykinin could be detected after staining for 2 h (Fig. 9). Separation of M_r markers (1)–(9) and myoglobin polypeptides A–F by SDS-PAGE using the new multiphasic buffer system followed by electroblotting into PVDF membranes and staining with Auro dye forte, according to the modified procedure (Fig. 10), showed that concentrations of single polypeptides should not exceed 50–100 ng per band, since smearing of overstained bands contributes to background staining. Among the polypeptides studied, horse heart myoglobin (Fig. 10, lane b, A) and melittin (Fig. 10, lane a, 8) yielded the lowest staining intensities. Proteins/peptides electroblotted into anion exchange membranes cannot be visualized with Auro dye forte because of the heavy background, due to ionic binding of the negatively charged colloidal gold particles to the positively charged diethylaminoethyl groups of the membrane.

3.5 Electrophoresis and molecular mass estimation of nondansylated proteins/peptides

Figure 11 shows the high resolution separation, of M_r markers (1)–(9) and of rat suprarenal gland and hypothalamus samples, obtained by SDS-PAGE with the new multiphasic buffer system, followed by glutardialdehyde fixation

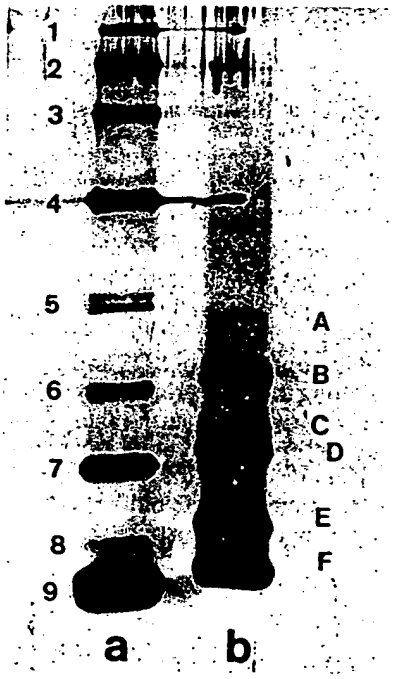

Figure 10. SDS-PAGE of (a) M_r markers (1)–(9) and (b) myoglobin polypeptides A–F, run in a 12%T, 5%C, 21.4% w/v glycerol separation gel (minigel version, new multiphasic buffer system) followed by electroblotting into a PVDF membrane (see Section 2.6). The membrane was pretreated with glutardialdehyde and stained with Auro dye forte for 2 h at 37°C (see Section 2.7). Only 50–100 ng of single protein/peptide were applied. As checked by glutardialdehyde fixation and colloidal Coomassie staining of the gel, all proteins/peptides except phosphorylase b and bovine serum albumin were completely transferred into the PVDF membrane.

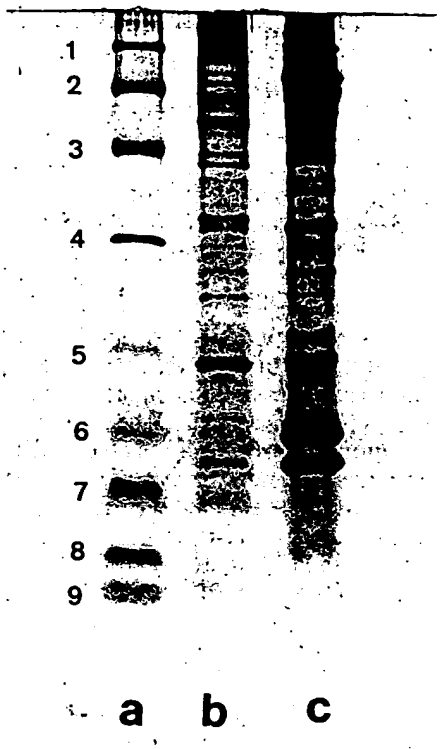

Figure 11. SDS-PAGE of: (a) M_r markers (1)–(9), (100 ng each), (b) rat hypothalamus crude protein/peptide preparation, (c) rat suprarenal gland crude protein/peptide preparation. The new multiphasic buffer system was applied. The separation gel was composed of 12%T, 5%C, 21.4% w/v glycerol (minigel version). Following SDS-PAGE the gel was pretreated with glutardialdehyde and stained with colloidal Coomassie.

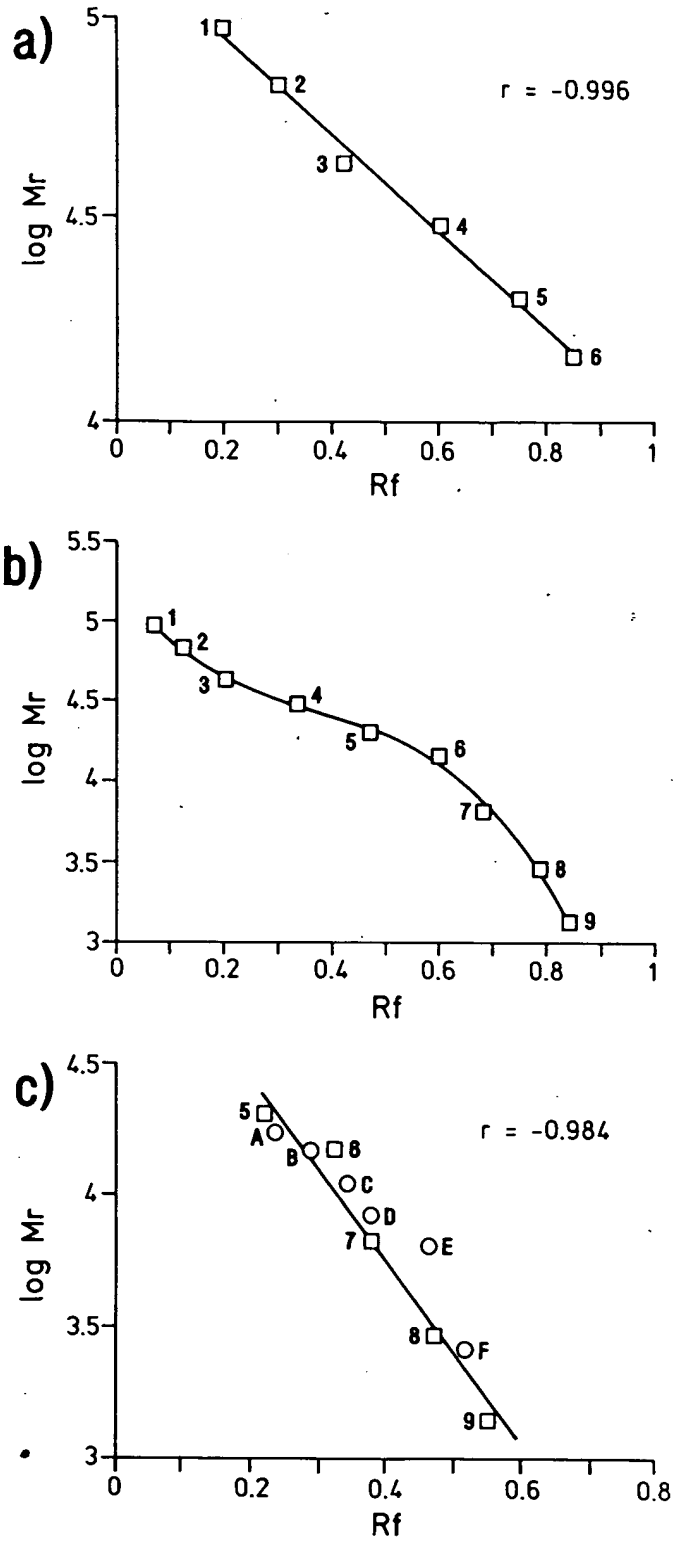

Figure 12. Plots of log M_r *versus* R_f for (a) M_r markers (1)–(6) (M_r range *ca.* 100 000–14 400, relative mean M_r prediction error 4.1%), (b) M_r markers (1)–(9) (M_r range *ca.* 100 000–1000), (c) M_r markers (5)–(9) and myoglobin polypeptides A–F (M_r range *ca.* 20 000–1000, relative mean M_r prediction error 18.8%). Apparent M_rs were obtained by linear regression lines (a, c) or a third-order polynomial (b). The relative M_r prediction error was defined as apparent $-M_r-$actual $M_r-\times$ actual $M_r^{-1} \times 100\%$. R_f measurements refer to SDS-PAGE of nondansylated polypeptides and are relative to moving boundary[29]. The separation gels were composed of (a) 9%T, (b) 12%T, and (c) 18%T, and 5%C, 21.4% w/v glycerol each (minigel version, new multiphasic buffer system). Gels were glutardialdehyde-fixed and stained with colloidal Coomassie.

and colloidal Coomassie staining. A 12%T separation gel is recommended for a first screening of a complex protein/peptide pattern within the M_r range of 100 000–1000. Such a gel will also tolerate higher sample loads than narrower pore size gels. However, the relationship between log R_f and M_r for the whole M_r range is sigmoidal, with an inflection point at about M_r 20 000 (Fig. 12b). Linear plots of M_r *versus* log R_f can only be obtained for distinct M_r ranges, *e.g.* for M_r 100 000–14 400 in 9%T, 5%C separation gels (Fig. 12a) or for M_r 20 000–1000 in 18%T, 5%C separation gels (Fig. 12c). The relative mean M_r prediction error (Fig. 12) in the M_r 20 000–1000 range was 18.8% with a standard deviation of ± 12.7%. Separation in presence of 8 M urea or application of different SDS-PAGE systems [10, 11] did not improve the validity of the M_r estimates in this range. By contrast, the relative mean M_r prediction error in the M_r 100 000–14 400 range was only 4.1%, with a standard deviation of ± 3.9%. Deviations between actual and predicted M_rs were most pronounced for alpha-lactalbumin, porcine ACTH (not included in Fig. 12a–c), and myoglobin fragment E, irrespective of whether they were separated as dansylated or nondansylated polypeptides. The atypical fast migration of alpha-lactalbumin was not observed in the 9%T separation gel (Fig. 12a); however, it became prominent when the impact of pore size on electrophoretic mobility was increased (Fig. 12b, c). This finding is probably due to an atypical K_r value of the alpha-lactalbumin-SDS complex, but construction of Ferguson plots for SDS-loaded proteins/peptides will be necessary to confirm this assumption.

4 Discussion

4.1 Physicochemical properties of the new multiphasic buffer system

4.1.1 General remarks

The precise physicochemical properties of the ionic system, as given by the equations in the Appendix, refer only to the native buffer system, since they are not valid *a priori* in the presence of SDS or additives. A full theoretical treatment would have to consider an incorporation of SDS and glycerol into the buffer system, along the lines proposed by Schafer-Nielsen and Svendsen [9]. However, a partial analysis of the new native multiphasic buffer system is sufficient to discuss its essential physicochemical properties in comparison with those of other native multiphasic buffer systems commonly used in SDS-PAGE and to illustrate the effect of two different counterions applied in the stacking and separating gels. In addition, sufficient empirical evidence [32] indicates that multiphasic buffer formulas originally designed for native PAGE can also be applied successfully to SDS-PAGE as long as the system accounts for the specific electrophoretic properties of SDS-protein/peptide complexes.

4.1.2 Stacking

In the present case Bicine was selected as trailing ion and a discontinuity was introduced between the stacking and sep-

arating gel with regard to the common ion: Bistris was applied in the stacking gel and Tris within the separating gel. Due to the "retrograde regulation" function of multiphasic buffer systems [1], this allowed us to establish great differences between trailing ion net mobilities in the stacking and separating gel at appropriate buffer values and ionic strengths within the generated electrophoretic phases. At a leading phase pH of 6.5 and a trailing phase pH of 7.6 in the stacking gel the corresponding relative trailing ion net mobility ($\bar{r}_1^{\varepsilon}$) is −0.11. This equals the minimum trailing ion net mobility during stacking that can be realized by multiphasic buffer formulas using Tris as common and glycine as trailing ion [6, 33]: $\bar{r}_1^{\varepsilon} = -0.091$, which is well below the lower stacking limit for SDS-protein complexes determined empirically as $r = -0.3$ by Wyckoff, Rodbard, and Chrambach [32]. By contrast, the desirable lower stacking limit for native acidic proteins approximates $r = -0.05$. As the present stacking system offers a minimum trailing ion net mobility of $\bar{r}_1^{\varepsilon} = -0.075$ at a trailing phase pH of 7.4 (see Appendix 6.2), a slightly modified version of the new buffer system may also be well suited for native PAGE of acidic proteins/peptides.

Using different common ions in the stacking and separating gel makes it possible to establish a great difference in trailing ion net mobilities between the two gel compartments, but may generate an additional moving boundary between the two common ions applied. Among other criteria, Bistris was selected as common ion in the stacking gel, thereby avoiding a moving boundary, ($mB^{\varepsilon\beta}$), with Tris as trailing and Bistris as leading ion, migrating opposite to the moving boundary between Bicine and SO_4^{2-} ($mB^{\alpha\beta}$) (see Appendix 6.3). Formation of a moving boundary is associated with a steep voltage gradient across the moving boundary, *i.e.* low conductivity in the trailing and high conductivity within the leading phase. However, because the moving boundary $^{\varepsilon\beta}$ is not generated, Tris migrates into phase $^{\beta}$ instead of the low conductivity trailing phase $^{\varepsilon}$. Due to the high conductivity of phase $^{\beta}$, the velocity of Tris ($V_4^{\beta} = 27.42 \times 10^{-5}$ cm s^{-1}) is slow compared to that of moving boundary $^{\alpha\beta}$ ($V^{\alpha\beta} = -80.2 \times 10^{-5}$ cm s^{-1}), which moves down at least 74.5% of the stacking gel height before it fuses with Tris (see Appendix 6.4.1–6.4.3). This results in adjoining phases with more than only one common component, *i.e.* Bistris and Tris, which means that the physicochemical properties of the trailing (Bicine + Tris + Bistris) and leading phase (Tris + Bistris + SO_4^{2-}) cannot be predicted by the present approach (see Appendix 6.4). If desired, a quantitative analysis can be obtained with the theory of telescope and snow electrophoresis [9]. Stacking of dansylated proteins/peptides was not adversely affected in the remaining 25.5% of the stacking gel (Fig. 1c). We did not visualize the stacking of acidic proteins/peptides on the remaining 25.5% of stacking gel during native PAGE; however, in contrast to SDS-PAGE a partial destacking may occur, as some sample components will have mobilities much closer to the lower stacking limit. (For native PAGE the restrictivity of comb and stacking gel should be reduced. Good results were obtained with gels composed of 5%T, 20%C). If we assume that the velocity of moving boundary$^{\alpha\beta}$ is not modified significantly on the remaining 25.5% of total stacking gel length (5 mm), and if we neglect the anionic detergent, it should enter the separating gel after 10.4 min, which is in good agreement with the 11 min determined empirically.

Due to the "retrograde regulation" function [1] of multiphasic buffer systems, the trailing-phase steady-state concentrations of Bistris and Bicine will be attained in the stacking gel, as predicted in Appendix 6.2. The calculated trailing phase composition is set up independently of the comb gel molarity in Bicine and Bistris; however, the time necessary to achieve this steady state condition is minimized in the present case because comb gel, applied sample, and trailing phase$^{\varepsilon}$ are composed identically with regard to Bicine and Bistris. Polymerization of a comb gel on top of the stacking gel [29] allows Bicine to enter the stacking gel at all points at the same time. Moving boundary$^{\alpha\beta}$ is formed as a straight line, which is not the case if the wells are formed in the stacking gel. In the latter case the optimized starting position would only result if the wells were filled to the top with stacking gel buffer, containing the sample, and if the upper electrophoresis buffer was composed equivalent to the trailing phase being generated. The extra effort of polymerizing a comb gel is especially justified if larger sample volumes have to be applied because lateral streaking or bending in one-dimensional SDS-PAGE can thus be completely avoided.

4.1.3 Destacking

As moving boundary$^{\alpha\beta}$ enters the separation gel a new trailing phase (phase$^{\gamma}$) is created, with Tris instead of Bistris as common ion. Proteins/peptides are separated at a trailing phase pH$^{\gamma}$ of 8.5, a relative trailing ion net mobility of $\bar{r}_1^{\gamma} = -0.413$, and an ionic strength of $(\frac{\Gamma}{2})^{\gamma} = 0.0954$ M (see Appendix 6.5.1). As separation takes place at comparatively high ionic strengths, moving boundary $^{\gamma\nu}$ creates a sharp refraction line within the separation gel. This refraction line may serve as a precise reference for R_f measurements at pore sizes where Bromophenol Blue already becomes destacked (> 9%T, 5%C). The high ionic strength attained favors the separation of hydrophobic compounds, makes the system insensitive to the extraneous salt content of samples, and improves band sharpening, as long as the extra heat generated is adequately dissipated.

Representative for multiphasic buffer formulas which use glycine as the trailing and Tris as the common ion, the physicochemical parameters of the system of Ornstein and Davies are used [6, 7]: pH$^{\gamma} = 9.43$, $\bar{r}_1^{\gamma} = -0.236$, and $(\frac{\Gamma}{2})^{\gamma} = 0.0153$ M. The data are taken from a computerized analysis of the system [3]. At separation gel concentrations, which do not impose difficulties in the control of polymerization, small polypeptides are not destacked at the relative trailing ion net mobility of glycine. In contrast, the trailing ion net mobility of $\bar{r}_1^{\gamma} = -0.413$, achieved by the new buffer system, is sufficient to destack Met-Lys-bradykinin (M_r 1320) and even Bromophenol Blue in separation gels composed of 12%T, 5%C. For the separation of dansylated proteins/peptides, the trailing ion net mobility of Bicine was further increased and the corresponding trailing phase values are pH$^{\gamma} = 8.84$, $\bar{r}_1^{\gamma} = -0.521$, and $(\frac{\Gamma}{2})^{\gamma} = 0.0548$ M (see Appendix 6.5.2). At a trailing ion net mobility of $\bar{r}_1^{\gamma} = -0.521$ and a gel concentration of 15%T, 5%C, even dansyldiethylamine becomes destacked (Fig. 2), clearly resolved from Bromophenol Blue, and migrates interposed between the dye and moving boundary$^{\gamma\nu}$.

4.2 SDS-PAGE of dansylated proteins/peptides

Dansylated peptides with M_rs even below 1000 are completely destacked and detected with high sensitivity, which may be further increased by electroblotting the compounds into ultrathin membranes; therefore this method may serve as a second analytical dimension to reversed phase high performance liquid chromatography (HPLC) and should be of particular value in protein chemistry when hydrophobic low M_r cleavage products of proteins are expected. In terms of resolving power and detection sensitivity the present discontinuous buffer system for dansylated proteins/peptides is superior to the homogeneous buffer formulation of Talbot and Yphantis [23], who achieved a detection limit of 10 ng for dansylated polypeptides separated by SDS-PAGE, as compared to 3 ng after electrophoresis and 1 ng after electroblotting in the present system. Irrespective of the separating gel concentration and nature of additive (glycerol, urea) applied, broadening of bands during separation was more pronounced for dansylated than for nondansylated proteins/peptides. This may be due to hydrophobic interaction with the polyacrylamide matrix, and a variable extent of side group (Lys, Tyr) dansylation, *i.e.* a more heterogeneous band composition.

4.3 SDS-PAGE of nondansylated proteins/peptides: Detection methods

4.3.1 Glutardialdehyde fixation

Small polypeptides, not prelabeled prior to separation, are frequently lost by conventional staining methods as a result of leaching during "fixation" (see Fig. 4a). *In situ* polymerization with glutardialdehyde at near neutral pH values, in the presence of borate, significantly improves the fixation of small polypeptides (Fig. 4c). Glutardialdehyde is a potent bifunctional cross-linking reagent, producing soluble and insoluble covalently linked protein polymers at both low (*ca.* 0.1%) and high (*ca.* 5%) concentrations [34]. Mainly free α-amino groups of *N*-terminal amino acids and ε-amino groups of lysine react with the two aldehyde groups of glutardialdehyde [35]. The reaction of glutardialdehyde with some free amino acids, such as glycine, gives colored derivatives, including substances of high M_r; therefore Avrameas and Ternynck [35] suggest that the reaction proceeds beyond the stage of a simple Schiff base formation, probably producing cyclic reaction compounds. The optimal polymerization pH in free solution varies from protein to protein; however, the reaction is significantly inhibited at values below pH 3.0 (see Fig. 6). According to Weston and Avrameas [36] the optimal pH values to link glutardialdehyde to free amino or amide groups, present in polyacrylamide beads, and to couple the proteins to the activated matrix, are pH 6.7 and 7.7, respectively. For the immobilization of Met-Lys-bradykinin in polyacrylamide gels by glutardialdehyde in the presence of borate we determined a pH optimum of 6.2. Within the pH range of 6–9, glutardialdehyde/borate fixation buffers were more effective than phosphate buffers. The reason for this difference in fixation efficiency, in dependence of the buffer ion used, will remain unclear without further experiments. We have neither investigated whether polypeptides are mainly immobilized by formation of insoluble oligomers or by covalent attachment to the polyacrylamide matrix *via* glutardialdehyde, nor have we determined to what extent effective fixation of small polypeptides depends on the number of lysine residues present.

4.3.2 Colloidal Coomassie staining

Recently Neuhoff *et al.* [18] described sensitive background-free staining of polyacrylamide gels with CBB G-250, utilizing the colloidal properties of the dye in the presence of ammonium sulfate. The present staining procedure is identical with an improved version [17] of the original method. Due to the addition of 20% v/v methanol to the staining solution, and higher concentrations of ammonium sulfate, the new method combines the advantages of much shorter staining time and complete staining of bands throughout the entire cross section of the gel with the high sensitivity and background-free staining of the original procedure. The colloidal Coomassie stain should be combined with the glutardialdehyde pretreatment of gels if polypeptides below approximately M_r 6000 are expected, since small polypeptides diffuse out of the gel matrix before they are immobilized as stable polypeptide-dye complexes by the colloidal Coomassie stain alone. For staining of proteins and polypeptides with $M_r > 6000$, direct colloidal staining may be preferred because this method yields a lower background and higher staining intensities. The present fixation buffer (see Section 2.4.2) turns yellow within 30 s after incubation of gels containing glycine, resulting in slightly increased background staining, probably caused by high molecular weight reaction products [35] of glycine and glutardialdehyde. Similarly, a reaction of glutardialdehyde with Tris might explain the slightly increased background of Bicine/Tris separating gels after glutardialdehyde fixation and colloidal Coomassie staining, as compared to gels directly stained with colloidal Coomassie. In contrast to Tris, the tertiary amine Bicine will not be involved in the reaction.

4.3.3 Colloidal gold staining of electroblotted proteins/peptides

For high sensitivity staining with Auro dye forte of small polypeptides electroblotted into PVDF membranes, the nonionic detergent Tween 20 has to be omitted in all washing steps and fixation with glutardialdehyde is required prior to adding the staining solution. The original procedure given by Moeremans *et al.* [31] includes washing the blotting membranes in phosphate buffered saline, supplemented with 0.3% v/v Tween 20, for 30 and 3 × 5 min. We found that small polypeptides were washed out of the membranes by this procedure and even at concentrations of 0.1% v/v Tween 20 most of the peptides were lost prior to staining. The commercial Auro dye forte staining solution contains 0.1% v/v Tween 20 and therefore electroblotted proteins/peptides had to be pretreated with glutardialdehyde to prevent additional leaching of peptides during staining. After staining for 2 h, the modified staining procedure can detect subnanogram amounts of polypeptides, down to approximately M_r 1000. Obviously, proteins/peptides pretreated with glutardialdehyde in the presence of borate at near neutral pH values are strongly hydrophobic and consequently yield high binding affinities to the hydrophobic PVDF matrix. One might expect that omitting Tween 20 in the washing step gives rise to heavy background staining because the nonionic detergent is antici-

pated to block the unspecific binding sites of the membranes and remove low molecular mass impurities prior to staining. We found that omission of Tween 20 and pretreatment with glutardialdehyde results in only low pinkish background staining but increases the sensitivity towards impurities present in reagents and inadequate handling of blotting membranes and gels. A brief discussion of factors relevant to clean working conditions is given by Moeremans *et al.* [31]. We generally recommend using an additional PVDF membrane at the cathodic gel side to absorb impurities released from the cathodic layers of filter paper. Whether this membrane may be omitted depends on the quality of filter paper applied and has to be checked in each case.

4.4 SDS-PAGE of nondansylated proteins/peptides: Relative molecular mass determination

SDS-PAGE is a widely used and accepted method to estimate the M_rs of proteins [37–39]. Electrophoretic migration (R_f value) is proportional to the effective molecular radius or approximately the M_r of proteins only if the following two conditions are met for the protein in question and the M_r standards used to construct the calibration line: (i) hydrodynamic homology, (ii) constant net charge per mass unit of the SDS/protein complex. Due to differences in conformation, and the variable content of hydrophobic or hydrophilic amino acid residues, as well as differences in intrinsic charge, (i) and/or (ii) may be violated. For most proteins, amino acid residues with atypical SDS binding will be compensated by a large number of residues with average SDS-binding properties, *i.e.* 1 molecule SDS is bound per 2 amino acid residues [40–42]. Correspondingly, the probability of atypical SDS binding will increase with decreasing length of the polypeptide chain, and electrophoretic mobilities of small polypeptides separated by SDS-PAGE will be more sensitive to differences in intrinsic charge or content of amino acids with nonaverage SDS-binding properties. In addition, the electrophoretic mobilities of small polypeptides are strongly influenced by their tertiary structure. For M_r estimates of polypeptides in the range M_r 20000–1000, separated in gels composed of 18%T, 5%C, 21.4% w/v glycerol, we obtained a relative mean M_r prediction error of 18.8%, with a standard deviation of ± 12.7%. Using the SDS-PAGE system of Swank and Munkres [10] with separation gels made up of 12.5%T, 9.1%C, and 8 M urea, we were not able to improve the validity of M_r estimates in the M_r 20000–1000 range. Obviously, atypical migration of small polypeptides seems to be more closely related to their specific amino acid compositon than to the specific properties of the SDS-PAGE system applied. Reliable data for the M_r range in question may be obtained by amino acid analysis, UV laser desorption/ionization mass spectrometry, or gas-phase sequencing of polypeptides electroblotted on PVDF membranes after separation by the SDS-PAGE system described [26]. Nonetheless, in many applications a simple and inexpensive method with high resolution, and which wastes only minimal amounts of sample, will be valuable in obtaining preliminary information on the approximate M_r of a protein/peptide not characterized so far.

We thank Dr. T. M. Jovin for carefully reading the manuscript. Dr. J. Wiltfang is supported by a postdoctoral fellowship of the Deutsche Forschungsgemeinschaft.

Received December 13, 1989; in revised form January 30, 1991

5 References

[1] Jovin, T. M., *Biochemistry* 1973, *12*, 871–879.
[2] Jovin, T. M., *Biochemistry* 1973, *12*, 879–890.
[3] Jovin, T. M., *Biochemistry* 1973, *12*, 890–898.
[4] Alberty, R. A., *J. Amer. Chem. Soc.* 1950, *72*, 2361–2367.
[5] Dismukes, E. B. and Alberty, R. A., *J. Amer. Chem. Soc.* 1954, *76*, 191–197.
[6] Ornstein, L., *Ann. N.Y. Acad. Sci.* 1964, *121*, 321–349.
[7] Davis, B. J., *Ann. N.Y. Acad. Sci.* 1964, *121*, 404–427.
[8] Chrambach, A., *The Practice of Quantitative Gel Electrophoresis*, VCH, Weinheim 1985.
[9] Schafer-Nielsen, C. and Svendsen, P., *Anal. Biochem.* 1981, *114*, 244–262.
[10] Swank, R. T. and Munkres, K. D., *Anal. Biochem.* 1971, *39*, 462–477.
[11] Anderson, B. L., Berry, R. W. and Telser, A., *Anal. Biochem.* 1983, *132*, 365–375.
[12] Kyte, J. and Rodriguez, H., *Anal. Biochem.* 1983, *133*, 515–522.
[13] Schägger, H. and von Jagow, G., *Anal. Biochem.* 1987, *166*, 368–379.
[14] Steck, G., Leuthard, P. and Bürk, R. R., *Anal. Biochem.* 1980, *107*, 21–24.
[15] Trah, T. J. and Schleyer, M., *Anal. Biochem.* 1982, *127*, 326–329.
[16] Auzan, C., Menard, J., Corvol, P. and Chrambach, A., *Sep. Purific. Methods* 1985, *14*, 97–107.
[17] Neuhoff, V., Arold, N., Taube, D. and Ehrhardt, W., *Electrophoresis* 1988, *9*, 255–262.
[18] Neuhoff, V., Stamm, R. and Eibl, H.-J., *Electrophoresis* 1985, *6*, 427–448.
[19] Rosemblatt, M. S., Margolies, M. N., Cannon, L. E. and Haber, E., *Anal. Biochem.* 1975, *65*, 321–330.
[20] Weidekamm, E., Wallach, D. F. H. and Flückiger, R., *Anal. Biochem.*, 1973, *54*, 102–114.
[21] Strottmann, J. M., Robinson, J. B. and Stellwagen, N. C., *Anal. Biochem. 1983, 132*, 334–337.
[22] Inouye, M., *J. Biol. Chem.* 1971, *246*, 4834–4838.
[23] Talbot, D. N. and Yphantis, D. A., *Anal. Biochem.* 1971, *44*, 246–253.
[24] Neuhoff, V. and Poehling, H.-M., *Hoppe-Seyler's Z. Physiol. Chem.* 1980, *361*, 77–78.
[25] Wiltfang, J., Arold, N. and Neuhoff, V., in: Radola, B. J. (Ed.), *Elektrophorese Forum '87*, Technische Universität München 1987, pp. 446–452.
[26] Kratzin, H. D., Wiltfang, J., Karas, M. and Neuhoff, V., Hilschmann, N., *Anal. Biochem.*, 1989, *183*, 1–8.
[27] Schulze, E. and Neuhoff, V., *Hoppe Seyler's Z. Physiol. Chem.* 1976, *357*, 225–231.
[28] Poehling, H.-M. and Neuhoff, V., *Electrophoresis* 1980, *1*, 90–102.
[29] Neuhoff, V., Cheong-Kim, K.-S. and Altland, K., *Electrophoresis* 1986, *7*, 56–57.
[30] Hirano, H., *J. Prot. Chem.* 1989, *8*, 115–130.
[31] Moeremans, M., Daneels, G., Raeymaeker, M., Wever, B. and Mey, J., *Electrophoresis* 1987, *8*, 403–409.
[32] Wyckoff, M., Rodbard, D. and Chrambach, A., *Anal. Biochem.* 1977, *78*, 459–482.
[33] Laemmli, U. K., *Nature* 1970, *227*, 680–685.
[34] Payne, J. W., *Biochem. J.* 1973, *135*, 867–873.
[35] Avrameas, S. and Ternynck, T., *Immunochemistry* 1969, *6*, 53–66.
[36] Weston, P. D. and Avrameas, J., *Biochem. Biophys. Res. Commun.* 1971, *45*, 1574–1580.
[37] Shapiro, A. L., Viñuela, E. and Maizel, J. V., *Biochem. Biophys. Res. Commun.* 1967, *28*, 815–820.
[38] Weber, K. and Osborn, M., *J. Biol. Chem.* 1969, *244*, 4406–4412.
[39] Dunker, A. K. and Rueckert, R. R., *J. Biol. Chem.* 1969, *244*, 5074–5080.
[40] Pitt-Rivers, R. and Impiombato, F. S. A., *Biochem. J.* 1968, *109*, 825–830.
[41] Fish, W. W., Reynolds, J. A. and Tanford, C., *J. Biol. Chem.* 1970, *245*, 5166–5168.
[42] Reynolds, J. A. and Tanford, C., *Proc. Natl. Acad. Sci. USA* 1970, *66*, 1002–1007.

6.0 Appendix: Physicochemical properties of the native multiphasic buffer system

6.1 General remarks

The theoretical treatment of multiphasic zone electrophoresis by T. M. Jovin [1–3] served as a rationale to design the physicochemical properties of the present buffer system. The definitions applied are summarized below and are those given by Jovin [1]. Equations are identified by their original Arabic numeration and correspond to the convention in sign notation proposed by Jovin. Relative ionic mobilities (r) and pK values of components are tabulated by Chrambach [8] and refer to 25°C and 0.01M ionic strength. In the following, "electrophoretic phases" are denoted by Greek letters and are defined as "homogeneous solutions demarcated by moving and/or stationary boundaries" [1]. The adjoining phases contain only two components, one of them being common to both. The entity of a leading and trailing phase, separated by a moving boundary, will be termed "electrophoretic unit". The Roman numeration of electrophoretic units refers to the subtypes (case I–IV) differentiated by Jovin [1]. Tables 1 and 3 summarize the components of the multiphasic buffer system and assign the corresponding physicochemical properties.

Definitions

- $\bar{c}_j$ component concentration of component j. Signed quantity, possessing the sign of the ion subspecies of the component. A component consists of a nondissociable species and all forms in equilibrium with it (M).
- $c_{j(i)}$ concentration of subspecies of component j with valence i; signed (M).
- u_j ion mobility of the ion subspecies of component j. Signed according to valence. For divalent weak electrolytes, the mobility of the univalent ion species is designated as $u_{j(1)}$ and that of the divalent ion species as $u_{j(2)}$ ($cm^2s^{-1}V^{-1}$).
- r_j relative ion mobility of the ion subspecies of component j = ratio of u_j to the mobility of the sodium ion determined at the same ionic strength and temperature. Signed. Same convention for divalent weak electrolytes as for u_j (dimensionless).
- $\bar{u}_j$ component mobility of component j. Signed quantity, representing the average mobility for the entire component ($cm^2s^{-1}V^{-1}$).
- $\bar{r}_j$ relative component mobility of component j. Signed (dimensionless).
- $\varkappa$ specific conductance (mhos cm^{-1}).
- σ relative conductance (C cm^{-3}).
- v boundary displacement, volume swept by a moving boundary during passage of one coulomb. Signed quantity, positive if the moving boundary moves in the same direction as the current, *i.e.*, toward the cathode. A double superscript is used to indicate both phases adjoining the moving boundary (cm^3C^{-1}).
- $\Gamma/2$ ionic strength = $^1/_2 \sum^{k} \sum^{n} / c_{j(i)} / i^2$
- E electric field strength = -potential gradient (V cm^{-1}).
- I current density = current per unit cross-sectional area (A cm^{-2}).
- ϕ_j fraction of component j dissociated into ion subspecies of greatest valence (dimensionless).
- θ absolute value of the ratio of component concentrations in an electrophoretic phase.

6.2 Stacking

On start of electrophoresis a moving boundary migrates toward the anode into the stacking gel and separates SO_4^{2-} and Bicine, thus creating an anodic leading (β) and cathodic trailing (α) phase within the stacking gel. The properties of phase$^\alpha$, composed of Bicine and Bistris, are entirely determined by the composition of phase$^\beta$ (SO_4^{2-}, Bistris), and are regulated *via* the set of moving boundary equations for each component [1].

Table 1. Electrophoretic unit I.1

Classification	Component (c)	Code	Valence of subtype (m)	pK	r
Trailing ion	Bicine	1	−1	8.3	−0.67
Common ion	Bistris	3	+1	6.5	+0.42
Leading ion	Sulfate	2	−2		−1.42

The fused moving boundary equation for components 1 and 2 is defined as

$$\mu^{\alpha\beta} = \frac{\bar{c}_1^{\alpha}}{\bar{c}_2^{\beta}} = m\,\frac{(1-r_3\,r_2^{-1})}{(1-r_3\,r_1^{-1})} \tag{40}$$

and for a multivalent leading ion ($m \neq 1$) the concentration relationships for component 3 are defined as

$$\Theta^{\alpha} = \frac{-\bar{c}_3^{\alpha}}{\bar{c}_1^{\alpha}} = 1 + (\Theta^{\beta} - m)/\mu^{\alpha\beta} \tag{44}$$

$$\Theta^{\beta} = \frac{-\bar{c}_3^{\beta}}{\bar{c}_2^{\beta}} = m + (\Theta^{\alpha} - 1)\,\mu^{\alpha\beta} \tag{45}$$

The present leading phase is composed of 0.4 M Bistris ($\bar{c}_3^{\beta} = 0.4$) and 0.1 M H_2SO_4 ($\bar{c}_2^{\beta} = -0.1$). Equations (24) and (23) define a pH$^\beta$ of 6.5:

$$\Theta^{\beta} = \frac{-\bar{c}_3^{\beta}}{\bar{c}_2^{\beta}} \tag{24}$$

$$\mathrm{pH}^{\beta} = \mathrm{p}K_3 - \log\left(\frac{\Theta^{\beta}}{m} - 1\right)^{-1} \tag{23}$$

According to Eqs. (40), (44), and (45) this leading phase determines a phase$^\alpha$ composed of 0.159 M Bicine ($\bar{c}_1^{\alpha} = -0.159$) and 0.359 M Bistris ($\bar{c}_3^{\alpha} = 0.359$).

The corresponding pH$^\alpha$ is given by

$$\Theta^{\alpha} = \frac{-\bar{c}_3^{\alpha}}{\bar{c}_1^{\alpha}} \tag{28}$$

$$\phi_1^{\alpha} = \left| |a| - [a(a+b)]^{1/2} \right| \tag{26}$$

with $a = 0.5\,(1 + \Theta^{\alpha})/(1-p)$

$$b = -2\,\Theta^{\alpha}/(1 + \Theta^{\alpha})$$

and $p = 10^{-(\mathrm{p}K_3 - \mathrm{p}K_1)}$

$$\mathrm{pH}^{\alpha} = \mathrm{p}K_1 - \log(1/\phi_1^{\alpha} - 1) = 7.6 \tag{29}$$

The relative component mobility of Bicine (r_1^{α}) in phase$^{\alpha}$ is obtained by

$$r_1^{\alpha} = \phi_1^{\alpha} \cdot r_1 = -0.11 \tag{3}$$

The minimum trailing phase pH that may be achieved is given by

$$pH^{\alpha}_{min} = 0.5\,(pK_1 + pK_3) = 7.4 \tag{51}$$

corresponding to a minimal relative trailing ion net mobility of

$$\bar{r}_1^{\alpha} = -0.075 \tag{3}$$

The present α and β-phase composition provides the requirement for a steady state moving boundary as inequality

$$r_2/r_1 > \phi_1^{\alpha} \tag{53}$$

is fulfilled.

6.3 Formation of moving boundary$^{\alpha'\beta'}$

So far the formation of a moving boundary with Bistris as leading ion in a leading phase termed β′, Tris as trailing ion in a trailing phase termed α′, and SO_4^{2-} as common ion, was not considered. In the following it will be demonstrated that a moving boundary$^{\alpha'\beta'}$, migrating opposite to the moving boundary$^{\alpha\beta}$, is not generated in the present multiphasic buffer system.

Table 2. Electrophoretic unit VI

Classification	Component (c)	Code	Valence of subtype (m)	pK	r
Trailing ion	Tris	4	+1	8.07	+0.50
Common ion	Sulfate	1	−2		−1.42
Leading ion	Bistris	3	+1	6.5	+0.42

The component concentration relationships between the adjoining phases are determined by

$$\mu^{\alpha'\beta'} = \bar{c}_4^{\alpha'}/\bar{c}_3^{\beta'} = m\,\frac{(1 - r_2 \cdot r_3^{-1})}{(1 - r_2 \cdot r_4^{-1})} \tag{40}$$

$$\Theta^{\alpha'} = -\bar{c}_2^{\alpha'}/\bar{c}_4^{\alpha'} = 1 + (\Theta^{\beta'} - m)/\mu^{\alpha'\beta'} \tag{44}$$

$$\Theta^{\beta'} = -\bar{c}_2^{\beta'}/\bar{c}_3^{\beta'} = m + (\Theta^{\alpha'} - 1)\,\mu^{\alpha'\beta'} \tag{45}$$

In the present α′ and β′ phase the fraction of monovalent weak electrolyte dissociated into ionic subspecies (ϕ_j) can be defined as

$$\phi_j = c_j/\bar{c}_j = [1 + 10^{-(pK_j - pH)}]^{-1} \tag{22}$$

and

$$\phi_j^{\alpha'} = \Theta^{\alpha'}\,|m|; \qquad \phi_j^{\beta'} = \Theta^{\beta'}\,|m| \tag{103}$$

with

$$pH^{\alpha'\beta'} = pK_j - \log\,(1/\phi_j - 1)^{-1} \tag{23}$$

Equations (40–45), (22), (23), and (103) and the pK and r values depicted in Table 2, applied to a β′ phase composed of 0.4 M Bistris and 0.1 M H_2SO_4, result in

$$pH^{\beta'} = 6.50, \quad pH^{\alpha'} = 8.13, \quad \phi_3^{\beta'} = 0.50, \quad \phi_4^{\alpha'} = 0.466$$

and

$$\phi_4^{\beta'} = 0.974, \quad \phi_3^{\alpha'} = 0.023$$

The dissociation fractions $\phi_4^{\beta'}$ and $\phi_3^{\alpha'}$ refer to trace amounts of Tris and Bistris, hypothetically placed in phases β' and α', respectively. The requirement for a steady state moving boundary of the type under consideration, defined as

$$r_3/r_4 > \phi_4/\phi_3 \tag{65}$$

for both phases β' and α', is not fulfilled.

In addition, inequality

$$\bar{r}_4^{\alpha'} < \bar{r}_3^{\beta'}$$

the basic requirement to generate the electrophoretic moving boundary, is not fulfilled. Note that at a running temperature of 0°C, instead of 25°C, condition (I) is confirmed, but not condition (65).

6.4 Fusion of Tris and moving boundary$^{\alpha\beta}$

As defined in Section 6.1, theoretical treatment is restricted to phases with only two components. Fusion of Tris, migrating to the cathode, and moving boundary$^{\alpha\beta}$, migrating to the anode, generates a phase composed of Bicine, Bistris, and Tris. The precise physicochemical properties of this condition, interposed between initial stacking (Section 6.2) and destacking (Section 6.5), can not be characterized by the present approach. To estimate the proportion of stacking gel length migrated by moving boundary$^{\alpha\beta}$ and Tris up to their fusion, their electrophoretic velocities have to be calculated.

6.4.1 Velocity of moving boundary$^{\alpha\beta}$ ($V^{\alpha\beta}$)

The moving boundary displacement (v) for the lower moving boundary$^{s\beta}$ of a sample (s) interposed between phase$^{\alpha}$ and phase$^{\beta}$ can be defined as $v^{s\beta} = v^{\alpha\beta} = \bar{r}_1^{\alpha}/\sigma^{\alpha}$ if the sample volume is equilibrated against a buffer solution with the same composition as phase$^{\alpha}$ [2]. The relative conductance σ^{α} and the velocity of moving boundary$^{\alpha\beta}$ ($V^{\alpha\beta}$) are given by

$$\sigma^{\alpha} = 96.5\,\bar{c}_1^{\alpha}\,\phi_1^{\alpha}\,(r_1 - r_3) \tag{38}$$

and

$$V^{\alpha\beta}_{(cm\,s^{-1})} = v^{\alpha\beta} \cdot I^{\alpha} \tag{163}$$

For the present current density of 0.02 A cm^{-2}, we obtain for the velocity of moving boundary$^{\alpha\beta}$

$$V^{\alpha\beta} = V^{s\beta} = -80.20 \times 10^{-5}\ cm\ s^{-1}$$

In this context the velocity of Bicine in phase$^{\alpha}$ is of interest

$$V_1^{\alpha} = \bar{u}_1^{\alpha} \times E^{\alpha} \quad \text{(IV)}.$$

To calculate $\bar{u}_1^{\alpha}$ and the corresponding electrical field strength

$$E^{\alpha} = I^{\alpha}/K^{\alpha} \quad (9)$$

with

$$K^{\alpha} \cong \sigma^{\alpha}\, u_{Na^+} \quad (6)$$

the sodium ion mobility function for 25°C, as given by Chrambach [8], has to be applied to the ionic strength of phase$^{\alpha}$:

$$u_{Na^+} = 51.921 - 42.876\sqrt{\left(\frac{\Gamma}{2}\right)^{\alpha}} + 52.247\left(\frac{\Gamma}{2}\right)^{\alpha} - 30.235\left(\sqrt{\left(\frac{\Gamma}{2}\right)^{\alpha}}\right)^3$$

The ionic strength of phase$^{\alpha}$ is given by

$$\left(\frac{\Gamma}{2}\right)^{\alpha} = \left|\bar{c}_1^{\alpha}\right|\phi_1^{\alpha} \quad (7).$$

In the case under consideration we obtain: $E^{\alpha} = 15.82$ V cm^{-1} and $V_1^{\alpha} = -80.12 \times 10^{-5}$ cm 5^{-1}

$E^{\alpha} = 15.82$ V cm^{-1} and $V_1^{\alpha} = -80.12 \times 10^{-5}$ cm s^{-1}

6.4.2 Velocity of Tris in phase$^{\beta'}$ ($V_4^{\beta'}$)

Let us consider an arbitrary amount of Tris placed in phase$^{\beta'}$. Due to the electroneutrality restriction, the ionic strength of phase$^{\beta'}$ is not affected. However, as the ion mobility of Tris is higher than that of Bistris the specific conductance of phase$^{\beta'}$ will increase and $E^{\beta'}$ will decrease ($I^{\beta'}$ = const.). With increasing amount of Tris placed in phase$^{\beta'}$, $pH^{\beta'}$ is increased and $u_4^{\beta'}$ decreased. According to Eq. (IV), in the following a maximal velocity is estimated for Tris, as we consider a trace amount of Tris hypothetically placed in phase$^{\beta'}$

$V_4^{\beta'} = 27.42 \times 10^{-5}$ cm s^{-1} and $I^{\beta'} = 1.391$ Vcm^{-1}

6.4.3 Fusion

If we define as "a" the length of total stacking gel height "A" that moving boundary$^{\alpha\beta}$ migrates and as "b" the length Tris migrates until both fuse, it follows that

$$V^{\alpha\beta}/V_4^{\beta'} = a/b \text{ and } a = A\left(\frac{V_4^{\beta'}}{V^{\alpha\beta}} + 1\right)^{-1} \quad \text{(V)}$$

The predicted low trailing ion mobility of $\bar{r}_1^{\alpha} = -0.11$ applies to at least 74.5% of the stacking gel height, as a maximum value was estimated for "b".

6.5 Destacking

As the moving boundary$^{\alpha\beta}$ enters the separation gel, a leading phase$^{\gamma}$ composed of Tris ($\bar{c}_4^{\gamma}$) and sulfate ($\bar{c}_2^{\gamma}$) determines a trailing phase$^{\pi}$ composed of Bicine ($\bar{c}_1^{\pi}$) and Tris ($\bar{c}_4^{\pi}$).

Table 3. Electrophoretic unit 1.2

Classification	Component (c)	Code	Valence of subtype (m)	pK	r
Trailing ion	Bicine	1	−1	8.3	−0.67
Common ion	Tris	4	+1	8.07	+0.50
Leading ion	Sulfate	2	−2		−1.42

6.5.1 Electrophoresis of nondansylated proteins/peptides

γ-Phase: $\bar{c}_2^{\gamma} = -0.1$, $\bar{c}_4^{\gamma} = 0.4$; $pH^{\gamma} = 8.07$. In equivalence to electrophoretic unit I.1 a set of equations with Tris as common ion instead of Bistris defines the following

π-Phase: $\bar{c}_1^{\pi} = -0.155$, $\bar{c}_4^{\pi} = 0.355$, $pH^{\pi} = 8.50$,

$$\left(\frac{\Gamma}{2}\right)^{\pi} = \left|\bar{c}_1^{\pi}\right|\phi_1^{\pi} = 0.0954 \quad (7).$$

6.5.2 Electrophoresis of dansylated proteins/peptides

γ-Phase: $\bar{c}_2^{\gamma} = -0.0456$, $\bar{c}_4^{\gamma} = 0.4$, $pH^{\gamma} = 8.60$.

π-Phase: $\bar{c}_1^{\pi} = -0.0706$, $\bar{c}_4^{\pi} = 0.379$, $pH^{\pi} = 8.84$,

$$\left(\frac{\Gamma}{2}\right)^{\pi} = \left|\bar{c}_1^{\pi}\right|\phi_1^{\pi} = 0.0548 \quad (7).$$

As inequality (53) is fulfilled for 6.5.1 and 6.5.2 the conditions for a steady-state moving boundary are met.

Mellerson, Kendra

From: Noguerola, Alex
Sent: Thursday, May 08, 2003 10:11 AM
T : STIC-EIC1700
Subject: articles request

Please order the following articles

09/728,378

L3 ANSWER 26 OF 28 CAPLUS COPYRIGHT 2003 ACS
AN 1976:147093 CAPLUS
DN 84:147093
TI Chromatography of hemoglobins on CM-cellulose with bis-tris and sodium chloride developers
AU Schroeder, W. A.; Pace, Laurence A.; Huisman, T. H. J.
CS Div. Chem. Chem. Eng., California Inst. Technol., Pasadena, CA, USA
SO Journal of Chromatography (1976), 118(3), 295-302
CODEN: JOCRAM; ISSN: 0021-9673
DT Journal
LA English

Bittech me
QD241.J5

Journal of Chromatography, 118 (1976) 295–302

CHROM. 8853

CHROMATOGRAPHY OF HEMOGLOBINS ON CM-CELLULOSE WITH BIS-TRIS AND SODIUM CHLORIDE DEVELOPERS

W. A. SCHROEDER and LAURENCE A. PACE

*Division of Chemistry and Chemical Engineering**, *California Institute of Technology, Pasadena, Calif. 91125 (U.S.A.)*

and

T. H. J. HUISMAN

Laboratory of Protein Chemistry and Sickle Cell Center, Medical College of Georgia, Augusta, Ga. 30902 (U.S.A.)

(Received October 28th, 1975)

SUMMARY

CM-Cellulose as an ion-exchange medium with Bis-tris as buffer and a gradient of sodium chloride provides a versatile system for the chromatography of hemoglobins. Changes in pH, Bis-tris concentration, and slope of the sodium chloride gradient provide means for markedly altering chromatographic behavior for special separations. Examples are given of the application of the method to normal samples and to those with hemoglobinopathies.

INTRODUCTION

Shortly after the first preparation of an ion-exchange cellulose by Sober and co-workers[1,2], CM-cellulose was applied to the chromatography of hemoglobin by Huisman *et al.*[3,4]. Later, as improved forms of CM-cellulose became available commercially, modifications have been described[5]. These procedures have separated the hemoglobins by means of a gradient of pH that was produced by phosphate buffers. In the development of microchromatographic methods for hemoglobins[6], buffers with Tris or Bis-tris and sodium chloride have been successfully applied. Indeed, with these buffers, human fetal hemoglobin (Hb-F) and adult hemoglobin (Hb-A) were well separated in contrast to their minimal separation in phosphate buffers with a pH gradient. Consequently, we have examined the behavior of human hemoglobins in this new system on more conventionally sized columns in order to ascertain its applicability to the analysis of complex mixtures.

* Contribution No. 5210.

MATERIALS AND METHODS

Blood samples

Blood from normal individuals and from those with various types of hemoglobinopathy were collected with EDTA as anticoagulant. Solutions for chromatography were prepared from blood by washing the cells three times with 0.9% NaCl, by hemolyzing with water equal to 1.5 times the packed cell volume plus 0.4 volume of carbon tetrachloride for 20 min at room temperature, by centrifuging twice to remove cellular debris, and finally by dialyzing the sample against a large volume of the appropriate developer overnight at 4°.

Solutions

Developer I is 0.03 *M* Bis-tris–HCl–0.03 *M* NaCl–0.01% KCN at pH 6.1 and contains 6.28 g Bis-tris [N,N-bis-(2-hydroxymethyl)-iminotris-(hydroxymethyl)-methane], 1.75 g NaCl, 0.1 g KCN, and HCl to pH 6.1 in 1 l.

Developer II is 0.03 *M* Bis-tris–HCl–0.12 *M* NaCl–0.01% KCN at pH 6.1 and is prepared by adding 5.25 g NaCl per liter to Developer I and adjusting the pH.

Developer III is 0.03 *M* Bis-tris–HCl–0.085 *M* NaCl–0.01% KCN at pH 6.1 and is prepared by adding 3.22 g NaCl per liter to Developer I and adjusting the pH.

Preparation of ion exchanger

A 50-g portion of CM-cellulose (CM-52, microgranular and pre-swollen; Whatman, Clifton, N.J., U.S.A.) was suspended in 300 ml of Developer I. After the ion exchanger had been settled twice in this buffer to remove fines, the pH of the stirred suspension was adjusted to pH 6.1, another settling was done, pH was checked, and finally the volumes of settled resin and supernatant fluid were adjusted to a ratio of 1:2. All chromatographic operations were done at room temperature.

Chromatographic procedure

A 20 × 1 cm column was poured from the slurry of equilibrated CM-52 and 50–100 ml of Developer I was passed through. After most of the liquid had been removed, the sample was carefully layered on the column and allowed to flow in. The tube above the column and the line through the pump to the gradient device were filled with Developer I. Development was accomplished with a linear gradient from a two-vessel system of which the mixer contained 650 ml of Developer I and the second vessel 650 ml of Developer II; this is the full gradient. Developer was passed through the column at 50 ml/h with a peristaltic pump. Fraction size was 5 ml. Absorbance was read at 415 nm for all fractions and at 280 nm in some instances. Conductance was determined on every tenth fraction. Because the conductance is a linear function of NaCl concentration, the NaCl concentration at any fraction of the chromatogram can be calculated easily from the measured conductance of the two solutions of a gradient.

If Hb-C is not present in the sample, the gradient may be decreased; 375 ml each of Developers I and III provide a shortened gradient of the same slope as the full gradient.

Other procedures

DEAE-Sephadex chromatography[7,8], starch gel electrophoresis[9], and amino acid analysis by Beckman amino acid analyzer followed published procedures.

RESULTS AND DISCUSSION

Figs. 1–5 depict the separations that may be obtained from a variety of normal and abnormal hematological conditions. The identity of the components was established in one or more of four ways: starch gel electrophoresis, comparison with DEAE-Sephadex chromatography or with microchromatography, and/or amino acid analysis.

Cord bloods with common abnormal hemoglobins

The data in Fig. 1A derive from the cord blood of a newborn infant with sickle cell trait. The separation of Hb-F, Hb-A, and Hb-S is excellent in this system and Hb-F_1 separates from Hb-F_0 as it does in most chromatographic systems. The newborn child with Hb-C trait has the pattern in Fig. 1B. The conditions of chromatography were chosen to provide a relatively rapid movement of hemoglobins on the column. If an electrophoretically fast moving hemoglobin at alkaline pH were present, it would be virtually unadsorbed under these conditions. However, as will be discussed below, a pattern such as that in Fig. 1A can be translated along the volume axis by changing the NaCl gradient at constant pH and Bis-tris and KCN molarity and thus the rate of movement of more rapidly moving components can be retarded.

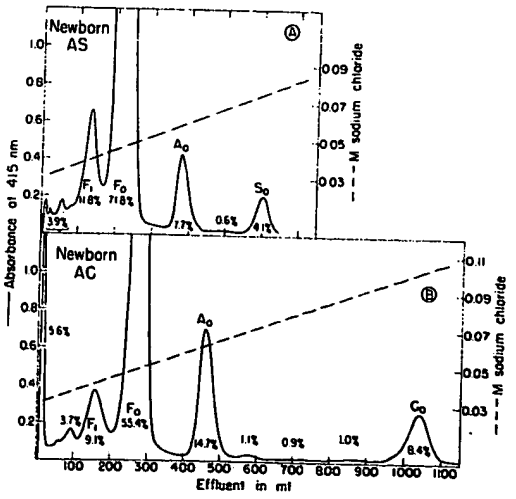

Fig. 1. Separation of hemoglobins in cord blood from an infant with sickle cell trait (A) and an infant with Hb-C trait (B). The shortened and full gradients respectively were used.

Adult samples with common abnormal hemoglobins

The hemoglobins of normal adults and of adults with combinations of hemoglobins A, S, and C yield chromatograms that are depicted in Figs. 2 and 3. In addition to Hb-A_2, a number of other minor components separate from the major Hb-A_0 of the normal individual (Fig. 2A). The very rapidly moving zones may contain some enzymes of the red cell[4] as well as the pyridoxal complex[10]. Traces of Hb-F_0 and minor components of Hb-A are not separable. Because no detailed study has been made of minor components and because they (with the exception of A_2 and F_1) have not been correlated with minor components as detailed by other chromatographic methods or by electrophoresis, they are labelled as A_x, A_y, etc. in the figures.

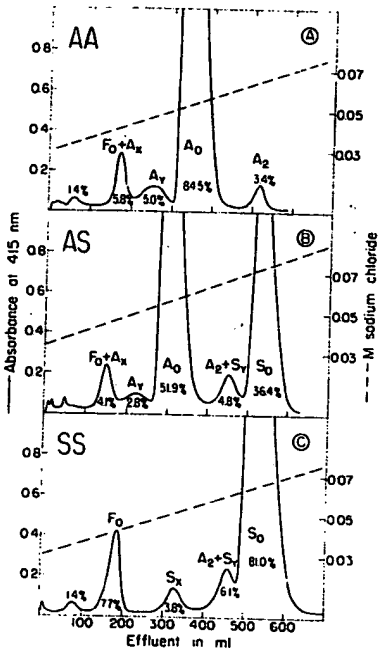

Fig. 2. Separation of hemoglobins of a normal adult (A) and of adults with sickle cell trait (B) and sickle cell anemia (C) by the shortened gradient.

When Hb-S is present, the separations in Figs. 2B (sickle cell trait) and 2C (sickle cell anemia) are obtained. A minor component(s) related to Hb-S (S_y) overlaps Hb-A_2 although in some chromatograms there may be partial separation (Fig. 4B). Hb-A_2, therefore, cannot be quantitatively determined in the presence of Hb-S by this method.

When Hb-C is present and the full gradient is used, Hb-C emerges, as shown in Figs. 1B, 3A, and 3B, before the end of the gradient. The separation of Hb-A_2 from

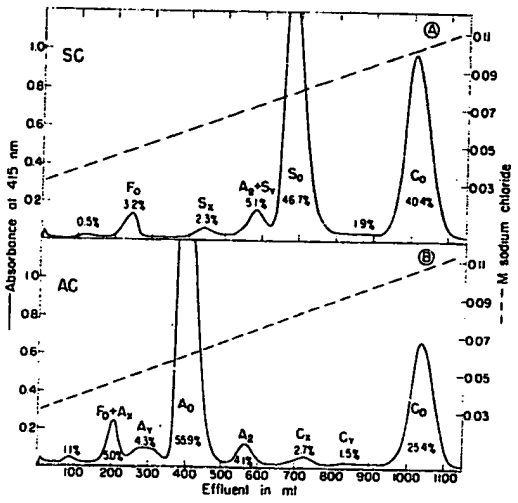

Fig. 3. Separation of hemoglobins of adults with SC disease (A) and Hb-C trait (B) by the full gradient

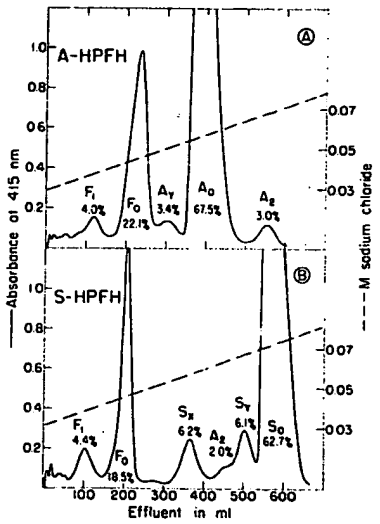

Fig. 4. Separation of hemoglobins in a heterozygote for the hereditary persistence of fetal hemoglobin (HPFH) (A) and in an HPFH individual with Hb-S (B) by the shortened gradient.

Hb-C is excellent and permits the quantitative determination of Hb-A_2 in the presence of Hb-C. Previous chromatographic procedures for this determination required about four days[5] in contrast to about a day by the present method.

Although the reproducibility of the procedure is good, slight changes in pH

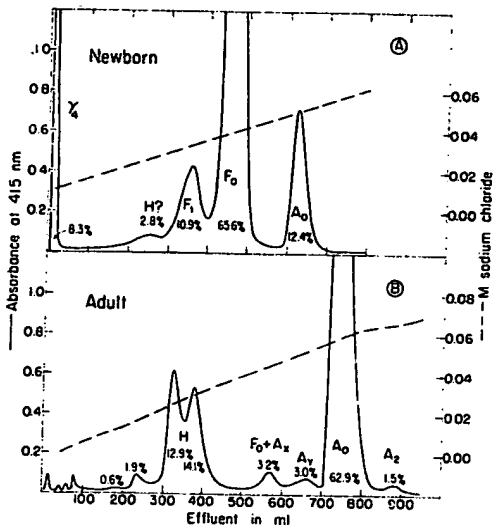

Fig. 5. Separation of hemoglobins in a newborn infant with Hb-Bart's (A) and in the father who has Hb-H disease (B) with a modified gradient (see text).

or NaCl concentration are responsible for the slightly different effluent volumes at which a given peak emerges. The NaCl molarity at the volume of emergence of the peak of any hemoglobin has been as follows: Hb-F_0, 0.039–0.050; Hb-A_0, 0.050–0.063; Hb-A_2, 0.060–0.074; Hb-S_0, 0.064–0.079; and Hb-C_0, 0.093–0.106. From these data as well as from a comparison of various chromatograms in Figs. 2 and 3, it is apparent that Hb-A_0 in an AS sample will be contaminated with a minor component of Hb-S (note the position of S_x in Fig. 2C and Fig. 3A as compared to Hb-A_0 in Fig. 2B). On electrophoresis on starch gel at pH 9, S_x does not behave like A_0 but is heterogeneous and moves like S_0 and F.

Other hemoglobinopathies and abnormal hemoglobins

The adult heterozygote for the hereditary persistence of fetal hemoglobin (HPFH) will have 15–30% Hb-F. The increased Hb-F of such a heterozygote is apparent in the chromatogram of Fig. 4A. When HPFH coexists with Hb-S, the chromatogram of Fig. 4B is obtained.

If Hb-S coexists with β-thalassemia, Hb-A is absent in the type termed S-β^0-thal and present in S-β^+-thal. The chromatogram of the former would have much the appearance of Fig. 4B except for a lower percentage of Hb-F. However, in S-β^+-thal, the S_x peak would contain Hb-A_0 and be present to the extent of 15–25%, and Hb-F would vary from case to case.

When other hemoglobins were chromatographed (not depicted), it was found that an Hb-D (possibly $D_{Los\ Angeles}$) moved more rapidly than Hb-S in a distinct peak although incompletely separated from Hb-S. Hb-Lepore (probably $Lepore_{Washington}$) has the mobility of Hb-A_2 as does Hb-E.

Figs. 5A and 5B present data from a Thailander in whom Hb-H(β_4) was detected by starch gel electrophoresis, and from his newborn child in whose hemoglobin Hb-Bart's (γ_4) was present. The mother had no electrophoretically abnormal hemoglobin. Because of the presence of these electrophoretically fast moving hemoglobins, the gradients were modified. For the chromatogram in Fig. 5A, the NaCl concentration in the two buffers was 0.01 *M* and 0.08 *M* in 0.03 *M* Bis-tris and 0.01% KCN at pH 6.1, the total gradient was 1000 ml, and the column had been equilibrated with 0.01 *M* NaCl. For that in Fig. 5B, the column was equilibrated with 0.01 *M* Bis-tris–no NaCl–0.01% KCN; 25 ml of this solvent was used for initial development with a subsequent 1000-ml gradient between no NaCl and 0.08 *M* NaCl in 0.03 *M* Bis-tris and 0.01% KCN at pH 6.1. The movement of hemoglobins is retarded under these conditions but the NaCl molarity at which a given peak emerges is within the range that is observed with the other gradient. The virtually unabsorbed peak in the chromatogram of the newborn (Fig. 5A) is Hb-Bart's and there is little or no Hb-H. Hb-H formed two peaks (Fig. 5B) which were readily identified by amino acid analysis. Because of the lability of Hb-H, different methods of preparing hemolysates gave varying ratios of the two peaks of Hb-H in other experiments.

Technical considerations

Bis-tris has been chosen as a buffer for these procedures because its pK_a is 6.5 and therefore the buffer capacity at the pH of choice is good. A few chromatograms in this study used only 0.01 *M* Bis-tris with a linear gradient of 1300 ml total volume and NaCl molarities of 0.03 and 0.12 at pH 6.1 in the gradient vessels. In this system, reproducibility of point of emergence was somewhat variable probably because of poorer pH control at this concentration of Bis-tris. Consequently, 0.03 *M* Bis-tris has been used and the reproducibility has improved.

A slower flow-rate or a longer column does not improve separations. Most of the chromatograms in the figures used a flow-rate of 25 ml/h, but in more recent work, the flow-rate has been 50 ml/h. Consequently, the chromatogram is complete in about a day. In fact, the flow-rate may be increased to 75 ml/h without significant deterioration in the separations. Visual observations of the movement of the hemoglobins on the column suggest that most of the separation occurs in the upper 10 cm, and that each hemoglobin washes virtually unretarded through the lower half of the column. The columns have been re-equilibrated as many as five times and used again successfully.

The developing conditions with the linear gradient of Developers I and II provide a good and rapid separation of the normal hemoglobins and common variants. However, modification of the NaCl gradient or Bis-tris concentration provides a versatility that can be used with less common mixtures of hemoglobins. As an example, Fig. 5A may be compared with Fig. 2A. The slope of the gradient was identical but the start at 0.01 *M* NaCl instead of 0.03 *M* NaCl retarded Hb-A_0 about 275 ml of effluent. Similar retardation occurs if the gradient is started at 0.03 *M* NaCl but the Bis-tris is 0.01 *M* instead of 0.03 *M*. In summary, an increase in pH, NaCl or Bis-tris concentration, or in slope of the NaCl gradient speeds the movement of any hemoglobin and vice versa. With some experience, these variables may be adjusted to provide correct conditions for special separations.

If the Bis-tris–NaCl system is replaced by a gradient of 0.02–0.08 *M* phosphate

at pH 6.1 or a gradient of 0.0 *M*-0.1 *M* NaCl in 0.02 *M* phosphate at pH 6.1, the separations are similar but less satisfactory.

ACKNOWLEDGEMENTS

These studies were supported in part by grants N01-HB-3-3007 and HL-02558 from the National Institutes of Health, U.S. Public Health Service. Dr. Darleen Powars and Dr. Richard Barnes supplied most of the blood samples that were used in this study.

REFERENCES

1 E. A. Peterson and H. A. Sober, *J. Amer. Chem. Soc.*, 78 (1956) 751.
2 H. A. Sober, F. J. Gutter, M. M. Wyckoff and E. A. Peterson, *J. Amer. Chem. Soc.*, 78 (1956) 756.
3 T. H. J. Huisman, E. A. Martis and A. Dozy, *J. Lab. Clin. Med.*, 52 (1958) 312.
4 T. H. J. Huisman and C. A. Meyering, *Clin. Chim. Acta*, 5 (1960) 103.
5 T. H. J. Huisman, *Clin. Chim. Acta*, 40 (1972) 159.
6 W. A. Schroeder, T. H. J. Huisman, D. Powars, L. Evans, E. C. Abraham and H. Lam, *J. Lab. Clin. Med.*, 86 (1975) 528.
7 T. H. J. Huisman and A. M. Dozy, *J. Chromatogr.*, 19 (1965) 160.
8 A. M. Dozy, E. F. Kleihauer and T. H. J. Huisman, *J. Chromatogr.*, 32 (1968) 723.
9 G. D. Efremov, T. H. J. Huisman, L. L. Smith, J. B. Wilson, J. L. Kitchens, R. N. Wrightstone and H. R. Adams, *J. Biol. Chem.*, 244 (1969) 6105.
10 S. K. Srivastava, C. van Loon, and E. Beutler, *Biochim. Biophys. Acta*, 278 (1972) 617.

Mellerson, Kendra

From: Noguerola, Alex
Sent: Thursday, May 08, 2003 10:11 AM
To: STIC-EIC1700
Subject: articles request

Please order the following articles

09/728,378

L3 ANSWER 17 OF 28 CAPLUS COPYRIGHT 2003 ACS
AN 1993:444830 CAPLUS
DN 119:44830
TI Purification of a mycobacterial adhesin for fibronectin
AU Ratliff, Timothy L.; McCarthy, Robert; Telle, W. Brian; Brown, Eric J.
CS Sch. Med., Washington Univ., St. Louis, MO, 63110, USA
SO Infection and Immunity (1993), 61(5), 1889-94
CODEN: INFIBR; ISSN: 0019-9567
DT Journal
LA English
CC 10-1 (Microbial, Algal, and Fungal Biochemistry)

Biotech mic
QR1.A47A35

INFECTION AND IMMUNITY, May 1993, p. 1889–1894
0019-9567/93/051889-06$02.00/0

Vol. 61, No. 5

Purification of a Mycobacterial Adhesin for Fibronectin

TIMOTHY L. RATLIFF,[1,2]* ROBERT McCARTHY,[3] W. BRIAN TELLE,[2] AND ERIC J. BROWN[3,4]

Departments of Pathology,[1] Medicine,[3] and Molecular Microbiology,[4] Washington University School of Medicine, and Department of Surgery (Urology), the Jewish Hospital of St. Louis, 216 South Kingshighway,[2] St. Louis, Missouri 63110*

Received 16 November 1992/Accepted 8 February 1993

Previous studies have demonstrated that mycobacteria attach to fibronectin (FN). The attachment of mycobacteria to FN is considered to be biologically important in *Mycobacterium bovis* BCG therapy for superficial bladder cancer, initiation of delayed hypersensitivity to mycobacterial antigens, and the phagocytosis of mycobacteria by epithelial cells. Therefore, we purified the mycobacterial receptor for FN. Culture supernatants from 3-week cultures of *Mycobacterium vaccae*, which contained proteins that bound FN and inhibited the attachment of both *M. vaccae* and BCG to FN, were used as a source of receptor. Lyophilized *M. vaccae* supernatants were reconstituted in 0.02 M bis-Tris (pH 6.0) and applied sequentially to an ACA 54 gel filtration column and a DEAE-Sephacel anion-exchange column. A purified inhibitory protein of 55 kDa (p55) was obtained. The purified p55 protein was observed to bind to FN and to inhibit ^{125}I-FN binding to viable BCG in a dose-dependent manner. Polyclonal and monoclonal antibodies to the protein were generated. The resulting polyclonal antiserum blotted a single protein band at 55 kDa in crude *M. vaccae* supernatants, cross-reacted with a 55-kDa BCG protein by Western blot (immunoblot), and recognized a 55-kDa band that was associated with the BCG cell wall, which is consistent with its function as a FN receptor. A monoclonal immunoglobulin M(λ) was isolated from mice immunized with purified *M. vaccae* p55 protein that was not functional in Western blots but inhibited the attachment of viable BCG to FN. These studies demonstrate that a protein or antigenically related proteins with M_rs of 55,000 function as FN receptors for at least two distinct mycobacteria.

Adjuvant intravesical *Mycobacterium bovis* bacillus Calmette-Guérin (BCG) is the most effective treatment for superficial transitional cell carcinoma of the bladder (10, 16, 17). Previous studies have demonstrated that a requisite step in BCG-mediated antitumor activity is retention of the bacteria within the bladder by attachment to fibronectin (FN) (13). BCG retention after intravesical instillation was inhibited by antibodies specific for FN but not by control antibodies to other basement membrane proteins. In addition, treatment of BCG prior to intravesical instillation with soluble monomeric FN, which had been shown to saturate bacterial surface receptors (4), also inhibited attachment (13). Further studies demonstrated that the retention of BCG within the bladder was dependent on attachment to FN most probably associated with the fibrin clot (11). In vivo functional studies showed that FN-mediated BCG attachment was necessary for (i) the induction of immunity to BCG after intravesical instillation, (ii) the expression of BCG-induced delayed-type hypersensitivity within the bladder, and (iii) mediation of antitumor activity (13).

In vitro characterization studies demonstrated that BCG, as well as all other mycobacteria tested, attached to FN-coated surfaces but not surfaces coated with laminin, fibrinogen, or type IV collagen (20, 21). The BCG-FN interaction was saturable, FN specific, essentially irreversible, and inhibited by pretreatment with protease, suggesting the presence of specific bacterial receptor (4). Further studies showed that BCG attachment to FN was inhibited by components contained in the supernatants of proliferating BCG, suggesting that the receptor(s) was released into the supernatant (2, 20). This hypothesis was supported by several independent observations: (i) radiolabelled proteins from BCG supernatants attached to FN-coated surfaces (2), (ii) the supernatant component(s) inhibited the attachment of BCG to FN (20), (iii) the inhibitory activity was removed by affinity chromatograph on FN-Sepharose (20), and (iv) proteins from BCG supernatants separated on sodium dodecyl sulfate-polyacrylamide gel electrophoresis (SDS-PAGE) and blotted to nitrocellulose bound FN (2). Therefore, we initiated studies to purify the inhibitor present in the mycobacterial culture supernatants. To this end supernatants from *Mycobacterium vaccae*, a fast-growing mycobacterial species, were used for purification because these supernatants inhibited FN attachment to BCG. This provided larger quantities of supernatant proteins for purification. We report herein the purification to homogeneity of the inhibitory factor and preparation of monoclonal and polyclonal antibodies against the protein. The data suggest that the inhibitor or a closely related molecule is a mycobacterial FN receptor.

MATERIALS AND METHODS

Chemicals. All chemicals were purchased from Sigma Chemical Co. (St. Louis, Mo.) and were reagent grade unless otherwise stated.

Bacteria. BCG was obtained from Armand Frappier, Quebec, Canada, as a lyophilized preparation containing 10^7 CFU mg^{-1} (manufacturer's specification). Before use, BCG was cultured in Youman's medium for 5 days at 37°C. The bacteria were harvested by centrifugation and resuspended in buffer to produce approximately 7×10^8 CFU ml^{-1} (determined by standard curves plotting optical density at 570 nm versus CFU). *M. vaccae* was obtained from the mycobacterial culture collection of John Stanford, University of London, London, England. *M. vaccae* was grown in Sauton medium and stored at −70°C as previously described (22).

* Corresponding author.

Preparation of ^{125}I-labelled FN. Human plasma FN was purified as previously described (13). The purified FN, 1.5 mg ml^{-1}, was labelled f r 15 min with 1 mCi (37 MBq) of ^{125}INa (Amersham) in a test-tube precoated with 200 μg f Iodo-Gen (1,3,4,6-tetrachloro-3,6-diphenylglycouril) as previously described (4). The labelled FN was then separated from unbound ^{125}I by chromatography on a 10-ml Sephadex G-25 column. The specific activities of the labelled FN preparations were routinely between 10^6 and 10^7 cpm μg^{-1}.

^{125}I-FN binding assay. The binding assay was performed as previously described (4). Briefly, 6 μg of ^{125}I-FN was added to 1.5-ml-volume microcentrifuge tubes (Eppendorf) precoated for 2 h with 1 ml of 1 mg of human serum albumin (HSA) ml^{-1}. Prior to ^{125}I-FN addition, 7 × 10^6 BCG suspended in 1.0 ml of 0.1 M Tris buffer, pH 6.0, was added. The ^{125}I-FN was mixed with either 300 μl of unlabelled FN (1 mg ml^{-1}) or 300 μl of Tris only to determine nonspecific and total binding, respectively. Specific binding was ascertained by subtracting nonspecific from total binding. The reaction mixtures were incubated for 1 h at 22°C. After incubation, the microcentrifuge tubes containing the reaction mixtures were centrifuged at 10,000 × *g* for 3 min in a Beckman microcentriiuge B. The supernatant, containing free radiolabelled FN, was carefully removed. The microcentrifuge tubes were sliced, and the pellets containing the radiolabelled FN bound to BCG were analyzed for radioactivity. Control experiments using ^{125}I-FN without bacteria produced background counts of approximately 500 cpm.

Attachment of BCG to FN-coated surfaces. The matrix attachment assay was performed by a modification of a previously described method (20). Briefly, a 5-day culture was washed twice with and resuspended in phosphate-buffered saline (PBS), pH 7.2, to a concentration of 10^8 CFU/ml. Next, 10^7 CFU (0.1 ml) was added to each well of a 96-well microtiter plate (Immulon II; Dynatech Laboratories, Inc., Chantilly, Va.) previously coated with FN (120 μg/ml) or HSA (120 μg/ml; background). Attachment was quantitated by reading the optical density at 570 nm on an enzyme-linked immunosorbent assay (ELISA) reader. The results are reported as optical density units. Results from a representative experiment are shown. Data were reproducible in at least two separate experiments.

Production of receptor-containing supernatants. *M. vaccae* was subcultured in 100 ml of Sautons medium to p'ateau growth phase. An inoculum of 8 × 10^8 bacteria was cultured in each of eight flasks containing 1.0 liters of Sautons. Cultures were maintained at 37°C in 7% CO_2 for 3 weeks. Supernatants were harvested by centrifugation, and residual bacteria were removed by filtration (2-μm-pore-size filters; Costar). The supernatant was concentrated 100 times on an Amicon filtration unit with a PM 10 filter. Concentrated *M. vaccae* culture supernatant was dialyzed against distilled H_2O and lyophilized.

Purification of the FN-binding protein. Concentrated *M. vaccae* culture supernatant was dialyzed against distilled H_2O and lyophilized. The lyophilized supernatant was reconstituted to 1.5 ml with 0.02 M bis-Tris (pH 6.0), and 0.7 ml was loaded onto an ACA 54 gel filtration column (0.6 by 75 cm) equilibrated with 0.02 M bis-Tris.

Inhibitory fractions were pooled and loaded onto 10 ml of DEAE-Sephacel. The column was washed with 0.02 M bis-Tris (pH 6.0) until the effluent was protein free. Protein was eluted with a 0 to 0.4 M NaCl gradient in bis-Tris. Fractions, 1.0 ml, were collected and dialyzed against bis-Tris, pH 6.0. SDS-PAGE and Western blots were performed as previously described (2).

Antibodies. P lyclonal rabbit antibodies to the purified adhesin (p55) were prepared by injecting subcutaneously 25 μg in alum. At 3-week intervals the rabbit was boosted with 15 t 20 μg in alum. Ten to 14 days after the second boost, antibody was harvested. Immunoglobulin G (IgG) was isolated from serum by 50% ammonium sulfate precipitation followed by DEAE-Sephacel ion-exchange chromatography. SDS-PAGE demonstrated only bands consistent with IgG heavy and light chains. All experiments using the polyclonal antibody were performed with DEAE-purified antibody.

Monoclonal antibody to the p55 protein was generated by the subcutaneous injection of BALB/c mice with 10 μg of p55 in alum. Mice were boosted three times at weekly intervals with 5 μg of p55 in alum. Mice were rested 3 to 4 weeks after the third boost and injected intravenously with 5 μg of p55 in PBS. Three days later, spleens were harvested and fused with the NS1 myeloma. Reactive clones were detected by ELISA with purified p55-coated microtiter wells. A single hybridoma showed consistent reactivity in an ELISA. The reactive hybridoma was cloned, and the antibody, designated mFNR.1, was isotyped as IgMλ.

p55 FN binding assay. Immulon wells were coated with FN or bovine serum albumin (BSA) as a control for nonspecific binding, as described above. The remaining attachment sites were blocked by the addition of 1% BSA in PBS for 30 min. Purified p55 in Tris buffer was added to appropriate wells (3 μg per well) and incubated for 30 min at room temperature. Wells were washed, and purified monoclonal anti-p55 (mFNR.1) diluted in PBS containing 0.1% BSA was added for 1 h at room temperature. The wells were washed, and a biotinylated anti-mouse immunoglobulin (Sigma) was added at a predetermined optimal concentration for 1 h at room temperature. The wells were washed, and the reaction was developed by the addition of *p*-nitrophenyl phosphate. Reactivity was read on an ELISA reader at a wave length of 405 nm. Controls included p55 added to BSA-coated wells, FN-coated wells without p55, and FN-coated wells with a nonspecific primary isotype control (RL172.4; a monoclonal IgM reactive with thy 1.2 on murine T cells [6]). Control absorbance for all controls was equal to or less than that of the isotype control.

BCG fractionations. BCG cells were separated into cell wall-associated (particulate) and cytoplasmic fractions as previously described (12). Briefly, BCG was collected after culture on Sautons as described above. Bacteria were resuspended in Tris buffer and subjected to probe sonication. Particulate material was sedimented by centrifugation and solubilized in SDS. The supernatant was considered the cytoplasmic fraction.

RESULTS

Previous studies suggested that mycobacterial supernatants contained proteins with functional activity consistent with the presence of soluble FN receptors (2, 20). In an effort to maximize supernatant protein production for purification, supernatants from *M. vaccae*, which were previously shown to contain proteins that attached to FN-coated surfaces, were tested for the presence of soluble receptors capable of inhibiting the attachment of ^{125}I-FN to BCG. The results demonstrate that concentrated *M. vaccae* supernatant contains a component that inhibits FN binding to BCG (Fig. 1). Purification of the inhibitory component(s) was initiated by applying supernatant to an ACA-54 gel filtration column previously equilibrated with bis-Tris, pH 6.0. The inhibitory activity was localized and pooled for further purification.

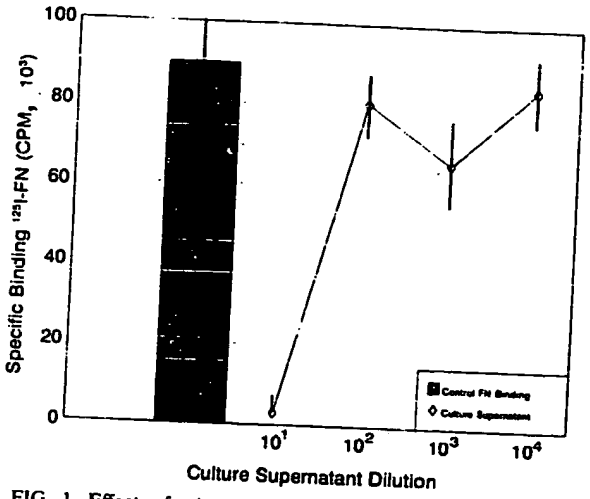

FIG. 1. Effects of culture supernatants from *M. vaccae* containing the putative mycobacterial FN receptor on ^{125}I-FN binding to BCG. Error bars, standard error of the mean for four replicates.

SDS-PAGE on the pooled fractions revealed a primary protein band at 55 kDa (p55; Fig. 2A, lane 1). The pooled ACA-54 inhibitory fractions were applied to a DEAE-Sephacel anion-exchange column equilibrated with 0.02 M bis-Tris, pH 6.0. Bound protein was eluted with a 0 to 0.4 M NaCl gradient in bis-Tris, pH 6.0. The peak inhibitory activity eluted at 0.3 M NaCl. SDS-PAGE on the 0.3 M fraction revealed a single 55-kDa protein band (Fig. 2B, lane 5). The protein from this fraction was used for all subsequent experiments and for immunization purposes. Protein purification is summarized in Table 1. Amino acid sequencing by Edman degradation was unsuccessful, presumably because the amino terminus of p55 was blocked.

The purified p55 was tested for its ability to inhibit ^{125}I-FN binding to BCG (Fig. 3). Purified p55 inhibited FN attachment to BCG in a dose-dependent manner.

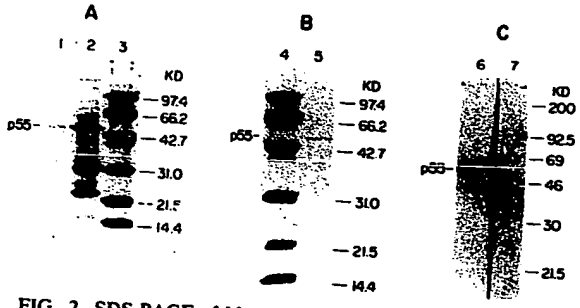

FIG. 2. SDS-PAGE of *M. vaccae* culture supernatant inhibitory fractions obtained from the ACA-54 gel filtration (A) and DEAE-Sephacel (B) columns. (C) Western blot of unfractionated *M. vaccae* supernatant with a polyclonal antibody prepared from the purified protein shown in panel B, lane 5. (A) ACA-54. Lane 1, pooled fractions that inhibited ^{125}I-FN binding to BCG; lane 2, concentrated, unfractionated *M. vaccae* supernatant; lane 3, molecular mass standards. (B) DEAE-Sephacel. Lane 4, molecular mass standards; lane 5, purified *M. vaccae* protein that inhibited ^{125}I-FN binding to BCG. (C) Lane 6, Western blot with rabbit polyclonal antibody to the purified FN receptor; lane 7, blot with preimmune serum.

TABLE 1. Purification of the *M. vaccae* FN-binding protein

Step	Protein (mg/ml)	Vol	Total protein	Fold purification
Concentrated supernatant	11.16	0.7	7.8	
ACA-54 gel filtration	0.07	8.0	0.57	13.7
DEAE-Sephacel (0–0.4 M NaCl)	0.16	2.0	0.32	24.3

Purified p55 was used as an immunogen to generate a rabbit polyclonal and a mouse monoclonal antibody. The resulting polyclonal antibody blotted a single protein band at 55 kDa in crude *M. vaccae* supernatants (Fig. 2C, lane 6). The single monoclonal antibody obtained was reactive by ELISA to purified p55 (Fig. 4) but was not effective in Western blots (immunoblots) (data not shown).

Further studies were performed to determine whether the purified p55 protein bound to FN. Microtiter wells were coated with FN as described in Materials and Methods, after which purified p55 was added. The binding of p55 to FN was detected by either the polyclonal or monoclonal antibodies. The results were identical for both. Data for the monoclonal antibody (mFNR.1) are shown in Fig. 5. The results demonstrate mFNR.1 binding to p55-treated FN-coated surfaces increases as a function of the input of p55, suggesting a p55-FN interaction. Thus, p55 inhibits FN binding to BCG and binds directly to FN. Taken together, the data show that the purified inhibitory component (p55) from the supernatant of *M. vaccae* is an FN-binding protein.

Because this *M. vaccae* FN-binding protein had been purified on the basis of its ability to inhibit FN binding to BCG, it was reasonable that BCG should contain a related protein. Therefore, we tested whether the polyclonal anti-p55 (made against *M. vaccae* FN-binding protein) recognized a BCG protein(s). BCG cells were fractionated into cytosolic and cell wall components as previously described (12). The crude cell fractions were subjected to Western blotting with the polyclonal anti-p55 (Fig. 6). An immunologically cross-reactive protein at 55 kDa was seen in the cell wall but not the cytosolic fraction from BCG. In addition, a protein at 100 kDa also faintly reacted with the antiserum. We are uncertain whether this represents an additional cross-reactive protein in BCG or a precursor of the mature

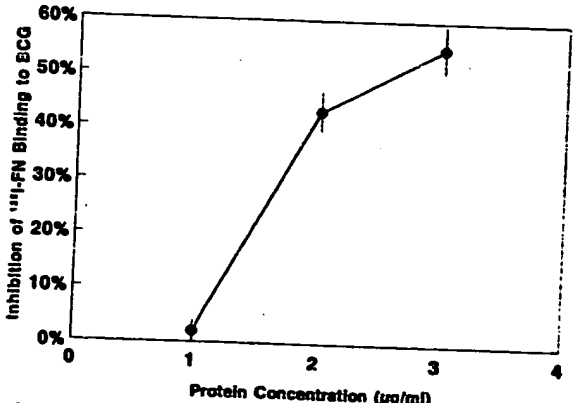

FIG. 3. Effects of purified *M. vaccae* FN receptor on ^{125}I-FN binding to BCG. Error bars, standard error of the mean for four replicate values.

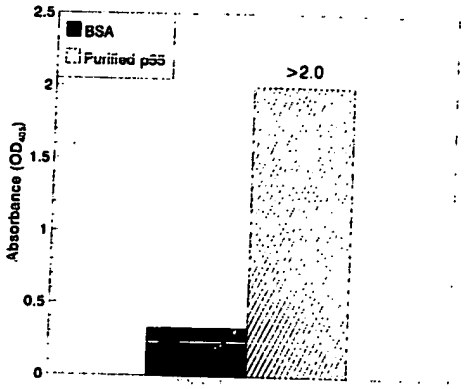

FIG. 4. Recognition of purified *M. vaccae* FN receptor (p55) by the monoclonal antibody mFNR.1. OD_{405}, optical density at 405 nm.

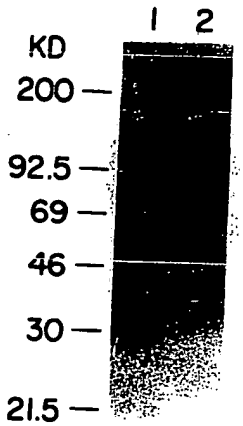

FIG. 6. Western blot of particulate and soluble BCG fractions with rabbit polyclonal antibody to the *M. vaccae* FN receptor (anti-p55). BCG were sonicated, and particulate and soluble fractions were separated as described in Materials and Methods.

p55. Thus, BCG expresses a protein(s) cross-reactive with the *M. vaccae* FN-binding protein in the cell wall.

Since the cell wall localization of p55 in BCG is consistent with its possible function as a FN receptor, we tested whether the monoclonal anti-p55 could inhibit the binding of intact, viable BCG to FN. As shown in Fig. 7, the anti-p55 monoclonal antibody inhibited BCG attachment to an FN-coated surface. Thus, an antigenically related protein is necessary for BCG binding to FN.

DISCUSSION

Previous reports have shown that BCG and other mycobacterial species attach to FN in a receptor-mediated manner (4, 11, 13, 21). Supernatants from proliferating mycobacteria contained a component(s) that bound FN and that inhibited the interaction between mycobacteria and FN (2). We have purified a 55-kDa protein (p55) from culture supernatant and have demonstrated its ability to bind directly to FN-coated surfaces. Our data are consistent with the hypothesis that p55 is a mycobacterial receptor for FN. Purified p55 was observed both to inhibit the binding of FN to BCG and to bind directly to FN-coated surfaces. In addition, p55 localizes to the particulate fraction of the bacterium, suggesting its availability for binding. Most convincingly, monoclonal antibody to p55 blocked the attachment of viable BCG to FN-coated surfaces. Importantly, although p55 was purified from *M. vaccae*, both the monoclonal and polyclonal antibodies recognize BCG. The monoclonal anti-p55 also inhibits the binding of *M. avium*, *M. tuberculosis*, and *M. kansasii* to FN-coated surfaces (19a). These data suggest that the 55-kDa protein is a highly conserved protein or a member of an antigenically related family of proteins that function as mycobacterial FN receptors.

Our data demonstrate that p55 is necessary for BCG attachment to FN. They do not rule out the involvement of additional components in FN binding. Since FN is known to interact with glycolipids, which are abundant in the mycobacterial envelope, there may be as-yet-unidentified components involved in binding. A multicomponent interaction might explain the extremely low dissociation rate previously reported for FN and mycobacteria (4). Furthermore, previous reports suggested that the mycobacteria expressed two FN-binding proteins with molecular masses of 55 and 32 kDa (1, 2). Subsequent studies using a cloned 32-kDa protein

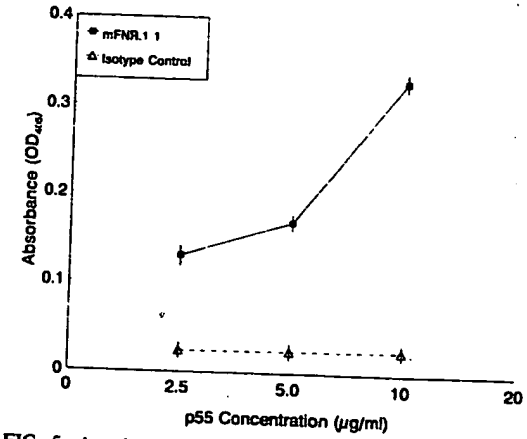

FIG. 5. Attachment of purified *M. vaccae* FN receptor (p55) to FN-coated surfaces. Standard error bars, standard error of the mean of eight replicate values. Statistics, Student's *t* test. Binding was significant for all datum points at a minimum $P < 0.01$. OD_{405}, optical density at 405 nm.

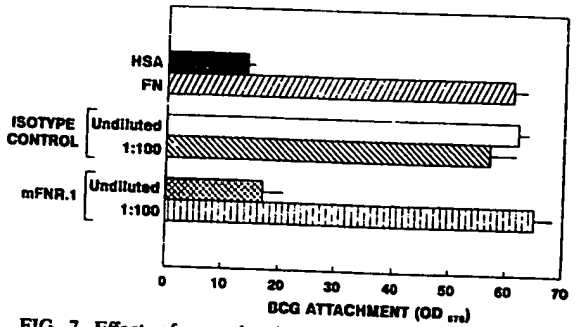

FIG. 7. Effects of monoclonal antibody to *M. vaccae* FN receptor (mFNR.1) on the attachment of BCG to FN-coated surfaces. Error bars, standard error of the mean of four replicate values.

from *M. leprae* demonstrated unequivocally that the recombinant 32-kDa protein bound FN in vitro (25). Two separate protein domains of the 32-kDa *M. leprae* protein, one containing amino acids 55 to 266 and the other containing amino acids 265 to 327, bound FN, suggesting that two separate binding sites exist in this protein. While it is clear that the 32-kDa protein binds FN in vitro, its role in the attachment of viable mycobacteria to FN-coated surfaces has not been established. Moreover, a recent report by Pessolani and Brennan (18) has questioned the FN-binding capacity of the 32-kDa proteins. Since the monoclonal anti-p55 inhibited the attachment of viable BCG to FN almost completely, p55 may be the primary mycobacterial FN receptor and the 32-kDa protein may function as an accessory molecule. However, the relationship between the 32- and the 55-kDa proteins and their respective roles in mycobacterial attachment to FN remain to be definitely established.

Previous reports have shown that several bacterial genera, including *Staphylococcus*, *Streptococcus*, *Escherichia*, *Salmonella*, and *Treponema*, attach to FN via specific bacterial receptors (3, 6, 7, 8, 14, 23, 26). The most studied bacterium-FN interaction is that of *Staphylococcus aureus*, for which the bacterial receptor has been cloned and the FN-binding region has been identified (8).

It is clear that the mycobacterial FN-binding protein possesses several physicochemical properties distinct from the FN-binding proteins of *S. aureus*, *Streptococcus pyogenes*, and *Treponema pallidum* (8, 23, 26). While the interaction between FN and *S. aureus* was enhanced by NaCl, concentrations as low as 0.04 M significantly inhibited FN attachment to BCG (4, 19). The pH maxima also differ with BCG possessing a range of 3.0 to 6.0, while little FN attachment to *S. aureus* is observed at pH 5.0 or lower. Finally, the location of the attachment site to FN is distinct for BCG. *S. aureus* attaches to the NH_2-terminal 29-kDa fragment of FN, while our unpublished data suggest that BCG attaches to the COOH-terminal heparin binding region of the FN molecule (3).

The biological role for the p55 protein is not known. The interaction between FN and the mycobacteria was first discovered in investigations aimed at gaining a better understanding of the mechanisms of action of BCG as an antitumor agent for superficial bladder cancer (21). In those studies it was determined that the attachment of BCG to FN present within the bladder was a requisite step in the antitumor response induced by BCG (13). Godfrey and associates (9) have suggested that mycobacterial FN-binding proteins inhibit cutaneous delayed-type hypersensitivity reactions to purified protein derivative in guinea pigs. Recent studies suggest that the FN-binding capacity of p55 is important in the phagocytosis of BCG by epithelial cells (15). Moreover, preliminary studies suggest that the p55-mediated ingestion process can be important in macrophage ingestion of *M. avium*. Whether the FN-binding activity of the mycobacteria is associated with pathogenicity, as has been suggested for other bacteria (24), remains to be determined. The capacity to bind FN has been observed in pathogenic mycobacteria, including *M. tuberculosis*, *M. kansasii*, *M. avium*, and *M. leprae* (20 and unpublished data). These data are consistent with a potential role for FN attachment in mycobacterial infections. If this is the case, interventions aimed at inhibiting mycobacterial binding to FN have the potential to be novel and useful agents for preventing the establishment of disease.

ACKNOWLEDGMENTS

This work was supported by USPHS grants CA 37926 and CA 44426 from the National Cancer Institute and a grant from the American Foundation for AIDS Research. W.B.T. was partially supported by the National Kidney Foundation.

REFERENCES

1. **Abou-Zeid, C., T. Garbe, and R. Lathigra.** 1991. Genetic and immunological analysis of *Mycobacterium tuberculosis* fibronectin-binding proteins. Infect. Immun. 59:2712–2718.
2. **Abou-Zeid, C., T. L. Ratliff, and H. G. Wiker.** 1988. Characterization of fibronectin-binding antigens released by *Mycobacterium tuberculosis* and *Mycobacterium bovis* BCG. Infect. Immun. 56:3046–3051.
3. **Abraham, S. N., E. H. Beachey, and W. A. Simpson.** 1983. Adherence of *Streptococcus pyogenes*, *Escherichia coli*, and *Pseudomonas aeruginosa* to fibronectin-coated and uncoated epithelial cells. Infect. Immun. 41:1261–1268.
4. **Aslanzadeh, J., E. J. Brown, S. P. Quillin, and T. L. Ratliff.** 1989. Characterization of soluble fibronectin binding to bacille Calmette-Guerin. J. Gen. Microbiol. 135:2735–2741.
5. **Beachey, E. H.** 1981. Bacterial adherence: adhesin-receptor interactions mediating the attachment of bacteria to mucosal surfaces. J. Infect. Dis. 143:325–345.
6. **Ceredig, R., J. W. Lowenthal, and M. Nabholz.** 1985. Expression of interleukin-2 receptors as a differentiation marker on intrathymic stem cells. Nature (London) 314:98–103.
7. **Faris, A., G. Froman, and M. Truszczynski.** 1986. *Escherichia coli* strains of serogroup 0139 isolated oedema disease of swine bind fibronectin. FEMS Microbiol. Lett. 34:221–224.
8. **Froman, G., L. Switalski, and P. Speziale.** 1987. Isolation and characterization of a fibronectin receptor from *Staphylococcus aureus*. J. Biol. Chem. 262:6564–6571.
9. **Godfrey, H. P., Z. Feng, and S. Mandy.** 1992. Modulation of expression of delayed hypersensitivity by mycobacterial antigen 85 fibronectin-binding proteins. Infect. Immun. 60:2522–2528.
10. **Herr, H. W., C. M. Pinsky, and W. F. Whitmore.** 1983. Effect of intravesical bacillus Calmette-Guerin (BCG) on carcinoma in situ of the bladder. Cancer 51:1323–1326.
11. **Hudson, M. A., E. J. Brown, J. K. Ritchey, and T. R. Ratliff.** 1991. Modulation of fibronectin-mediated bacillus Calmette-Guerin attachment to murine bladder mucosa by drugs influencing the coagulation pathways. Cancer Res. 51:3726–3732.
12. **Hunter, S., M. McNeil, R. Modlin, V. Mehra, B. Bloom, and P. Brennan.** 1989. Isolation and characterization of the highly immunogenic cell wall-associated protein of *Mycobacterium leprae*. J. Immunol. 142:2864–2872.
13. **Kavoussi, L. R., E. J. Brown, J. K. Ritchey, and T. L. Ratliff.** 1990. Fibronectin-mediated Calmette-Guerin bacillus attachment to murine bladder mucosa. J. Clin. Invest. 85:62–67.
14. **Kristiansen, K., S. B. Baloda, and J. L. Larsen.** 1987. Toxins, putative cell adhesions and fibronectin binding properties of *Salmonella dublin*. Acta Pathol. Microbiol. Immunol. Scand. Sect. B 95:57–63.
15. **Kuroda, K., E. J. Brown, W. B. Telle, D. G. Russell, and T. L. Ratliff.** 1993. Characterization of the internalization of bacillus Calmette-Guerin (BCG) by human bladder tumor cells. J. Clin. Invest. 91:69–76.
16. **Lamm, D. L., B. A. Blumenstein, and E. D. Crawford.** 1992. A randomized trial of intravesical doxorubicin and immunotherapy with bacille Calmette-Guerin for transitional-cell carcinoma of the bladder. N. Engl. J. Med. 325:1205–1209.
17. **Lamm, D. J., D. E. Thor, and V. D. Stogdill.** 1982. Bladder cancer immunotherapy. J. Urol. 128:931–935.
18. **Pessolani, M. C. V., and P. J. Brennan.** 1992. *Mycobacterium leprae* produces extracellular homologs of the antigen 85 complex. Infect. Immun. 60:4452–4459.
19. **Proctor, R. S., D. F. Mosher, and P. J. Olbrantz.** 1982. Fibronectin binding to *Staphylococcus aureus*. J. Biol. Chem. 257:14788–14794.

19a. **Ratliff, T. L., and E. J. Brown.** Unpublished data.

20. **Ratliff, T. L., J. A. McGarr, and C. Abou-Zeid.** 1988. Attachment of mycobacteria to fibronectin-coated surfaces. J. Gen.

Microbiol. 134:1307–1313.
21. **Ratliff, T. L., J. O. Palmer, and J. A. McGarr.** 1987. Intravesical bacillus Calmette-Guerin therapy for murine bladder tumors: initiation of the response by fibronectin-mediated attachment of bacillus Calmette-Guerin. Cancer Res. 47:1762–1766.
22. **Sher, N. A., S. D. Chaparas, and J. Pearson.** 1973. Virulence of six strains of *Mycobacterium bovis* (BCG) in mice. Infect. Immun. 8:736–742.
23. **Speziale, P., M. Höök, L. M. Switalski, and T. Wadström.** 1984. Fibronectin binding to a *Streptococcus pyogenes* strain. J. Bacteriol. 157:420–427.
24. **Stanislawski, L., H. S. Courtney, and W. A. Simpson.** 1987. Hybridoma antibodies to the lipid-binding site(s) in the amino-terminal region of fibronectin inhibits binding of streptococcal lipoteichoic acid. J. Infect. Dis. 156:344–349.
25. **Thole, J. E. R., R. Schoningh, and A. A. M. Janson.** 1992. Molecular and immunological analysis of a fibronectin-binding protein antigen secreted by *Mycobacterium leprae*. Mol. Microbiol. 6:153–163.
26. **Thomas, D. D., J. B. Baseman, and J. F. Alderete.** 1985. Fibronectin mediates *Treponema pallidum* cytadherence through recognition of fibronectin cell-binding domain. J. Exp. Med. 161:514–525.

Jacob, Rebecca (ASRC)

From: STIC-ILL
Sent: Thursday, May 08, 2003 11:39 AM
To: Jacob, Rebecca (ASRC)
Subject: FW: articles request

-----Original Message-----
From: Mellerson, Kendra
Sent: Thursday, May 08, 2003 11:34 AM
To: STIC-ILL
Subject: FW: articles request

4/4910

-----Original Message-----
From: Noguerola, Alex
Sent: Thursday, May 08, 2003 10:11 AM
To: STIC-EIC1700
Subject: articles request

Please order the following articles

09/728,378

L1 ANSWER 3 OF 3 CAPLUS COPYRIGHT 2003 ACS
AN 1972:523540 CAPLUS
DN 77:123540
TI Amine-citrate buffers for pH control in starch gel electrophoresis
AU Clayton, J. W.; Tretiak, D. N.
CS Freshwater Inst., Fish. Res. Board Canada, Winnipeg, MB, Can.
SO Journal of the Fisheries Research Board of Canada (1972), 29(8), 1169-72
CODEN: JFRBAK; ISSN: 0015-296X
DT Journal
LA English

AGL COMPLETED
OR
LC
5/9
SMP
Missing

Amine-Citrate Buffers for *p*H Control in Starch Gel Electrophoresis

J. W. CLAYTON AND D. N. TRETIAK

Fisheries Research Board of Canada
Freshwater Institute, Winnipeg, Man. R3T 2N6

CLAYTON, J. W., AND D. N. TRETIAK. 1972. Amine-citrate buffers for *p*H control in starch gel electrophoresis. J. Fish. Res. Bd. Canada 29: 1169–1172.

Amine-citrate buffer systems for *p*H control in starch gel electrophoresis gave good resolution of some dehydrogenase isozymes. The pK's of three new amine buffers, N-(3-aminopropyl)-morpholine, pK_2 25 C, 6.12; N-(3-aminopropyl)-diethanolamine, pK_2 25 C, 6.90; and 1,3-bis(dimethylamino)-2-propanol, pK_2 25 C, 7.55, were determined at 5 C intervals in the range 10–40 C. These compounds, together with N, N-bis(2-hydroxyethyl)iminotris(hydroxymethyl)methane (bis-Tris) and tris-(hydroxymethyl)-methylamine(Tris), provide a series of amine buffers with pK's at 0.5 unit intervals in the *p*H range 6.1–8.1.

CLAYTON, J. W., AND D. N. TRETIAK. 1972. Amine-citrate buffers for *p*H control in starch gel electrophoresis. J. Fish. Res. Bd. Canada 29: 1169–1172.

L'emploi de systèmes tampons amines-citrates pour le contrôle du *p*H dans l'électrophorèse sur gel d'amidon a fourni une bonne résolution de quelques isozymes de la déshydrogénase. Les valeurs de pK pour trois nouveaux tampons amines, N-(3-aminopropyl)-morpholine, pK_2 25 C, 6.12; N-(3-aminopropyl)-diéthanolamine, pK_2 25 C, 6.90 et 1,3-bis(diméthylamino)-2-propanol pK_2 25 C, 7.55 ont été déterminées à intervalles de 5 C sur une gamme de 10 à 40 C. Ces composés, de même que N, N-bis(2-hydroxyéthyl)-iminotris(hydroxyméthyle)-méthane (bis-Tris) et tris-(hydroxyméthyl)-méthylamine(Tris), fournissent une série de tampons amines avec des valeurs de pK à intervalles de 0.5 unités sur la gamme de *p*H de 6.1 à 8.1.

Received March 15, 1972

STARCH gel electrophoresis of specific proteins and enzymes has become one of the central techniques of biochemical genetics. One of the advantages of the technique is that the investigator may, in principle, vary the *p*H of the gel medium over a range sufficient to maximize the differences in mobility of the particular proteins under study. In practice, some limitations arise that are related to the necessity of providing adequate *p*H buffering capacity while at the same time keeping the ionic strength of the gel as low as possible in order to minimize electrical currents and undesirable heating of the gel. In studies of enzymes it is also essential to use a buffer system that is compatible with the preservation of enzymatic activity.

Our search for buffer systems that might be useful for starch gel electrophoresis, particularly for the resolution of the abundant isozymes of dehydrogenases in fish, has been influenced by earlier investigations of dehydrogenases that showed the protective effects of coenzymes, citrate ions, and polyhydroxy compounds. Citrate and coenzymes protected lactate dehydrogenase from inactivation by urea (Di Sabato and Kaplan 1965) and also promoted the reactivation of malate dehydrogenase following inactivation by guanidine hydrochloride (Chilson et al. 1965a). More extensive investigations have shown the beneficial effect of citrate in the reactivation of lactate and malate dehydrogenase after guanidine hydrochloride inactivation, as well as in the protection of malate dehydrogenase from heat inactivation (Chilson et al. 1966). In studies of the freezing and thawing of several enzymes it was found that some coenzymes and a number of polyhydroxy compounds prevented the loss of catalytic activity and also, evidently, inhibited the dissociation of multimeric enzymes into their monomeric subunits (Chilson et al. 1965). A general conclusion that may be drawn from these studies is that citrate, coenzymes, and, to some extent, polyhydroxy compounds probably exert a protective effect on the catalytic activity of several dehydrogenases. It therefore appeared likely that buffers for electrophoresis of these enzymes could advantageously be made up with citric acid buffered with an appropriate polyhydroxyamine. The combination of tris-(hydroxymethyl)-methylamine (Tris) buffered citrate has

Printed in Canada (J2474)

proven to be useful in a number of investigations (Clayton and Gee 1969; Clayton et al. 1971; Williscroft and Tsuyuki 1970).

It has become clear that it would be desirable to have a series of amines available to buffer citrate over a range of *p*H in order to bring out all the variability present in some isozyme systems. This paper describes the ionization constants and the suitability for electrophoretic studies of a number of amine buffers that range in pK from 6.1 to 8.1 in approximately 0.5 unit intervals.

Materials and Methods

The whitefish (*Coregonus clupeaformis*) used in this investigation were collected from Clear Lake, Riding Mountain National Park, Man. The walleye (*Stizostedion vitreum vitreum*) was taken from Lake of the Woods, Ont.

The amine buffers were obtained from the following suppliers: N, N-bis (2-hydroxyethyl) iminiotris (hydroxymethyl) methane (bis-Tris), General Biochemicals, Chagrin Falls, Ohio; 2-amino-2-methyl-1, 3-propanediol, Sigma Chemical Co., St. Louis, Mo.; N-(3-aminopropyl)-morpholine, N-(3-aminopropyl)-diethanolamine, and 1,3-bis (dimethylamino)-2-propanol, Aldrich Chemical Co., Milwaukee, Wisc.; tris-(hydroxymethyl)-methylamine, "Analar grade," B.D.H. Chemicals, Toronto, Ont.; triethanolamine was "Baker Analyzed" from Canlab, Toronto, Ont. These amines were used for titrations and also as *p*H buffers in electrophoresis as received from the suppliers. Other chemicals used were of laboratory reagent grade.

Starch gel electrophoresis was conducted with the apparatus described by Tsuyuki et al. (1966). The general methods of extract preparation, electrophoresis, and enzyme staining have been described previously (Clayton and Gee 1969; Clayton et al. 1971). As in the previous work, starch was gelled in buffers prepared by adjusting 0.00200 M citric acid to the desired *p*H with an appropriate amine at room temperature, approximately 22 C. The electrode buffers were made similarly with 0.0400 M citric acid. These concentrations give ionic strengths similar to the citric acid/phosphate buffers described by Fine et al. (1963).

In the present work, muscle extracts were prepared by homogenizing tissue with a distilled water solution of nicotinamide adenine dinucleotide (NAD), 300 mg/liter in a ratio of 1 g muscle to 3 ml NAD solution.

The pK values for the amines were determined graphically from titration curves obtained with an automatic titrator. The titration equipment was obtained from Radiometer, Copenhagen, and consisted of a model 26 *p*H meter, a model GK2021c combination calomel/glass electrode, a SBR 2c Titrigraph and a SBUld Syringe Burette. The meter and electrode were standardized with buffers recommended by Bates (1964).

The amines (8 ml, 0.050 M solution) were titrated with 0.200 N hydrochloric acid under nitrogen in a jacketed, temperature-controlled vessel. The actual temperature of the solution titrated was observed directly with a small thermometer. For amines with two nitrogen atoms per mole the titration of the more acidic nitrogen was conducted on a stock solution that was already partly neutralized with hydrochloric acid. Eight titrations were made with each amine at each temperature.

Buffer values $\frac{\Delta B}{\Delta pH}$ (Van Slyke 1922; Bates 1964) were determined by measurement of the change in *p*H produced by the addition of 1 ml of standardized hydrochloric acid or sodium hydroxide to 100 ml of amine-citrate buffer. The concentration of acid or base used was determined in a trial experiment to be sufficient to produce a *p*H change of 0.1–0.2 unit. The temperature of the amine-citrate buffer was controlled at 25± 0.1 C and each buffer was tested in triplicate.

The conductivities at 25 ± 0.1 C of amine-citrate buffers were measured in the usual way with a conductivity "bridge" and platinized cell.

Results and Discussion

The application of amine-buffered citric acid to starch gel electrophoresis is shown in Figs. 1–3. Malate dehydrogenase isozymes in white muscle of a C^1C^1 homozygous walleye (Clayton et al. 1971) are well separated at *p*H's between 6.1 and 7.5 (Fig. 1), but in the much-used Tris-citrate at *p*H 8.0 two of the isozymes are no longer clearly separable. Lactate dehydrogenase in red muscle of a FF homozygous lake whitefish (Clayton and Franzin 1970) appears as two groups of isozymes in the *p*H range 6.1–8.5 (Fig. 2). However, the existence of multiple muscle-type isozymes, the least anodal group, is only evident at *p*H 7.8, 8.0, and 8.5, while the multiplicity of the heart-type isozymes is clearly evident at all *p*H's studied. The multiplicity of both sets of isozymes that has been used as evidence for tetraploidy in salmonids (Klose et al. 1968; Ohno et al. 1968; Massaro and Markert 1968) would be completely missed in this species if electrophoresis was carried out at *p*H 7.5 or lower. Electropherograms of lake whitefish malate dehydrogenase (MDH) show (Fig. 3) a fish with an apparent symmetrical heterozygous phenotype similar to that found in rainbow trout and Pacific salmon by Bailey et al. (1970). The full multiplicity of MDH isozymes, with the most anodal isozymes occurring as progressive sets of one, two, and three isozymes each, was seen only at *p*H 6.5 and 6.1. At *p*H 8.0, the isozyme pattern is so contracted that it no longer has any resemblance to the *p*H 6.1 pattern or to the phenotypes shown by Bailey et al. (1970). It was suggested in the introduction that amines with hydroxyl groups would be desirable in order to combine the protective effects of polyhydroxy compounds with the buffering capacity of amines. In our search for

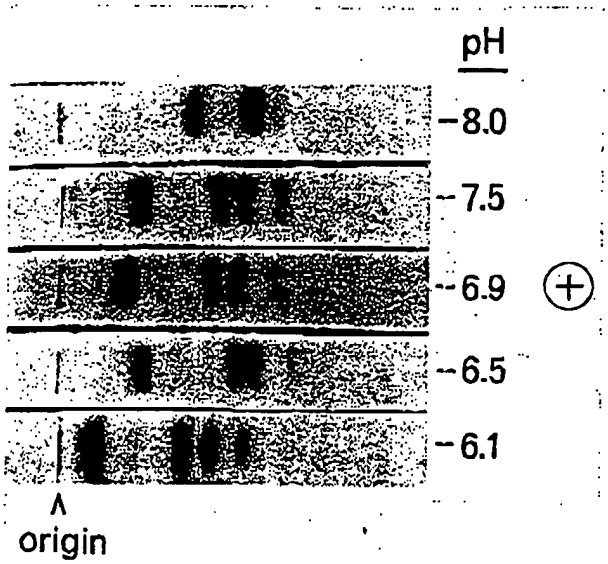

FIG. 1. Walleye malate dehydrogenase electrophoresis amine-citrate buffers: *p*H 6.1, N-(3-aminopropyl)-morpholine; *p*H 6.5, bis-Tris; *p*H 6.9, N-(3-aminopropyl)-diethanolamine; *p*H 7.5, 1,3-bis(dimethylamino)-2-propanol; *p*H 8.0, Tris.

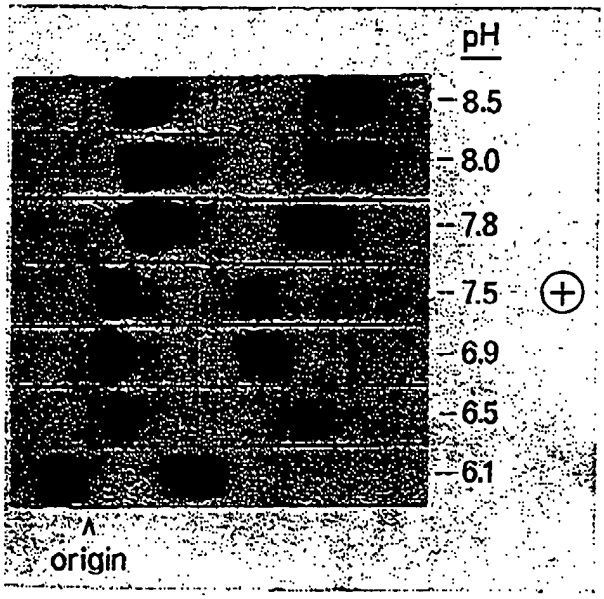

FIG. 2. Lake whitefish lactate dehydrogenase electrophoresis, amine-citrate buffers; *p*H 6.1, N-(3-aminopropyl)-morpholine; *p*H 6.5, bis-Tris; *p*H 6.9, N-(3-aminopropyl)-diethanolamine; *p*H 7.5, 1,3-bis(dimethylamino)-2-propanol; *p*H 7.8, triethanolamine; *p*H 8.0, Tris; *p*H 8.5, 2-amino-2-methyl-1,3-propanediol.

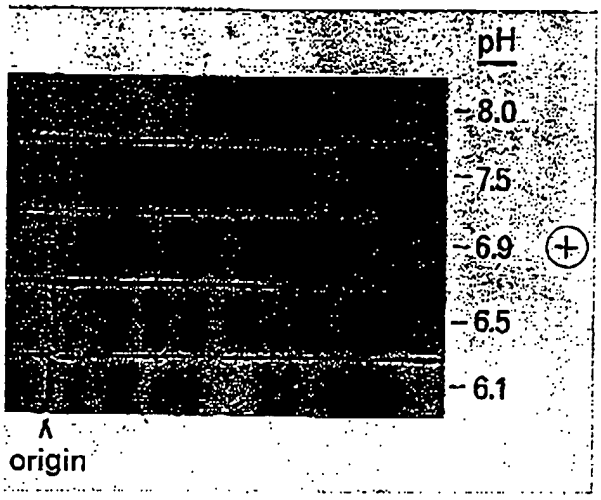

FIG. 3. Lake whitefish malate dehydrogenase electrophoresis amine-citrate buffers: *p*H 6.1, N-(3-aminopropyl)-morpholine; *p*H 6.5, bis-Tris; *p*H 6.9, N-(3-aminopropyl)-diethanolamine; *p*H 7.5, 1,3-bis(dimethylamino)-2-propanol; *p*H 8.0, Tris.

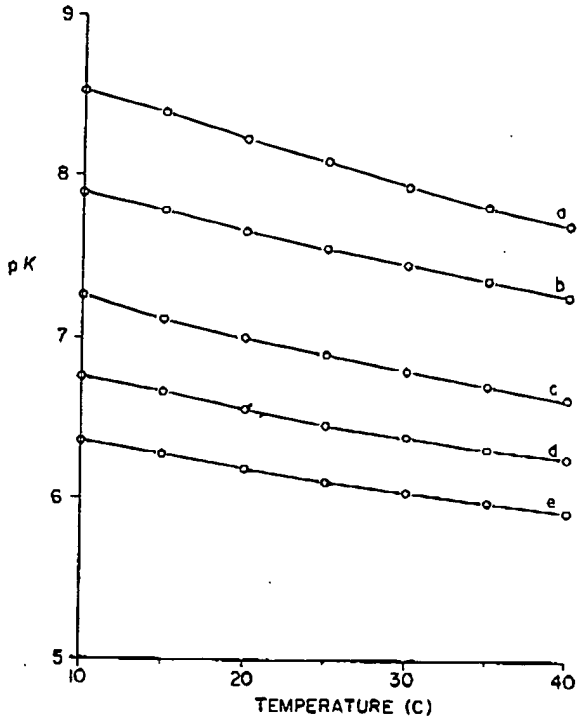

FIG. 4. Effect of temperature on pK of amine buffers: a, Tris; b, 1,3-bis(dimethylamino)-2-propanol (second ionization); c, N-(3-aminopropyl)-diethanolamine (second ionization); d, bis-Tris; e, N-(3-aminopropyl)-morpholine (second ionization).

TABLE 1. pk apparent for amines in 0.05 M solution.

Temp.	N-(3-aminopropyl)-morpholine $H_2NCH_2CH_2CH_2N\langle O \rangle$ pK_2	Bis-Tris $(HOCH_2CH_2)_2NC(CH_2OH)_3$ pK	N-(3-aminopropyl)-diethanolamine $H_2NCH_2CH_2CH_2N(CH_2CH_2OH)_2$ pK_2	1,3-bis(dimethylamino)-2-propanol $(CH_3)_2NCH_2CHOHCH_2N(CH_3)_2$ pK_2	Tris $H_2NC(CH_2OH)_3$ pK	Tris $H_2NC(CH_2OH)_3$ -log K_{ba}*
40±0.2 C	5.91±0.013	6.25±0.012	6.63±0.019	7.25±0.010	7.69±0.014	7.6774±0.0011
35±0.1 C	5.98±0.008	6.32±0.016	6.71±0.019	7.35±0.014	7.81±0.018	7.8031±0.0010
30±0.1 C	6.04±0.017	6.39±0.016	6.80±0.009	7.44±0.017	7.93±0.019	7.9344±0.0010
25±0.2 C	6.12±0.011	6.47±0.013	6.90±0.015	7.55±0.006	8.09±0.015	8.0746±0.0006
20±0.2 C	6.19±0.012	6.56±0.015	7.00±0.015	7.64±0.015	8.23±0.018	8.2138±0.0009
15±0.2 C	6.28±0.019	6.67±0.029	7.11±0.027	7.78±0.020	8.39±0.019	8.3616±0.0008
10±0.3 C	6.36±0.028	6.76±0.026	7.25±0.031	7.89±0.039	8.53±0.017	8.5164±0.0008
	pK_1		pK_1	pK_1		
25±0.2 C	9.99±0.015		10.26±0.013	9.37±0.015		

*Data of Bates and Hetzer (1961).

TABLE 2. Buffer value and conductance of 0.00200 M amine-citrate buffers at 25 C.

Amine buffer	Nominal *p*H	Buffer value × 10^3 HCl $\left(\frac{\Delta B}{\Delta pH}\right)$	Buffer value × 10^3 NaOH	Specific conductance × 10^4 (*mhos/cm*)
N-(3-aminopropyl)-morpholine	6.1	2.9	2.8	3.6
Bis-Tris	6.1	3.7	4.2	3.7
Bis-Tris	6.5	6.2	6.7	4.2
Bis-Tris	6.9	10.0	9.1	4.6
N-(3-aminopropyl)-diethanolamine	6.9	2.4	2.5	4.0
1,3-bis(dimethylamino)-2-propanol	7.5	2.1	2.5	4.2
Triethanolamine	7.5	3.7	4.2	5.2
Tris	7.5	2.0	2.5	5.0
Tris	8.0	4.6	5.3	5.1

amines with pK's in the *p*H range 6–8, we were not always able to find compounds that combined both properties of desirable pK and the presence of a large number of hydroxyl groups. The amines we have investigated do seem to perform well in our electrophoretic procedures (Figs. 1-3), in spite of the number of hydroxyl groups.

A solution of coenzyme (NAD) was used to make the tissue extracts. We have found that the level of enzymatic activity is usually enhanced in extracts with NAD compared to water extracts. We have also found that much clearer electropherograms are obtained, with some enzymes, when coenzyme is also added to the starch and electrode buffers (Clayton et al. unpublished data). In the present work this further addition of coenzyme did not seem to be necessary.

The results of the pK determinations (Table 1, Fig. 4) show that a set of amine buffers is now available with intervals of pK of about ½ unit from *p*H 6 to 8. The new or little-used compounds, N-(3-aminopropyl)-morpholine, N-(3-aminopropyl)-diethanolamine, and 1, 3-bis (dimethylamino)-2-propanol, have pK's that are temperature-dependent like many other amines (Bates 1961). We have measured the first dissociation for these three compounds only at 25 C. These ionizations are probably too alkaline to be of any particular interest as biological *p*H buffers. In the original description of bis-Tris (Lewis 1966), the pK at 25 C was reported to be 6.46; the present value of 6.47 is in good agreement. The variation of pK with temperature for bis-Tris has apparently not previously been reported. The present results confirm the prediction of Lewis (1966) that the pK of bis-Tris would vary with temperature in a manner similar to other amines.

Our data for the pK apparent of Tris may also be compared (Table 1) with pK_{bh} determinations of Bates and Hetzer (1961). The pK_{bh} values contain numerous corrections in comparison with the present results; however, it may be seen that the agreement with the present data is sufficient for all practical purposes related to the choice of a *p*H buffer. We have not investigated the effect of concentration on the pK's of these amines because it has already been shown by Bates (1961, 1964) that the pK's of amines are little affected by concentration at near neutral *p*H of biological interest.

In addition to the amines listed in Table 1, we have found triethanolamine and 2-amino-2-methyl-1, 3-propanediol to be satisfactory as *p*H buffers in electrophoresis (Fig. 2). The physical properties of these amines and many others have been reported by Bates (1961).

The term "buffer value" was suggested by Van Slyke (1922) to describe the effectiveness of a *p*H buffer in resisting *p*H change resulting from the addition of acid or base. Buffer value was defined quantitatively as $\frac{dB}{dpH}$, the slope of the titration curve at any particular *p*H. In practice it is easier to use $\frac{\Delta B}{\Delta pH}$ where the ΔB is a macroscopic addition of base (or acid) and ΔpH is the macroscopic *p*H change. We have measured (Table 2) buffer values and conductivities for a number of amine-citrate buffer systems of the concentration normally used as the gel buffer in starch gel electrophoresis. The results show the superiority of bis-Tris as a *p*H buffer over the other amines. This is due mainly to the way in which these buffers are prepared, whereby the amine is added in quantity sufficient to titrate the citric acid, and thus the concentration of monofunctional amines like bis-Tris is considerably higher than that of difunctional amines like N-(3-aminopropyl)-morpholine. The reduced buffer capacity of some of the difunctional amine buffer systems does not seem to have had any deleterious effect on the isozyme resolution that actually is obtained in electrophoresis (Figs. 1–3). There were no important differences in the conductivity of the various buffer systems (Table 2). The general trend for lower conductivities at lower *p*H is convenient to a practical electrophoretic procedure, since it is usually necessary to increase the voltage to compensate for decreased cationic character of proteins as the *p*H decreases.

In summary, this investigation illustrates the good resolution of the multiple isozymes of some fish dehydrogenases that is produced in starch gel electrophoresis when the gel *p*H is controlled by amine-citrate buffer systems. These systems produce electrophoretic separations that may be interpreted directly in terms of the *p*H of the medium and are not influenced by the character of any particular buffer species. Three previously unused amines together with Tris and bis-Tris provide a series of amine buffers with pK's at 0.5 *p*H unit intervals in the *p*H range 6.1–8.1. The observed differences in the buffering capacity of the electrophoresis buffers did not seem to affect the quality of the electropherograms. The ionization of all the amines tested was, as expected, markedly temperature-dependent, and reproducible electropherograms are likely to depend upon adequate temperature control during both buffer preparation and electrophoresis.

Acknowledgments

We thank R. E. K. Harris of the Freshwater Institute for preparing the electropherograms.

BAILEY, G. S., A. C. WILSON, J. E. HALVER, AND C. L. JOHNSON. 1970. Multiple forms of supernatant malate dehydrogenase in salmonid fishes. J. Biol. Chem. 245: 5927–5940.

BATES, R. G. 1961. Amine buffers for *p*H control. Ann. N.Y. Acad. Sci. 92: 341–356.

1964. Determination of *p*H theory and practice. John Wiley and Sons Inc., New York, N.Y.

BATES, R. G., AND H. B. HETZER. 1961. Dissociation constant of the protonated acid form of 2-amino-2-(hydroxymethyl)-1,3-propanediol (tris-[hydroxymethyl-aminomethane]) and related thermodynamic quantities from 0 to 50°. J. Phys. Chem. 65: 667–671.

CHILSON, O. P., L. A. COSTELLO, AND N. O. KAPLAN. 1965. Effects of freezing on enzymes. Fed. Proc. Suppl. 24: 55–65.

CHILSON, O. P., G. B. KITTO, AND N. O. KAPLAN. 1965a. Factors affecting the reversible dissociation of dehydrogenases. Proc. Nat. Acad. Sci. USA 53: 1006–1014.

CHILSON, O. P., G. B. KITTO, J. PUDLES, AND N. O. KAPLAN. 1966. Reversible inactivation of dehydrogenases. J. Biol. Chem. 241: 2431–2445.

CLAYTON, J. W., AND W. G. FRANZIN. 1970. Genetics of multiple lactate dehydrogenase isozymes in muscle tissue of lake whitefish (*Coregonus clupeaformis*). J. Fish. Res. Bd. Canada 27: 1115–1121.

CLAYTON, J. W., AND J. H. GEE. 1969. Lactate dehydrogenase isozymes in longnose and blacknose dace (*Rhinichthys cataractae* and *R. atratulus*) and their hybrid. J. Fish. Res. Bd. Canada 26: 3049–3053.

CLAYTON, J. W., D. N. TRETIAK, AND A. H. KOOYMAN. 1971. Genetics of multiple malate dehydrogenase isozymes in skeletal muscle of walleye (*Stizostedion vitreum vitreum*). J. Fish. Res. Bd. Canada 28: 1005–1008.

DI SABATO, G., AND N. O. KAPLAN. 1965. The denaturation of lactic dehydrogenases. II. The effect of urea and salts. J. Biol. Chem. 240: 1072–1076.

FINE, I. H., N. O. KAPLAN, AND D. KUFTINEC. 1963. Developmental changes of mammalian lactic dehydrogenases. Biochemistry 2: 116–121.

KLOSE, J., U. WOLF, H. HITZEROTH, H. RITTER, AND S. OHNO. 1968. Duplication of the LDH gene loci by polyploidization in the fish order clupeiformes. Humangenetik 5: 190–196.

LEWIS, J. C. 1966. Mono- and bis(2-hydroxyethyl) aminotris(hydroxymethyl)-methane, "mono-tris", and "bis-tris": new buffer bases with pK^T, 7.83 and 6.46. Anal. Biochem. 14: 495–496.

MASSARO, E. J., AND C. L. MARKERT. 1968. Isozyme patterns of salmonid fishes: evidence for multiple cistrons for lactate dehydrogenase polypeptides. J. Exp. Zool. 168: 223–238.

OHNO, S., U. WOLF, AND N. B. ATKIN. 1968. Evolution from fish to mammals by gene duplication. Hereditas 59: 169–187.

TSUYUKI, H., E. ROBERTS, R. H. KERR, AND A. P. RONALD. 1966. Micro starch gel electrophoresis. J. Fish. Res. Bd. Canada 23: 929–933.

VAN, SLYKE, D. D. 1922. On the measurement of buffer values and on the relationship of buffer value to the dissociation constant of the buffer and the concentration and reaction of the buffer solution. J. Biol. Chem. 52: 525–570.

WILLISCROFT, S. N., AND H. TSUYUKI. 1970. Lactate dehydrogenase systems of rainbow trout — evidence for polymorphism in liver and additional subunits in gills. J. Fish. Res. Bd. Canada 27: 1563–1567.